This is to certify that the

dissertation entitled

PRACTICAL CONSIDERATIONS FOR THE USE OF IMMOBILIZED ENZYMES IN FLOW INJECTION ANALYSIS

presented by

Cheryl Lynn Mattson Stults

has been accepted towards fulfillment
of the requirements for

Ph.D. degree in Chemistry

Major professor

Date July 7, 1987

PRACTICAL CONSIDERATIONS FOR THE USE OF IMMOBILIZED ENZYMES IN FLOW INJECTION ANALYSIS

By

Cheryl Lynn Mattson Stults

A DISSERTATION

Submitted to
Michigan State University
in partial fulfillment of the requirements
for the degree of

DOCTOR OF PHILOSOPHY

Department of Chemistry

1987

ABSTRACT

PRACTICAL CONSIDERATIONS FOR THE USE OF IMMOBILIZED ENZYMES IN FLOW INJECTION ANALYSIS

By

Cheryl Lynn Mattson Stults

Numerous practical issues concerning the use of immobilized enzymes in flow injection analysis (FIA) have been investigated. Immobilized glucose oxidase (GO) was used predominantly. The enzyme reaction was coupled with a modified Trinder reaction in an FIA system. The basic components of the apparatus were: a peristaltic pump, a pneumatically actuated sample injection valve, single bead string reactors (SBSRs), and a miniaturized filter colorimeter. Data acquisition, sample injection and pump speed were controlled by a microcomputer.

The procedure for immobilizing GO on nonporous glass beads was studied and improved. Simplex optimization was used to find an optimum set of operating conditions for the FIA system containing a GO SBSR. Seven variables were specified: carrier pH, reagent pH, temperature, flow rate, aminoantipyrine concentration, dichlorophenolsulfonate concentration, and peroxidase concentration. The results were similar to those obtained by univariate experiments.

Several extended applications of the GO SBSR were investigated. The enzyme coated beads were used to make a microconduit SBSR. The response obtained was equivalent to that of the conventional SBSR. A GO SBSR was used to study the mutarotation of D-glucose in the presence of

phosphate. The mutarotation coefficients obtained were in good agreement with the literature values. Galactose oxidase (GA) was immobilized by a procedure similar to that for glucose oxidase. A GA SBSR was combined with a GO SBSR to make a parallel FIA system. The results obtained from the analysis of real samples matched known values.

Two other issues that are related to the use of immobilized enzymes were also studied. First, the effect of temperature on dispersion was examined for four classes of reactions—none, fast, medium, and slow. A dye was used to establish the effect of temperature. The reactions were: p-nitrophenol with sodium hydroxide, nickel with 4-(2-pyridylazo)resorcinol, and the GO/Trinder reaction. The results indicate that it may be possible to calibrate FIA systems for temperature changes. Second, a partially automated system on which flow reversal/merging zones experiments may be carried out was designed and characterized. The results illustrated the advantage of using a second detector and two dimensional mapping of reaction surfaces from a single injection.

ACKNOWLEDGEMENTS

I'm glad for the opportunity to officially thank those who have contributed to this achievement in my life. First and foremost, I am thankful for Professor Crouch's continuous, positive encouragement and patience. Special thanks are extended to Professor Watson for being my Second Reader, and to the other members of my Guidance Committee (Professors Dye and Nocera) for their helpful suggestions and insight.

I am indebted to Dr. Adrian Wade for his friendship, gentle pushing, and essentially "taking me under his wing". Without the help of Paul Kraus (AKA: my cohort in crime) I might still be taking data on a chart recorder. A big thank-you is in order for letting me use his version of the "Bruce Bus", and for the camaraderie we've shared. The friendship and support of the other members of the Crouch group is also much appreciated.

It was a special privelege to teach for Professor Timmick, Professor Allison, and Dr. Funkhouser. A special note of thanks to Marty Rabb and the other members of the technical support groups in the Chemistry Department for going out of their way to be helpful. I am also grateful for the graphics assistance provided by Bill Draper.

I owe special thanks to Dr. Peggy Hine and other teachers who have encouraged me throughout my life to pursue goals that I mistakenly thought were unattainable. I must also thank my mom and dad for always

believing in me and lending a hand when things got a little crazy in this last year. Last, but certainly not least, I am deeply grateful to my husband, John, for his constant support and taking care of the details of our personal life so that I could complete my work; and to my son, Michael, for providing happy moments of diversion during my writing binges.

TABLE OF CONTENTS

LIST OF TABLES

LIST OF FIGURES

CHAPTER 1

WHAT'S IN THE BOOK

The immobilization of enzymes is no longer a novel concept. Application of these reusable reagents has gained notoriety in the fields of food processing, clinical chemistry, and analytical chemistry. Research in the area of immobilized enzymes has focused primarily on immobilization procedures, reactor designs, and analytical applications. The research reported in this dissertation focuses on the practical considerations that must be made in order to utilize immobilized enzyme technology to its fullest.

This work centered around the use of glucose oxidase (GO) immobilized on nonporous glass beads in the form of a single bead string reactor (SBSR). This enzyme is inexpensive, has good activity, and can be bonded to a variety of insoluble substrates. Primary consideration was given to the use of the SBSR in a flow injection analysis (FIA) system. In this system the GO reactor is coupled with a reaction that utilizes the hydrogen peroxide formed from the enzyme reaction to produce a colored dye.

Fundamental background information is provided in Chapter 2. A review of current immobilized enzyme methodology is provided along with a more specific orientation to the analytical applications of these reagents in FIA. A brief review of the principles of flow injection analysis is presented; the SBSR is introduced.

Chapter 3 describes the characteristics of the GO SBSR. A more efficient immobilization procedure is enumerated. The activity, useful

lifetime, catalase activity, and specificity of the reactor are discussed in detail. Another matter of practical interest, optimum operating conditions, is treated in Chapter 4. Three methods by which the response of the FIA system can be increased are presented. Several extended applications of the system are given in Chapter 5. The potential for using the immobilized enzyme beads in a microconduit is explored. A preliminary investigation of ascorbate interference is described. A novel use of the system, to study a batch reaction, is presented. Finally, the knowledge gained from the work on glucose oxidase was applied to galactose oxidase and resulted in a parallel analyzer. The design, construction, and use of the system for the simultaneous determination of two sugars in real samples are discussed.

Two topics of practical interest are presented following the enzyme work. In Chapter 6 the effect of temperature on the FIA profile is examined. Four different reaction conditions are presented. The design and characterization of an FIA system which combines the flow reversal technique with merging zones is discussed in Chapter 7. Ideas for future projects are given in Chapter 8.

The practical information obtained in the course of this research should prove beneficial to those who continue to work with immobilized enzymes in coming years. It should be possible to extend the procedures developed here to other immobilized enzyme systems.

CHAPTER 2

BACKGROUND INFORMATION

This chapter provides a condensed review of the topics with which familiarity is assumed in the subsequent chapters. There are two major areas of focus: immobilized enzymes and flow injection analysis (FIA). The first section gives the reader a perspective on the general methodology employed with immobilized enzymes in analytical chemistry. More complete information on the subject of immobilized enzyme technology can be found in recent books (1-11) and general review articles (12-18). Specific procedures for enzyme immobilization can be found in Reference 8. The second section deals with some of the fundamental aspects of FIA which are common to all of the systems in the following chapters. Discussion of subtopics which relate only to the material in one chapter are delayed until then. The authoritative book on FIA by Ruzicka and Hansen was published in 1981 (19). A recent monograph by Valcarcel and Luque de Castro (20) provides a review of current FIA technology. An excellent bibliography containing 811 references to the work accomplished in this field was published in a recent review written by the same authors (21). A complete bibliography has also been published by Tecator which covers the period from 1974 through February 1985 (22).

Introduction to Immobilized Enzymes

An enzyme is a protein which acts as a biological catalyst. It differs from an ordinary catalyst in that it has a high turnover rate at

ordinary temperatures, is selective with respect to a particular reaction pathway, and may be specific for one or for only a few compounds. Enzyme solutions are useful as analytical reagents, but they have a few major disadvantages. Some enzymes are unstable in solution, most cannot be used in organic solvents, and all are very sensitive to elevated temperatures. Enzymes are expensive reagents. Once an enzyme is used in solution it is not easily recovered, therefore making the use of these catalysts rather uneconomical.

The immobilization of these biocatalysts has been a major factor in the popularity which they have achieved in the past few decades. By rendering the enzyme water-insoluble many of the disadvantages of the soluble form are eliminated and some advantages gained. The enzyme retains its activity over a broader range of pH and temperature. The enzyme is reusable in this form and so provides an economical alternative to other methods. An additional advantage of this feature is that the enzyme is easily manipulated. It has been suggested that there are fewer interferences with immobilized enzymes (11); thus, complex samples are relatively easy to analyze.

Methods of Enzyme Immobilization

The methods for enzyme immobilization fall into four categories: adsorption, cross-linking, entrapment, and covalent binding. The initial discovery by Nelson and Griffin of enzyme activity retention upon immobilization involved the adsorption of invertase on charcoal (23). This type of immobilization occurs any time an enzyme is adsorbed on some type of insoluble support. The chemical conditions required for

this process are very mild. However, as easily as the enzyme adsorbs to a surface it also desorbs. This is a significant problem if the immobilized enzyme is to be used in a system where it is exposed to a continuous flow of solution.

Entrapment provides a sturdier environment than adsorption. A common method of entrapment involves creation of a polymer in the presence of the enzyme. The enzyme becomes enclosed in a lattice. Polyacrylamide is often used to immobilize enzymes in this way. Gels of this type are commonly used in enzyme electrode applications. An alternative type of entrapment is accomplished by encapsulation of the enzyme in a semipermeable polymeric membrane. This usually involves a tedious and time consuming immobilization procedure.

A somewhat more harsh chemical method is cross-linking. The enzyme is covalently bonded with a bi- or multifunctional reagent to create an intermolecular cross linkage. Glutaraldehyde is commonly used as a linking agent.

Of the four methods of immobilization covalent binding of the enzyme to a water-insoluble support provides the sturdiest environment. This is the most commonly used method of immobilization. Some type of chemically modified glass provides an ideal inert support. The methods of enzyme attachment to the glass are as varied as the number of applications.

Analytical Applications of Immobilized Enzymes

For a complete review of the many ways in which immobilized enzymes have been used in analytical chemistry the reader is referred to

the book by Guilbault (11). There are two main areas of application. Immobilized enzymes have been coupled with amperometric or potentiometric electrodes in a number of ways. The enzyme may be bound directly to the surface of the sensor, but is more commonly attached in the form of a membrane. These probes have gained great popularity in biological and clinical applications.

Immobilized enzyme reactors (IMERs) constitute the other major area of application. Many types of such reactors have been developed. They take the form of packed beds, open tubes, and single strings of beads. Packed bed reactors typically contain the enzyme immobilized on very small particles (37-74 μm) which are packed into a column. They have been used in batch as well as continuous flow methods. The great advantage of these reactors is the large surface area over which the enzyme is spread. However, when used with flowing streams, these reactors may develop channels and high dispersion may result.

Open tubular reactors contain the enzyme immobilized on the inner surface of the tube (usually about 1 mm i.d.). These are commonly used in air-segmented continuous flow analysis. The small surface area available per length of tubing results in very low enzyme activity. There have been various attempts to increase the surface area of the inner wall of the tube. Onuska *et al* (24) demonstrated the use of ammonium hydrogen difluoride to grow whiskers on the inside of glass tubes. A recent report indicated that controlled pore glass particles had been embedded on the walls of plastic tubing (25).

The single bead string reactor (SBSR) is used in flow injection analysis applications. Such reactors are made by immobilizing the

enzyme on porous or nonporous beads. These are packed into a tube which has an i.d. that is 1.3-1.7 times the diameter of the bead. The dispersion in such reactors is low while the enzyme activity is high. More will be presented about this type of reactor in the following section.

Introduction to Continuous Flow Analysis

Continuous flow analysis is the technique by which a sample undergoes treatment as it is carried by a flowing stream through a manifold made of interconnected tubing. It can be divided into two major areas: air-segmented and non-segmented continuous flow analysis. Skeggs is accredited with the development of the former technique (26), which is most often referred to simply as continuous flow analysis (CFA). In this, air segments are introduced into the analytical stream at regular intervals so that the stream is divided into a train of identical segments. The sample is introduced onto the manifold by aspiration for a defined period of time. In each segment complete mixing takes place so that the signal obtained at the output has a rectangular shape similar to what would be expected in the ideal case of a plug-shaped sample. This technique has been used extensively in clinical analysis applications; the best known commercial CFA instrument is the Technicon Autoanalyzer.

Principles of Flow Injection Analysis

The other branch of continuous flow analysis was developed by two separate groups, but has since emerged as a singular technique known as

flow injection analysis (FIA). The approach of Stewart, Beecher, and Hare (27) was a conceptual outgrowth of liquid chromatography, whereas that of Ruzicka and Hansen (28) was founded as an alternative to CFA. In any case, the driving force for the development of this technique was the ability to manipulate and reproduce dispersion of the sample. This technique involves the injection of a sample into a nonsegmented carrier stream. Since the conditions are usually such that laminar flow is predominant, the development of a parabolic velocity profile is responsible for the dispersion of the sample along the axis of the tube. This dispersion, although much greater than that found in CFA, can be controlled by appropriate choices of tubing length and inner diameter, flow rate, sample size, and other components such as valves and flowcells which determine the overall volume of the reactor in the FIA system.

Ruzicka and Hansen have proposed an empirical method by which dispersion can be measured (19). The sample has an initial concentration of C° as it enters the carrier stream. As the plug travels through the manifold, axial and radial mixing take place. This results in a predominantly Gaussian-shaped signal profile. The maximum concentration sensed by the detector, C^{max}, is only a fraction of C°. The formula for the dispersion is:

$$D = \frac{C^\circ}{C^{max}} = \frac{H^\circ}{H} \times \frac{const'}{const''}$$

The height of the peak obtained with the undiluted sample is H°. After the sample has traversed the manifold a lower peak height, H, will be obtained due to dispersion. If the two constants are equal, as in the

case of photometric detection for a system that adheres to Beer's law, the peak heights of the signals can be used to determine the dispersion of the FIA system. This empirical value is classified as limited (D = 1-3), medium (D = 3-10), or large (D > 10). The amount of dispersion that can be tolerated in an FIA system depends on the application for which it is intended. For mere transportation of a sample, limited dispersion is ideal. On the other hand, when a chemical reaction requiring reagent addition must take place, medium or large dispersion is desirable.

Types of FIA Manifolds

One way of manipulating dispersion is by selection of the appropriate type of manifold. A comparison between various types of FIA manifolds was carried out by Ruzicka and Hansen (29). Straight open tubes yield relatively large amounts of dispersion. Coiled tubes show less dispersion due to the presence of secondary flow. This type of flow is a result of the centrifugal forces which affect the flow perpendicular to the axis of the tube. The same phenomenon is observed in 3-D coiled tubes (tubes with regularly spaced knots tied in them). A relatively small amount of dispersion has been found in the use of packed tubes. This is due to the fact that the parabolic profile is broken up as the sample passes through the packed material. The high pressure drop associated with tubes that have been packed with very small diameter particles makes them difficult to use with the peristaltic pumps normally present in an FIA system.

The single bead string reactor (30) has gained acceptance as a viable alternative to open tubes and those packed with small particles. The SBSR consists of a tube packed with beads that have a diameter 60% to 80% of the tube inner diameter. This type of reactor has the advantage of decreased dispersion due to the break up of the velocity profile. The pressure drop is small. Therefore the SBSR can be used to provide longer residence times without an increase in dispersion. An example of typical signal profiles obtained with an SBSR and an open tube of the same length and volume is shown in Figure 1. (Each length of open tubing had the same internal diameter). Although the arrival time of the peak at the detector did increase with reactor length, the point of injection is not given for the sake of simplicity. For use with immobilized enzymes an added advantage of the SBSR is the additional surface area available compared to that of an open tube.

Measurement Tools in FIA

Following the development of an FIA system with the appropriate amount of dispersion, the analyst must choose a measurement tool from a variety of peak characteristics. The complete signal is usually recorded either on a chart recorder or by a computer data acquisition system. The most commonly used measurement is that of peak height. In this case the FIA system may be simplified by the use of a peak detector. In some cases the height at some other place on the peak than the maximum is used (e.g., in gradient techniques). The full width of the peak at half the maximum height (FWHM) can be used as a measure of sample dispersion. Peak area may also be used as an analytical

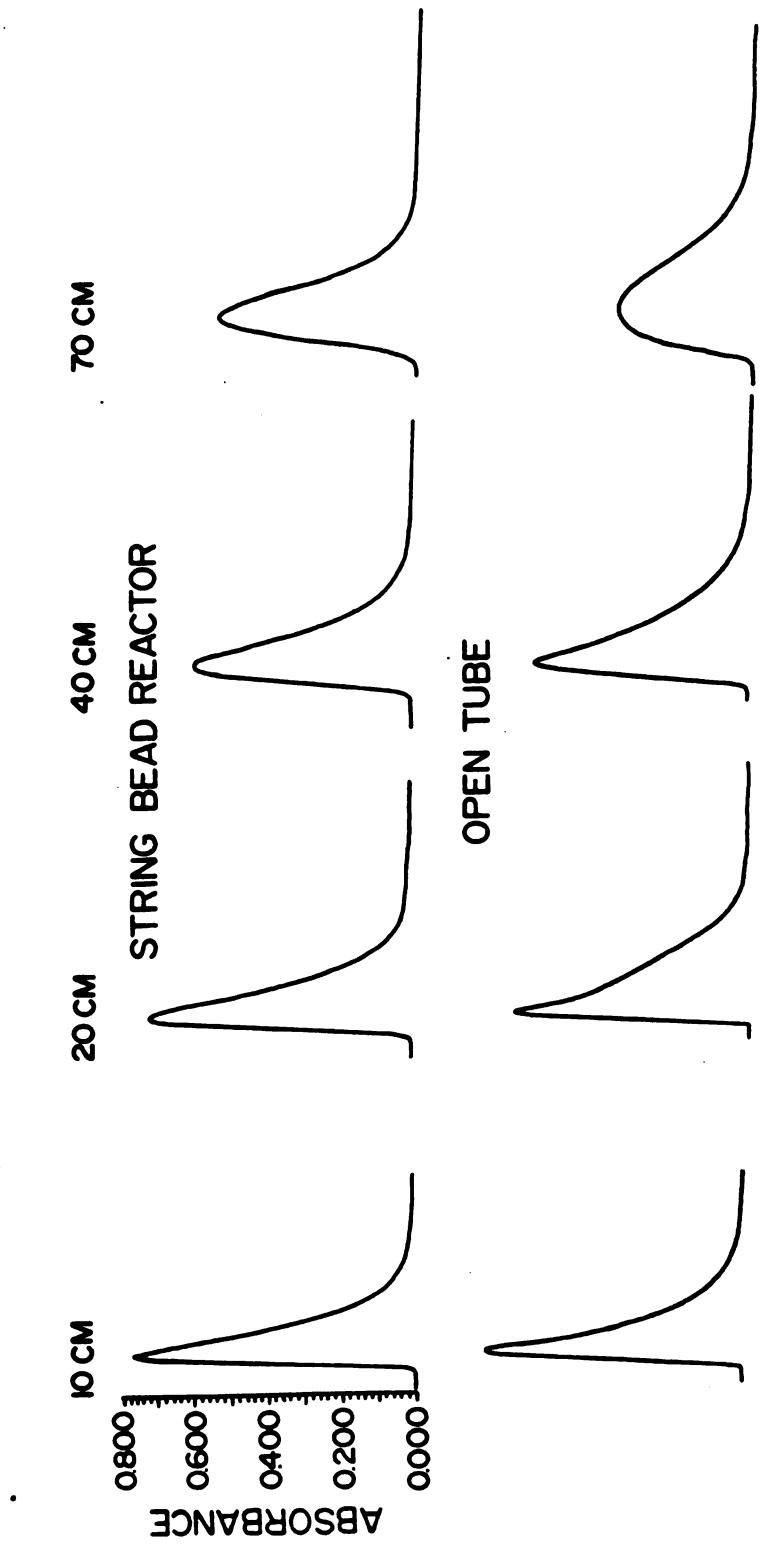

FIGURE 1 Comparison of FIA profiles obtained with an SBSR and an open tube. Signal traces are only in the region of interest (see text for further explanation).

measurement tool. This measure is most easily obtained by a commercially available integrator or by computer processing of the acquired signal. The time at which the peak maximum occurs has been found to be useful in kinetic measurements (31).

Use of Immobilized Enzymes in FIA

Hicks and Updike used a nonsegmented flowing stream with an immobilized enzyme column prior to the development of the technique called, "flow injection analysis". Glucose oxidase was immobilized in a polyacrylamide gel and packed into a miniature chromatographic column. Colorimetric (32) and electrochemical (33, 34) detection methods were employed.

Cremonisi was the first to inject a sample into a nonsegmented stream which flowed through an immobilized enzyme reactor (35). Glucose oxidase was peptide-bonded to CNBr-activated cellulose and packed into a small HPLC-type column. Since then FIA has become increasingly popular for use with immobilized enzymes. The references listed in Table 1 are just a few of the more recent examples. The works listed are mainly in the area of sugars' analysis since that is the thrust of the work presented here. For a general overview of the use of immobilized enzymes in FIA the reader may consult References 45 through 47.

TABLE 1 Examples of immobilized enzymes.

Reactor Type	Detection Method	Immobilization Method	Enzyme	Reference
Bi-enzyme electrode	Amperometric	Covalent attachment to nylon mesh	Glucose oxidase/ Peroxidase Xanthine oxidase/ Peroxidase	36
Electrode & Packed Bed	Amperometric	Cross-linked with bovine serum albumin Covalent attachment to silica gel	Peroxidase Glucose oxidase	37
Packed Bed	Amperometric	Covalent attachment to porous alumina	Glucose oxidase	38
Packed Bed	Amperometric	Covalent attachment to controlled pore glass	Glucose oxidase Mutarotase Invertase	39
Packed Bed	Potentiometric	Covalent attachment to controlled pore glass	Glucose dehydrogenase	40
Packed Bed	Spectrophotometric	Covalent attachment to controlled pore glass	Glucose oxidase Mutarotase Invertase	41
Packed Bed	Chemiluminescence	Covalent attachment to controlled pore glass	Glucose oxidase Mutarotase Invertase Catalase	42
SBSR	Spectrophotometric	Covalent attachment to nonporous glass beads	Glucose oxidase	43
SBSR	Fluorescence	Covalent attachment to polyaminostyrene beads	Glucose oxidase Peroxidase	44

CHAPTER 3

THE GLUCOSE OXIDASE SBSR

As was reported previously (Chapter 2) there is a minimal amount of dispersion associated with an SBSR made of nonporous glass beads; this allows longer residence times which are desirable in enzyme applications. Glucose oxidase was chosen as a model enzyme since it is inexpensive, highly active, and easily obtained. The development of the procedure used to immobilize this enzyme on nonporous glass beads is described. The dimensions of the SBSR assembled with these beads are given in Figure 2. In order to use an immobilized enzyme single bead string reactor effectively one must first know its characteristics. In some cases it is desirable to know the amount of enzyme actually immobilized. A method for such a determination is presented. Since it is desirable to work with a reactor that retains its activity for a long period of time, the useful lifetime of the immobilized glucose oxidase SBSR is discussed. One problem with many enzyme preparations is that they sometimes contain small amounts of impurities which can be immobilized along with the enzyme. These impurities sometimes affect the apparent activity of the enzyme. The presence of catalase in glucose oxidase preparations can be problematic in this respect. Results of the investigation of catalase activity in the reactor are presented. The specificity of the reactor is also examined.

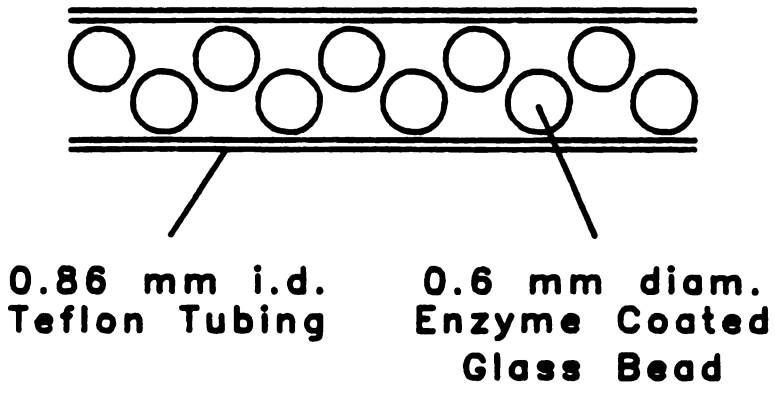

FIGURE 2 **Single bead string reactor.**

Immobilization Procedure for Glucose Oxidase

Covalent attachment of enzymes to an inert matrix provides a sturdy environment and yet allows the enzyme to be readily accessible for reaction in continous flow reactors. Glass provides an ideal inert support because of its low reactivity toward most compounds and mechanical stability. Nonporous glass beads provide added surface area without increased dispersion. For these reasons, covalent bonding of glucose oxidase to nonporous glass beads was the method of choice for the reactor to be incorporated into a flow injection system. Glucose oxidase is commonly attached to glass by glutaraldehyde linkage. The specific conditions for this type of immobilization as enumerated by Thompson (43) were used initially. There are four steps in the procedure: cleaning, whisker formation, silanization, and enzyme attachment. The aim of this work was to minimize the amount of time required to perform the immobilization and to establish a procedure that gave reproducible results.

The conditions for a given step were varied while those for the other three steps were held constant. In each case all four steps were carried out on a 0.5 g sample of nonporous glass beads. After the immobilization of the glucose oxidase the beads were put into Teflon tubing (10 cm in length) and incorporated into the FIA system described in Chapter 4. A calibration curve was obtained with glucose standards in the 0 to 800 ppm range. The slope of the calibration curve was taken as a measure of the activity of the enzyme on the beads.

Cleaning Procedure

In order to immobilize an enzyme efficiently it is necessary to eliminate any contaminants from the surface of the glass before the procedure is begun. There are a variety of ways by which glass surfaces can be cleaned. The most common chemical methods are by chromic acid, hydrochloric or nitric acids, or alcoholic potassium hydroxide. Chromic acid cleaning is a very harsh treatment that ensures the oxidation of any carbonaceous material. Other acids are used to leach any heavy metals from the surface of the glass. As shown in Table 2 the initial procedure specified treatment of the glass beads with both chromic and hydrochloric acids. It is known that in order for an acid treatment to be effective it must be carried out at elevated temperatures (48).

The use of warm concentrated acids can be hazardous and is therefore not a highly desirable method of treatment. Also, when the beads were cleaned with chromic acid they darkened during the whisker formation process. These two factors suggested that an alternative cleaning process would be advantageous. Since the glass beads are not extremely dirty it is not mandatory that chromic acid be used. As an alternative cleaning solution, alcoholic KOH was chosen. The beads obtained by cleaning with only the alcoholic KOH did not darken and were found to have a level of activity similar to those treated with chromic and hydrochloric acids. This would suggest that the beads do not have an excess of heavy metals at the surface; these would require leaching by HCl.

TABLE 2 Initial immobilization procedure.

Step	Reagent	Time	Temperature (°C)
Cleaning	Chromic Acid	15 min.	23
	6 M HCl	10 min.	"
Rinse	Distilled H_2O		"
	Acetone		"
Dry	N_2		"
Whisker Formation	5% (w/v) NH_4F HF/MeOH	1 hr.	23
Dry	N_2		"
Heat		3 hr.	450
Silanize	2% (v/v) 3-aminopropyl-triethoxysilane/ acetone	30 min.	23
Decant			
Heat		24 hr.	90
Glutaral-dehyde	1% solution in pH 8.0 buffer	30 min.	23
Enzyme	5 mg/ml glucose oxidase in pH 6.85 buffer	24 hr.	4

Whisker Formation

The best conditions for whisker formation were found by Onuska (24) and were not altered. This step involves soaking the beads in methanol saturated with ammonium hydrogen difluoride for an hour, decanting the solution and drying the beads, followed by heating them in a sealed glass tube at 450°C for three hours. The effectiveness of the treatment with ammonium hydrogen difluoride was investigated. Three experiments were conducted. The first involved treating the beads in the specified manner. In the second the heating of the beads in a closed tube was eliminated. The third experiment involved no treatment with ammonium hydrogen difluoride.

It was expected that the beads from the first experiment would have the highest activity. Since the second experiment was carried out at room temperature it was expected at most that only a limited amount of etching would take place; this was expected to result in only a small increase in surface area and thus a small increase in enzyme activity over that obtained from the beads in the third experiment. The activity of the beads was found to vary as expected. The beads from the second experiment exhibited only 58% of the activity of those from the first; the beads from the third experiment had an activity that was only 49% of that associated with those from the first. This indicates that indeed the surface area is greatly increased by this treatment. It should be noted, however, that the enhancement is not due to the formation of real whiskers. Mottola has shown that the surface looks more like a series of "volcanic crater erosions" (45). The same author points out that

there is not a great advantage to be gained by roughening the surface of the tube and immobilizing the enzyme on its surface as well.

Silanization

The silanization of the beads proved to be the most problematic part of the immobilization procedure. It was found that heating the beads with the 3-aminopropyltriethoxysilane in acetone caused the coverage to be quite non-uniform. It was suspected that the rapid evaporation of the solution was the reason for this. Therefore, it was thought that an aqueous solution might give better results. The silanization procedure specified by Mosbach (8) was tried. The resulting beads had low activity.

A "trial and error" approach was used to arrive at a silanization procedure which gave reproducible results. The concentration of the solution, the temperature, and reaction time were varied. It was found that a 1% (v/v) solution gave sufficient coverage without leaving an excessive residue on the bottom of the beaker. By allowing the solution to evaporate from the beads at room temperature in the fume hood more uniform silane coverage was obtained. The temperature and reaction time were decreased in order to prevent darkening of the beads (a sign of silane decomposition). The time required for this part of the procedure was significantly reduced from 24 hours to 15 hours.

Since the solution used to silanize the beads was made with acetone it was assumed that washing the beads with acetone after the treatment would be sufficient. However, the beads stuck to the bottom of the beaker. One solution to this problem would be to use Teflon

beakers instead of glass. However, the more economical solution proved to be the dropwise addition of distilled water (DW) to the acetone until the beads were loosened. If too much water is added the beads float. Thus, it can be concluded that this part of the procedure seems to be much more of an "art" than a "science".

Glutaraldehyde Attachment

The glutaraldehyde was attached to the silane group as specified in Table 2. A 1% (v/v) solution of glutaraldehyde in pH 8.0 phosphate buffer was allowed to react with the silanized beads. This step was not modified. However, it was observed that the beads become salmon colored when this part of the procedure is successful. It was noted that the time required for the color change to take place was in the range of 0.5-2 hours.

Enzyme Attachment and SBSR Construction

The covalent binding of the enzyme was carried out under the same conditions as in the initial procedure (Table 2). A 5 mg ml^{-1} solution of glucose oxidase (E.C.1.1.3.4, Sigma Type II from Aspergillus niger, specific activity approximately 17,800 U g^{-1} at 35°C) in phosphate buffer was allowed to react with the glutaraldehyde treated beads for 24 hr. It is desirable to immobilize the enzyme in its most active state. The use of a 0.05 M phosphate buffer, pH 6.85, facilitates this. After this step was complete, a single bead string reactor was made by placing a suitable portion of the beads in a length of Teflon tubing. This task was most easily accomplished by crimping one end of the tubing

and inserting it into the end of a syringe. The tube was then filled by applying suction. The beads remaining were transferred to a glass vial. In any case the beads were stored in 0.05 M phosphate buffer at 4°C. The final immobilization procedure is summarized in Figure 3.

Alternate Method of Immobilization

While periodically retesting the SBSRs, a rapid decrease in activity was observed during the first few days of use. This was attributed to enzyme being adsorbed on the surface. One remedy for the situation is to flush the SBSR with copious amounts of buffer prior to use. An alternative is to prevent adsorption from occurring in the first place. Therefore, the possibility of immobilizing glucose oxidase by continuously circulating the enzyme solution was investigated. The immobilization procedure was carried out in the usual manner up to the point of the glutaraldehyde attachment. The beads were then put into a suitable length of Teflon tubing which was connected to a pump tube. A small two-channel peristaltic pump (Ismatec) circulated the enzyme solution at the rate of 0.8 ml min^{-1}. The resulting beads exhibited very low activity compared to that of beads obtained by the usual method. The trade-off of providing the beads with a continuous stream of "fresh" solution versus the time needed for attachment at the surface proved to be in favor of the latter. Perhaps a very low flow rate (e.g., 0.05 ml min^{-1}) would provide a suitable environment for the immobilization.

1. Silanization

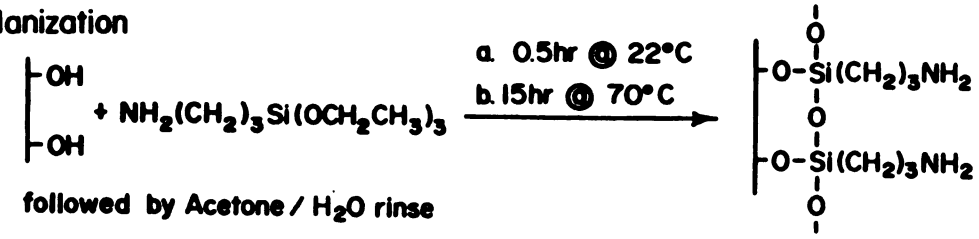

followed by Acetone / H_2O rinse

2. Glutaraldehyde Addition

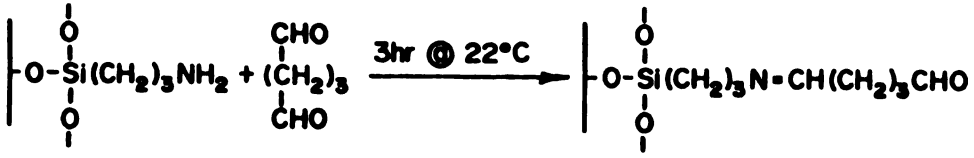

followed by 0.05 M phosphate buffer rinse

3. Enzyme Attachment

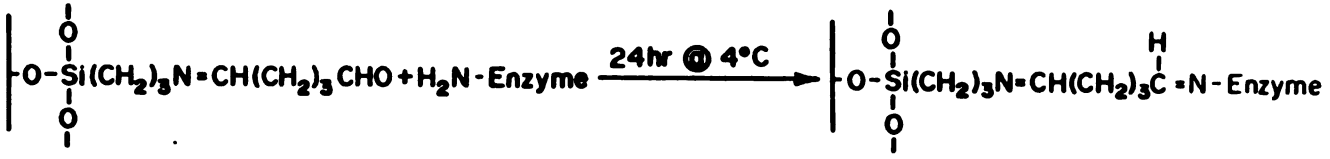

followed by rinsing with and storage in 0.05 M phosphate buffer

FIGURE 3 Final immobilization procedure.

Determination of Amount Immobilized

The are two viewpoints concerning the amount of enzyme immobilized. The first is the literal interpretation--what quantity of enzyme is on each bead. The second is more pragmatic in nature--what equivalent amount of enzyme must be used in solution in order to do the same analysis. There are a number of ways to arrive at an answer for the first case. One might choose to do a nitrogen analysis. This would not guarantee an exact result unless the aminosilane content were previously known (or determined). An alternative would be quantitation of the protein present. However, the small amounts of other enzymes present as impurities would result in a positive error. In either case, the enzyme is destroyed in the process. Professor Mottola's group at Oklahoma State University has been working on a nondestructive solution to this problem, but has only published a method for the determination of aldehyde groups on glass surfaces (49). It therefore seemed appropriate to pursue another method of enzyme determination.

The method chosen was that of an assay by difference. A glucose oxidase solution was prepared, half of which was used for the covalent binding step in the immobilization procedure and the other half as a control. After the enzyme was attached to the beads the reacted GO solution was poured into a volumetric flask. The washings were combined with this and the mixture was diluted to the mark with distilled water. The final solution was used as the carrier solution in the FIA apparatus with a plain SBSR in place of a GO SBSR. Dilutions of the control solution were used in a similar manner to construct a calibration curve. For each GO solution a 400 ppm glucose standard was injected and the

absorbance measured. The absorbance of the reacted solution was located on the calibration curve. After correcting for the dilution factors, the amount of glucose oxidase immobilized per gram of beads was determined to be 7.3 mg (approximately 1.4 $\mu g\ mm^{-2}$).

From a more practical standpoint (the second viewpoint mentioned), the activity of the GO on a 10-cm SBSR was found to be equivalent to a solution containing 0.5 mg of enzyme per ml. Combining the results from the two determinations, it would take less than two hours under continous operation (a flow rate of 0.5 ml min^{-1}) to use the entire amount of glucose oxidase needed for the immobilization. These results were based on the initial activity of the GO SBSR. In order to make a more realistic comparison one must take into account the drop in activity that occurs.

A typical scenario of the loss in activity is shown in Figure 4. It can be seen that after about 150 days the activity of the stored beads would match that of the beads which had been used for periodic testing. The activity in this particular SBSR (one of the first assembled for this research) dropped to approximately 56% of the original. The GO SBSR used in the determination of the amount of enzyme immobilized was found to retain 66% of its original activity after one year (the immobilization method was improved). Thus, it can be concluded that the glucose oxidase immobilized by the modified method presented in Figure 3 has a very long useful lifetime. This evidence substantiates the cost advantage of enzyme immobilization.

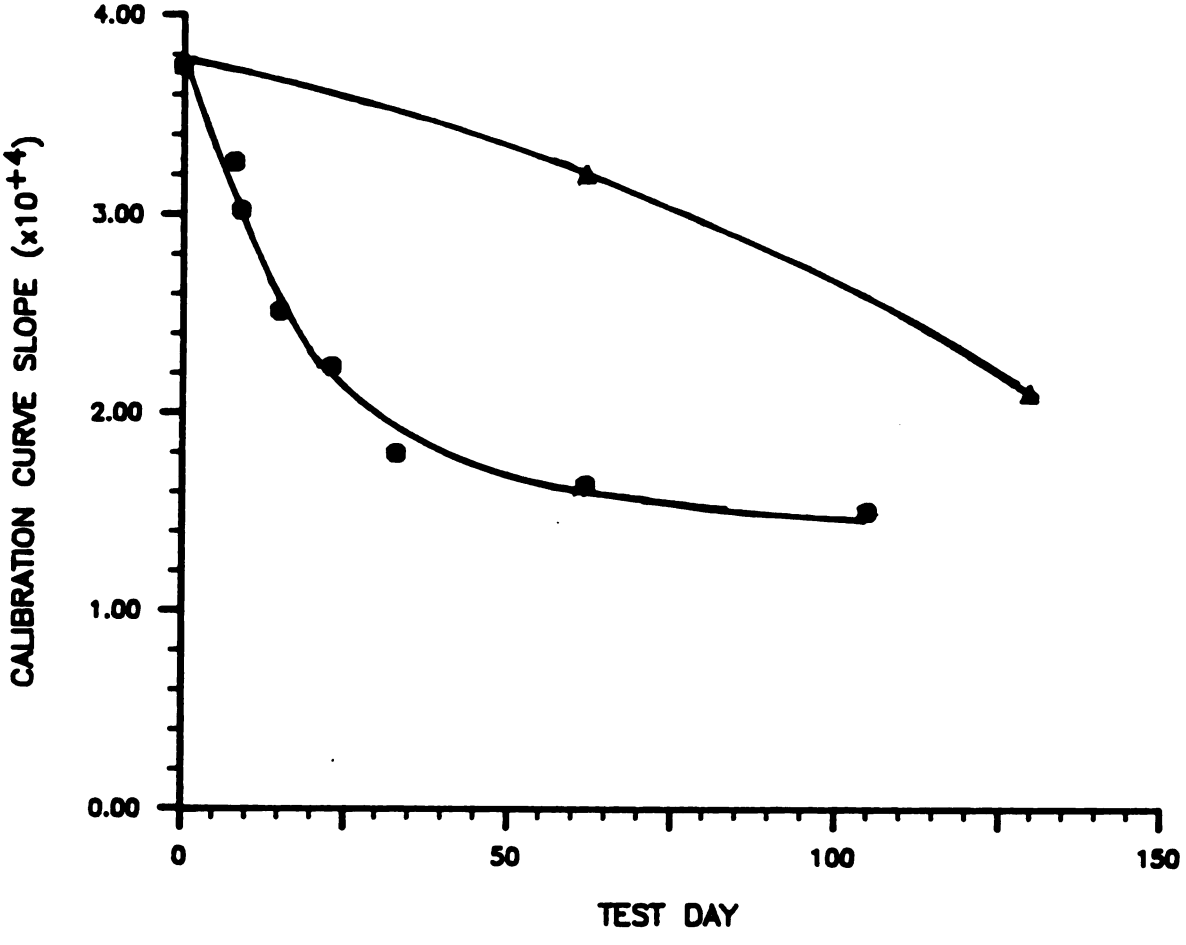

FIGURE 4 Loss of glucose oxidase activity for routinely used beads (●) and stored beads (▲).

Catalase Activity

In all immobilizations there is a risk of immobilizing impurities which will interfere with the reaction of interest. Catalase is a major problem in the case of glucose oxidase since it destroys the peroxide formed. In order to get some idea of the extent of the catalase activity in the GO SBSR, an experiment was carried out in which three 10-cm reactors were tested individually and then connected together to make reactors 20 and 30-cm long. The expected absorbance was obtained by adding the appropriate absorbances for the two- or three-unit reactors used. As can be seen in Figure 5 there is a significant difference between the expected values and those actually obtained. In an effort to eliminate some of this effect the color-forming reagent stream was placed before the glucose oxidase SBSR. A wider range of linearity was found, but there was still a significant deviation from the expected results.

Specificity of Immobilized Glucose Oxidase

Since the ultimate intended use for the GO SBSR is in the analysis of real samples it was necessary to ensure that the reactor is specific for glucose compared to other sugars. Nine nutritionally-significant sugars were tested by preparing 3.3 mM standards of each and using them in the place of β-D-glucose. The responses were then taken as a percentage of that obtained for β-D-glucose. The results are compared in Table 3 to those found in the literature (50). The experimental values designated by a "-" indicate that the value obtained could not be differentiated from the baseline. All values except that obtained for

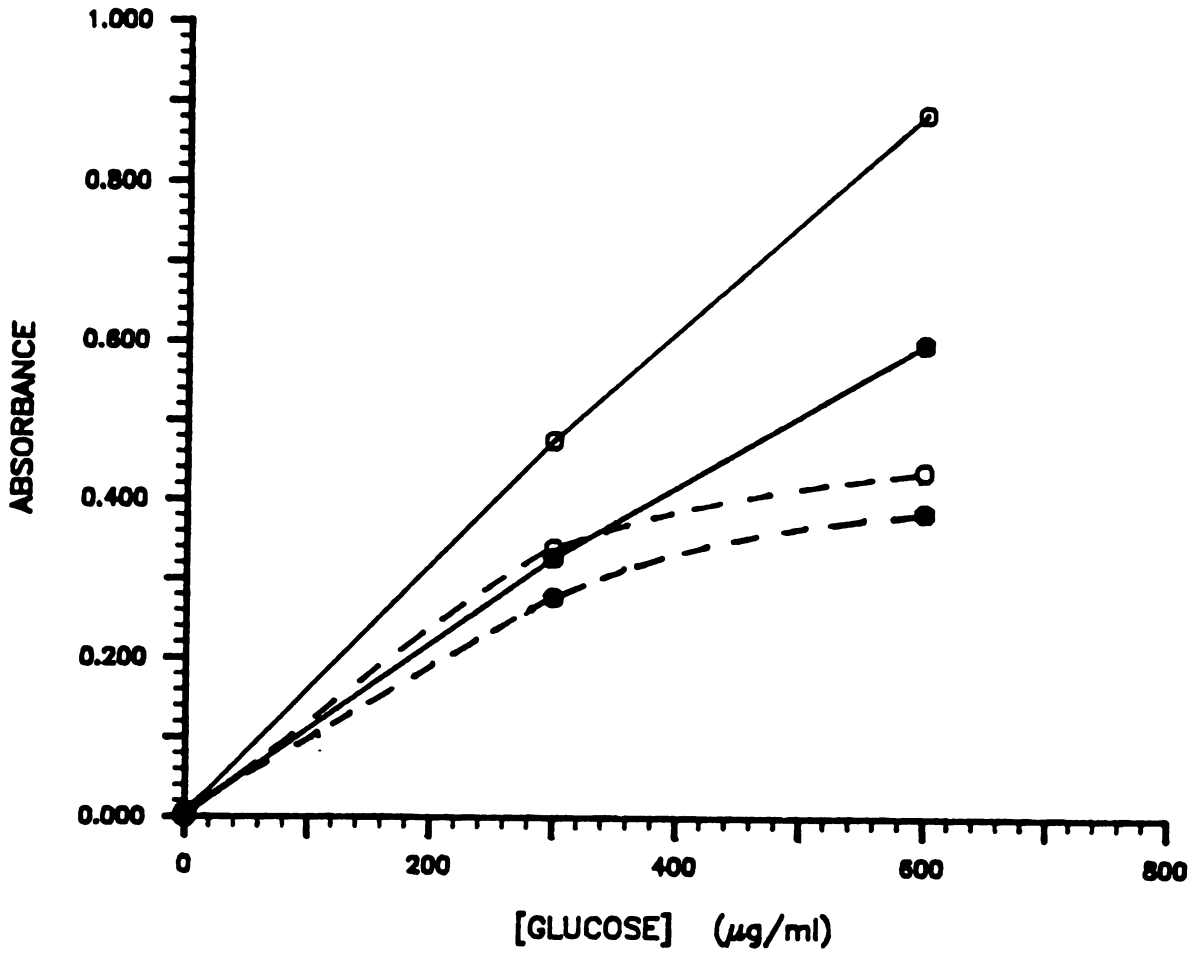

FIGURE 5 Actual (- -) and expected (——) effect of catalase in a 20-cm SBSR (●) and a 30-cm SBSR (○).

TABLE 3 Glucose oxidase activity toward other sugars.

	Response Ratio	
Sugar	SBSR	Literature
β-D-glucose	1.00	1.00
α-D-glucose	0.89	0.0064
galactose	-	0.0014
fructose	-	na
mannose	0.011	0.0098
2-deoxyglucose	0.18	0.25
maltose	0.015	0.0019
xylose	0.0062	0.0098
glucosamine	-	<0.0005
sucrose	-	na

"-" denotes no distinguishable response
"na" means not available

α-D-glucose are as good as or better than those indicated in the literature. The unusually high value for α-D-glucose was a result of phosphate catalysis of the mutarotation of this species. A more detailed discussion of this is undertaken in Chapter 5.

In summary, an immobilization procedure for glucose oxidase has been improved and characteristics of single bead string reactors made from nonporous glass beads containing the enzyme have been established. In the next chapter some practical considerations concerning the use of this reactor are discussed.

CHAPTER 4

OPTIMIZATION OF THE FIA SYSTEM

The glucose oxidase/Trinder reaction (51) is one of the most commonly used methods for the colorimetric determination of glucose. The reaction scheme originally proposed involves the reaction of glucose and molecular oxygen in the presence of glucose oxidase (GO) to produce hydrogen peroxide. The H_2O_2 then reacts with 4-aminoantipyrine (AAP) (also known as 4-aminophenazone) and phenol in the presence of peroxidase (PO) to produce a colored dye with an absorbance maximum at 505 nm. Trinder later found that when the phenol was replaced by 3,5-dichloro-2-hydroxyphenyl sulfonic acid (DCPS) the reaction was four times more sensitive and the absorbance maximum shifted to 510 nm (52). In this work the latter Trinder reaction was coupled with the GO reaction as shown in Figure 6.

Other workers have immobilized glucose oxidase and used it in flow injection analysis systems in conjunction with the Trinder reaction (45, 53, 54). However, this work is the first to be published (55) regarding the optimization of such systems.

In this chapter the computer controlled FIA system incorporating the GO SBSR with the Trinder reaction is described. The salient features of the instrumentation are enumerated. Three different approaches toward improving system performance are discussed.

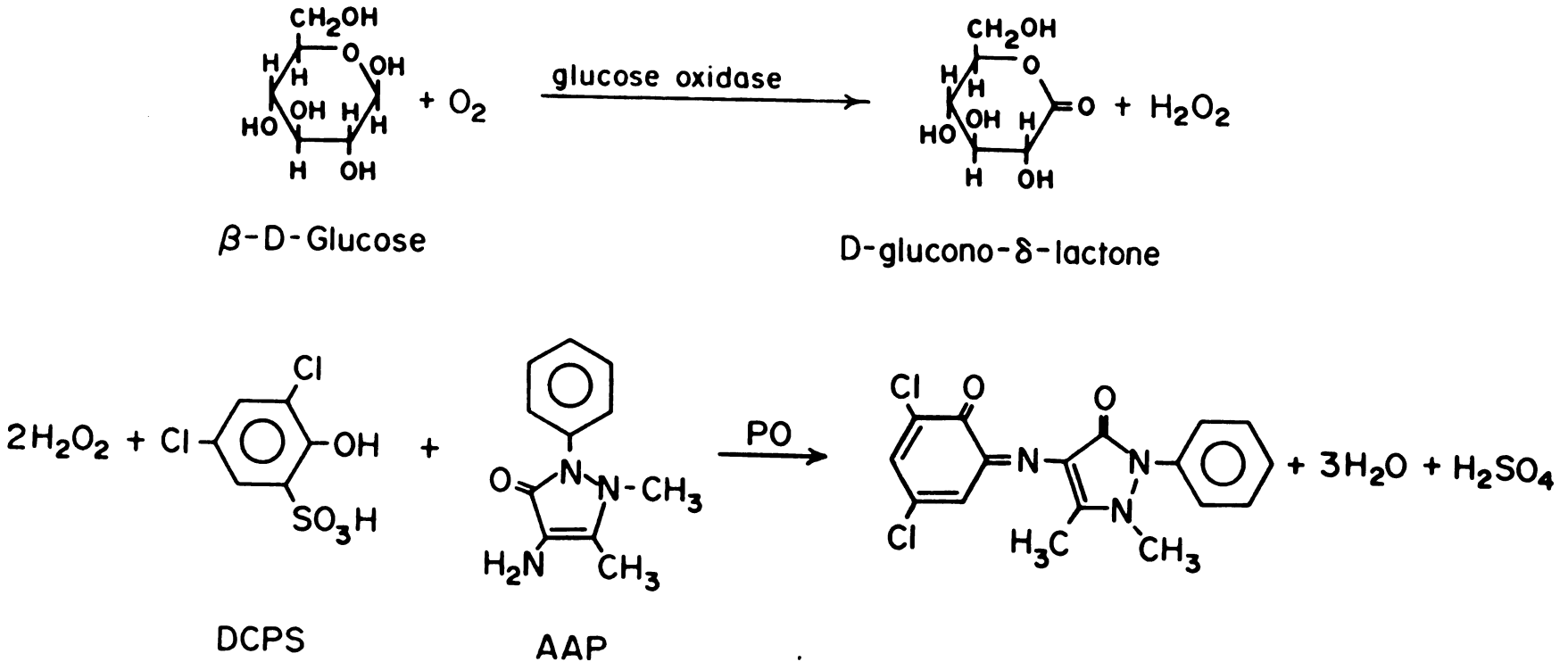

FIGURE 6 Glucose oxidase/Trinder reaction.

Instrumentation

A diagram of the apparatus is shown in Figure 7. The temperature of the solutions and the GO SBSR was controlled by a thermostatted circulating water bath. The temperature of the reagents was controlled by placing each solution in a jacketted beaker or flask. A jacket was made for the GO SBSR. This consisted of a piece of glass tubing (that fit snugly around the 10-cm length of Teflon tubing) fused into the open ends of a small condenser.

The sample was injected via a pneumatically actuated 6-port sample injection valve with a 30-µl sample loop (Rheodyne) into the carrier stream which was pumped by a 12-channel peristaltic pump (Ismatec). Flow rated pump tubing (Technicon) was used for delivery of the reagents to the manifold. The sample first passed through the GO SBSR. It was then joined at a tee by a solution containing PO, AAP, and DCPS. The sample/reagent mixture then passed through an SBSR made with unmodified glass beads (also referred to as a "plain" SBSR) in order to promote mixing without added dispersion. After reaction the sample/reagent mixture entered a miniaturized flow-through filter colorimeter which was designed by Patton *et al* (56) and assembled in our laboratory. Data acquisition, sample injection, and pump speed were controlled by a microcomputer as discussed below.

Choice of Fixed Parameters

Initially there were a number of parameters that, for convenience, were fixed. These were: SBSR lengths, sample size, flow ratio of the carrier (buffer) and reagent streams. As mentioned previously

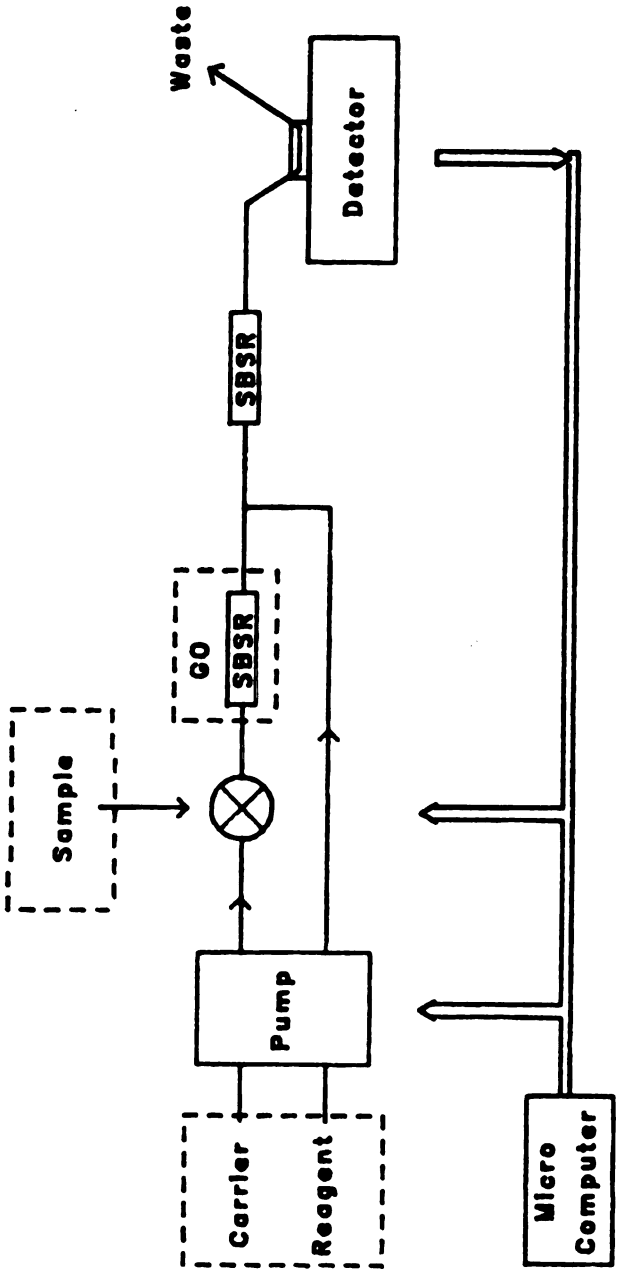

FIGURE 7 FIA system for glucose determination.

(Chapter 3) the effect of the catalase, as the GO SBSR is made longer, invokes the "law of diminishing returns". Therefore, a 10-cm length was chosen since its activity gave acceptable absorbance values. This also minimized the back pressure which results when a packed reactor is used in a flowing stream. A 40-cm SBSR consisting of unmodified glass beads was used as the reaction manifold for the Trinder part of the reaction. This length was necessary to allow sufficient time for reaction between reagent addition and detection.

The placement of the PO reagent solution was also of interest. Theoretically, it would be better to add this solution prior to the glucose reaction so that any effect of catalase would be minimized. The hydrogen peroxide would be immediately consumed by the color-forming reaction and have less chance of coming into contact with catalase as the reacting plug travels through the manifold. A comparison of the calibration curves obtained with the reagent addition before and after the GO SBSR revealed that there was no significant increase in slope or linearity for a 10-cm length. The 20 and 30-cm lengths did exhibit a significant increase in linearity. Thus the choice of a 10-cm length was confirmed as the best one. The reagent solution could be added after the glucose reaction without loss in sensitivity and without risking contamination of the immobilized glucose oxidase.

A sample volume of 30 µl was chosen to match the internal volume of the glucose oxidase single bead string reactor. In order to investigate the relationship of absorbance to sample size a 6-port sample injection valve was connected in such a way that the sample size was regulated by the amount of time the valve spent in the "inject"

position. The injection time multiplied by the flow rate of the sample stream was used to determine the sample volume. The sample injection time was varied from 1 s to 25 s in 1 s increments with a flow rate of 0.44 ml min^{-1}. The peak heights obtained are plotted in Figure 8 versus sample volume. It is interesting to note that the relationship between absorbance and peak height is linear from 7 µl to 81 µl. The greatest sensitivity is attainable in this region and, thus, makes the 30-µl sample volume desirable. Beyond that region the response increases by successively smaller amounts and finally approaches the maximum amount of glucose that can be converted--approximately 74 µg (185 µl of a 400 ppm standard). In previous experiments related to this project (43), double peaks were obtained with volumes greater than 65 µl for a 20-cm GO SBSR through which the reagent stream was passed concurrently with the sample. This resulted in an optimum sample volume of 45 µl. No incidence of double peaks was observed for this system which indicates that complete mixing occurs in the manifold.

The ratio of the flow rate of the carrier stream to that of the reagent stream was adjusted by appropriate choices of pump tubing. A range of ratios from 4:1 to 20:1 was investigated. The overall flow rate was kept at 0.5 ml min^{-1}. The resulting peaks are shown in Figure 9. There was no sampling time advantage to be gained since the baseline widths of all peaks are similar. The peaks obtained with the two highest flow ratios showed some distortion. Therefore, a 10:1 ratio was selected. This also helped minimize both the consumption of PO and dilution of the sample.

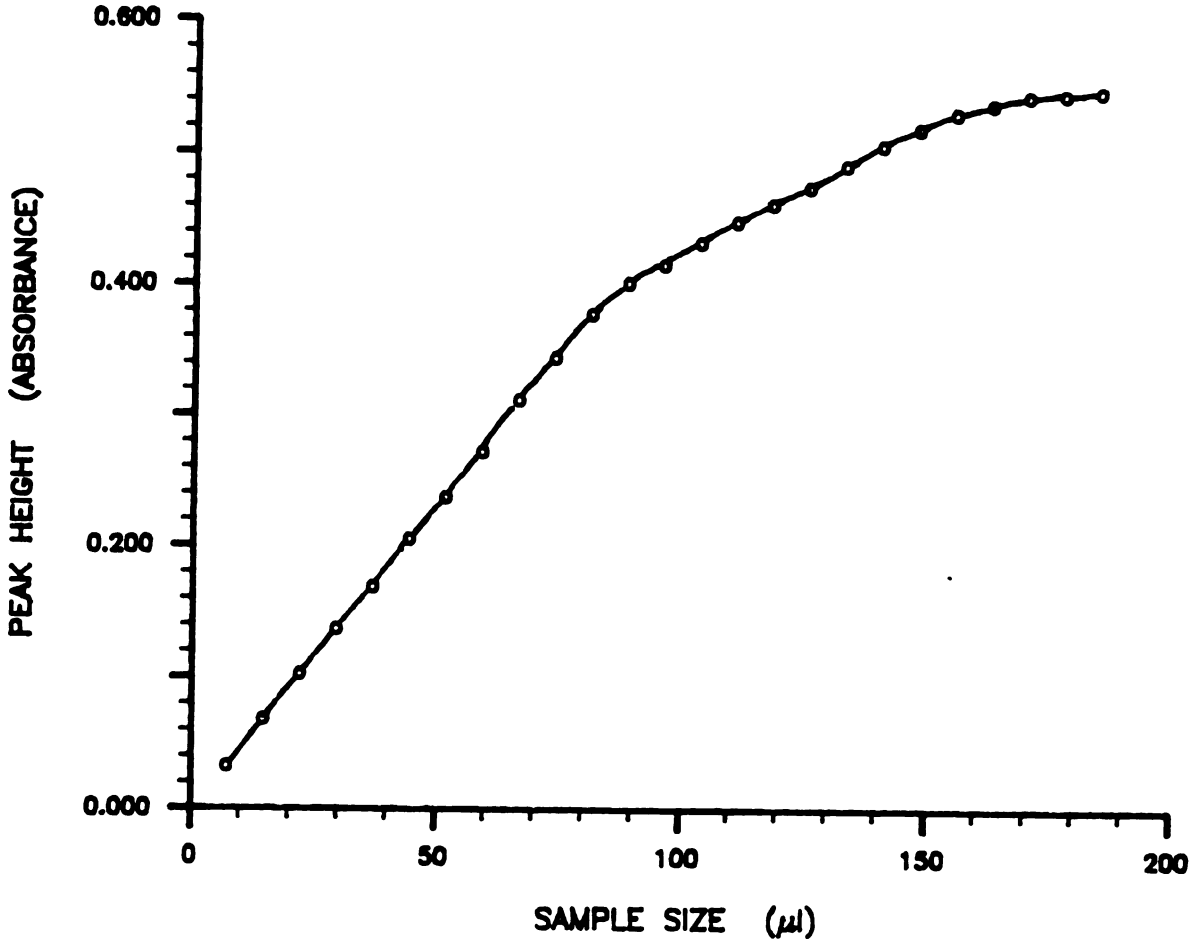

FIGURE 8 Effect of varied glucose sample size.

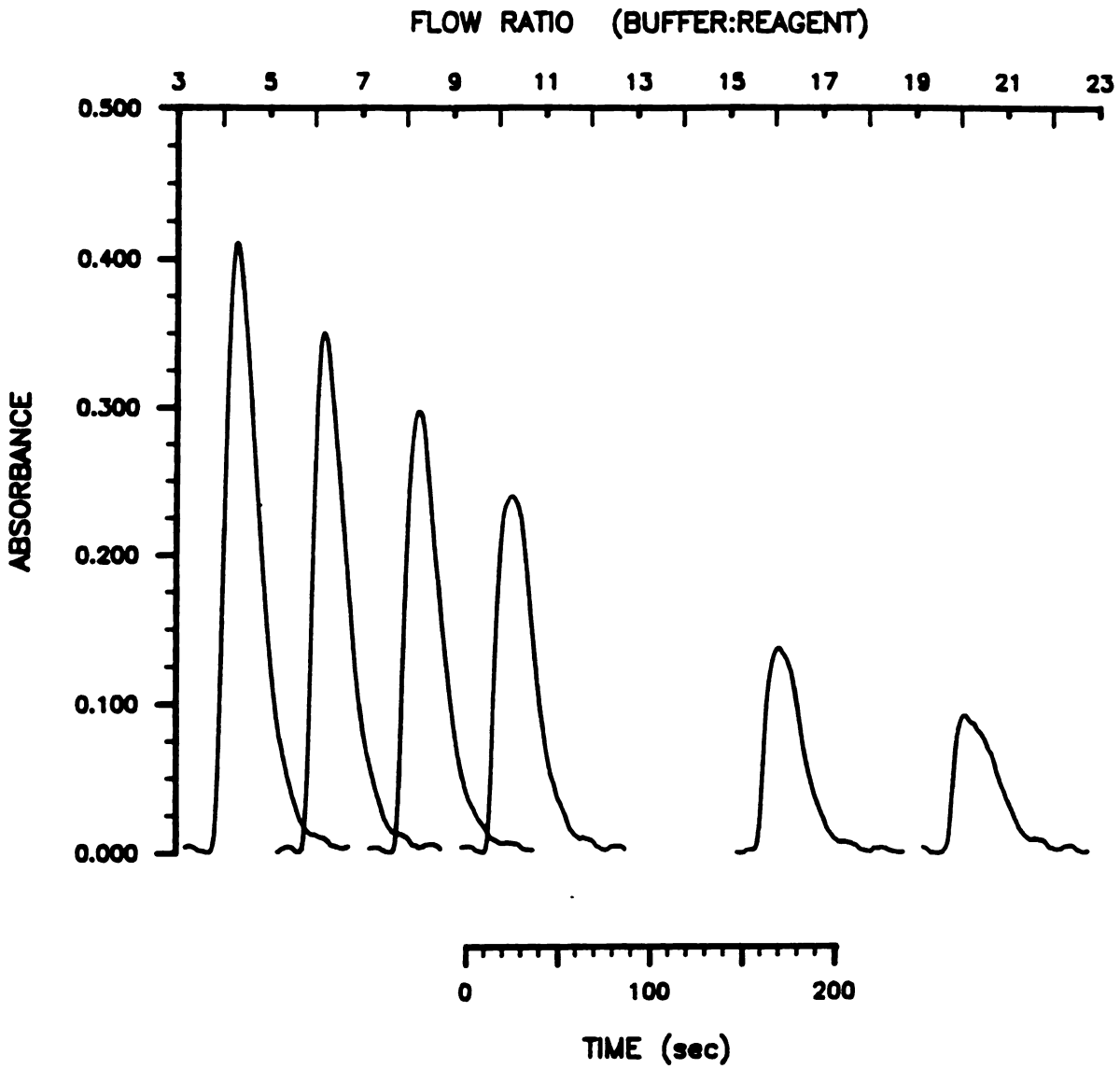

FIGURE 9 Effect of flow ratio (Buffer : Carrier) on FIA profile.

Temperature Calibration

Since it was necessary to control the temperature of the FIA manifold, a method had to be devised to monitor the temperature. The temperature of the solution flowing through the GO SBSR was not the same as that of the water bath. A high precision 30-kΩ thermistor was placed in a thin piece of protective Teflon tubing which was subsequently inserted into a glass tee (see Figure 10). The junction was sealed with Teflon tape to minimize the dead volume and prevent leakage. This temperature probe was calibrated by immersing it in a water bath at the same level as a thermometer. The temperature of the bath was increased in 2° or 3° increments and the resistance recorded after a stable value was reached. The calibration curve is shown in Figure 11. The relationship of resistance to temperature was fitted for 10° segments to the Steinhart-Hart equation ($T^{-1} = A + B*(\ln R) + C*(\ln R)^3$, taken from Reference 57). The resulting coefficients are presented in Table 4. The probe was then connected to the terminal end of the GO SBSR. Once again the temperature of the bath was increased in small increments and the resistance measured. After converting the resistance to temperature, the following linear relationship between the temperature at the end of the reactor and that of the water bath was found: $T = 0.505 * T_B + 11.1$, where T is the temperature at the GO SBSR and T_B is that of the water bath.

Microcomputer Interface to FIA System

Originally an in-house designed (58) Intel 8088-based microcomputer (also known as the "Bruce Bus") controlled the pump speed,

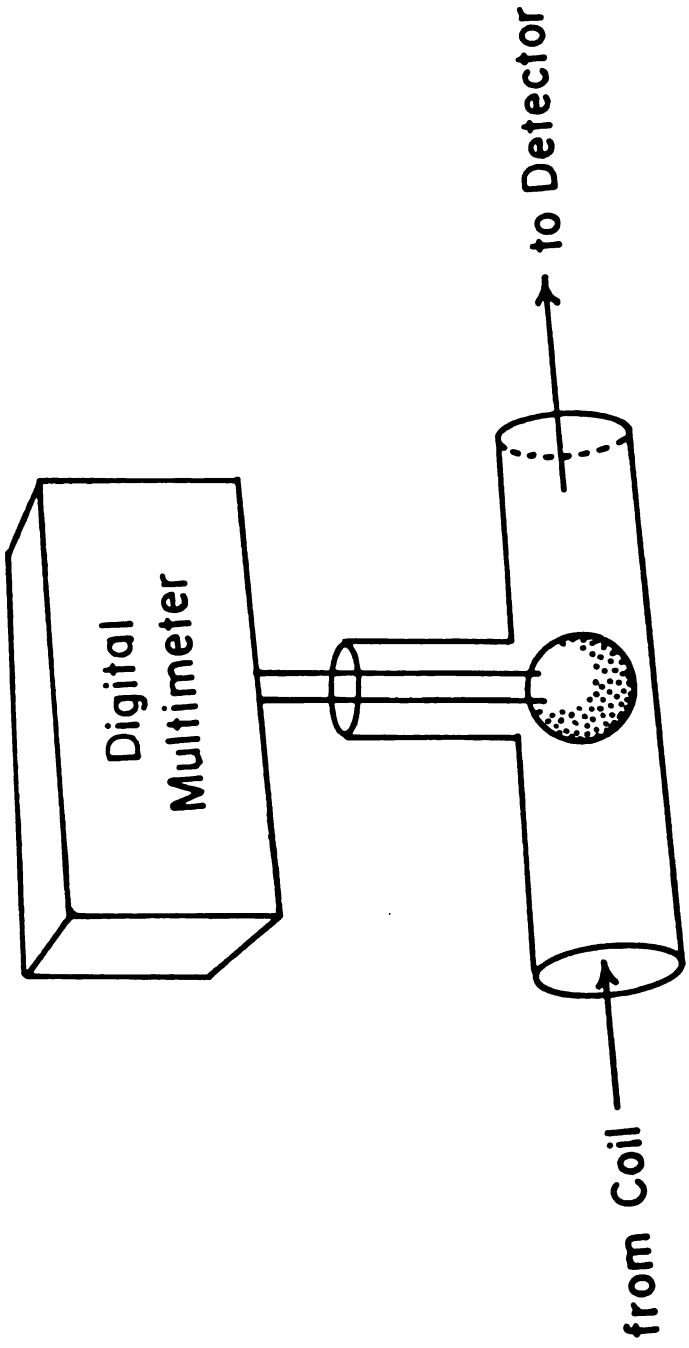

FIGURE 10 T-piece containing 30-kΩ thermistor.

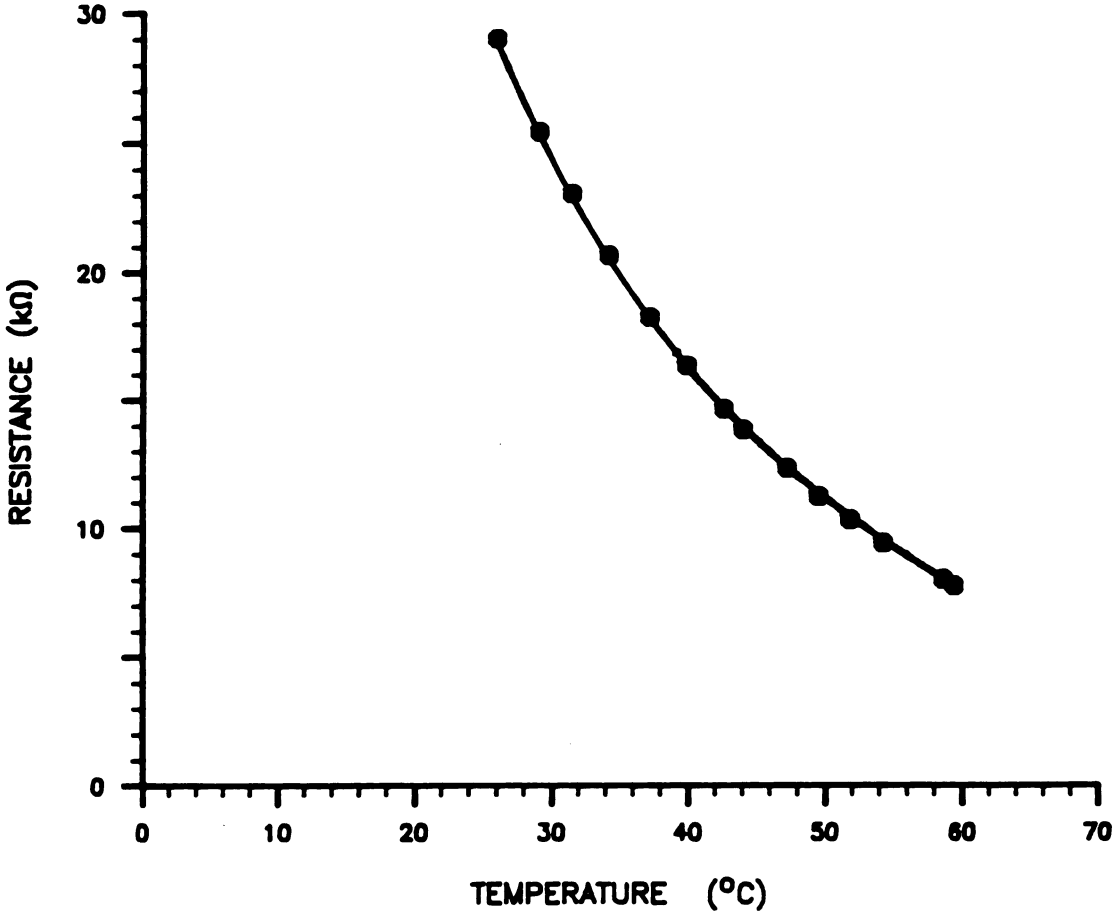

FIGURE 11 Thermistor response curve.

TABLE 4 Coefficients of the Steinhart-Hart equation for different flow rates.

Equation: $T^{-1} = A + B (\ln R) + C (\ln R)^3$

T = temperature R = resistance

Temperature Range (°C)	A	B	C
21-30	0.133	-0.0595	0.00279
31-40	0.0535	-0.0226	0.00159
41-50	0.0358	-0.0145	0.00137
51-60	0.0100	0.00112	0.000527

injection, and data acquisition. The software was written in FORTH (Forth, Inc., Hermosa Beach, CA). Most of the "words" used in this work were strings of "core words" which had been written or modified by Paul Kraus. The final word, "PEAKS", combined injection timing, data acquisition of 100 points over a specified period of time, automatic storage of the data on a floppy, and repetition of the process for a specified number of times. More extensive information on the configuration of the microcomputer can be found in Reference 59.

In the latter phase of the project computer control was relinquished to an IBM PC compatible microcomputer (Bentley-model T). The machine was also Intel 8088-based. It was equipped with two floppy drives, 512 Kb of memory, a color graphics board (IBM), and an RTI-815 interface board (Analog Devices). All routines were written with QuickBASIC (Microsoft). The timing routines were written in assembly and made use of the AM9513A counter/timer that was part of the interface board. Control of the pneumatic actuator on the injection valve was accomplished by connection to a digital output port on the interface board. The data acquisition routines utilized direct memory access (DMA). Plotting routines were developed for three different graphics modes--EGA, CGA, and HERCULES (the HERCULES drivers were provided by Mark Victor, a graduate assistant in the Chemistry department). The initial DMA and plotting routines written by Pete Wentzell, a graduate assistant in the Chemistry department, were modified for this work.

The main program "FIADATA" is a menu-driven program. A number of features were built into the program to make it flexible enough that almost any flow injection analysis experiment could be carried out on

the equipment presently available in the laboratory. One important aspect in this regard is that either the sample output (± 10 V) or the "log-ratio" output (± 1 V) from the colorimeter can be monitored. The gain selection option on the interface board is controlled by the software. The general characteristics of the program are: user-selected experimental parameters, a flow reversals experiment option, data acquisition from one or two channels at a rate selected by the user, immediate data storage on a floppy, screen plots of the data, and printouts of the file containing the data. This program was modified to allow variation of the injection time; "FIAINJ" was the result.

The need also arose for the capability to plot (on the screen) or print data from files previously stored on a floppy. "FIAPLOT" incorporates a routine that will read the data regardless of its format. The only stipulation is that the comments be prefaced with ";" and confined to the beginning lines of the file. By calculating the number of data points and the number of lines of data, the number of columns of data is empirically determined. The user selects which columns of data are to be used for the plot—one x and one or two y values. There is also an option in the program that allows the user to print the data file. Eventually, the three programs may be merged into one large generic program that will do everything but turn the computer on for you.

An interface box was constructed in order to facilitate easy connection to the interface board. The mounts for 50-pin and 34-pin connectors were soldered to the back side of a solderless breadboard. The breadboard was then mounted into an aluminum box along with 6 BNC

and 6 banana plug connectors. The appropriate size ribbon cables were used to attach the box to the interface board. This arrangement provides a versatile way of linking the computer to the analytical system.

Data Acquisition

In either case each experiment involved injection followed by monitoring the output voltage of the detector. Each data point shown in the figures represents the average of the values obtained from 3-5 sequential injections. The baseline voltage was maintained at 5.0 V. The detector voltage was converted to a digital signal by the microcomputer's 12-bit analog to digital converter (ADC). For the in-house built microcomputer the ADC counts were stored in a file on a floppy disk. The files were later transferred to a DEC LSI 11/23 minicomputer, and the ADC values converted to absorbance units after first calculating transmittance values. The software for the PC compatible computer was written such that the absorbance was calculated immediately following the data acquisition period and stored on the floppy. In both cases the resultant data file contained time, absorbance pairs. Further data manipulation was usually carried out on the LSI 11/23.

Improvement of System Performance

The complete FIA system, when first assembled, was functional but it was felt that better sensitivity and sample throughput could be achieved. As mentioned earlier three approaches were used. The first

two approaches were focused mainly toward improving the sensitivity. In essence the goal was to achieve the largest peak absorbance possible. A third approach incorporated the achievement of higher sample throughput as well. In the first and third cases an optimum set of operating conditions was sought for six experimental variables; these were the flow rate, temperature, pH, and the concentrations of PO, AAP,and DCPS.

All solutions were prepared using distilled water (DW) and filtered as necessary. A peroxidase solution was prepared by dissolving 20.0 mg of Horseradish peroxidase (E.C.1.11.1.7, Sigma Type II, specific activity approximately 200 U mg^{-1} at 20°C) in 2.000 ml DW immediately before use to avoid decomposition. The reagent solution consisted of the desired volumes of PO solution, 10 mM 4-aminoantipyrine (Sigma), and 10 mM 3,5-dichloro-2-hydroxyphenyl sulfonic acid (Sigma) mixed together and then diluted with buffer to 10.00 ml in a volumetric flask. The reagent solution was prepared immediately before use.

Glucose (Sigma) standards were made by diluting with buffer the appropriate quantities of a 2 g (α-D-glucose) l^{-1} stock solution that contained 0.5 g l^{-1} benzoic acid as a preservative (the stock solution was stored at 4°C). This stock solution was prepared at least 24 hours in advance so that mutarotation equilibrium was reached. Unless otherwise noted, a 400 ppm (2.2 mM) standard was used. The concentrations of PO, AAP, and DCPS were 0.8 mg ml^{-1}, 1 mM, and 1 mM, respectively, unless otherwise stated.

Phosphate buffer (0.05 M), pH 6.85, was used in the univariate and delay flow experiments. Universal buffer (60) was used in the simplex experiments. Alternative buffers tested in the univariate experiments

were Tris and Borax. The recipes for all but the Universal buffer can be found in the Chemical Rubber Co. Handbook. All experiments were carried out at room temperature (22°C) except, of course, those in which the temperature was varied.

Univariate Experiments

The most common method of optimizing analytical systems is the univariate approach. In this, one parameter is varied while all others are held constant. The six variables mentioned previously were studied by this method.

The flow rate was the first parameter investigated. As can be seen in Figure 12 there is a marked decrease as the flow rate is increased. The flow rate (FR) is related to the pump speed (PS) by the following equation: $FR = 0.0141*PS + 0.00167$. A rate of 0.5 ml min^{-1} was chosen for subsequent experiments. This gave an absorbance that was large enough to give very reproducible results yet small enough that values obtained with more concentrated samples would not be beyond the range of detection. This also allowed an acceptable sampling rate of one per minute.

The effect of the concentrations of the two color-forming reagents was explored. In the initial study the DCPS concentration was fixed at 1 mM while the concentration of the AAP was varied from 0.1 mM to 2.0 mM. The AAP/DCPS ratio that gave the best results was 1:2. This was found to be the case for pH values between 6.0 and 8.6 as evidenced in Figure 13. From the reaction stoichiometry one would assume that the ratio ought to be 1:1. This caused suspicion as to whether or not the

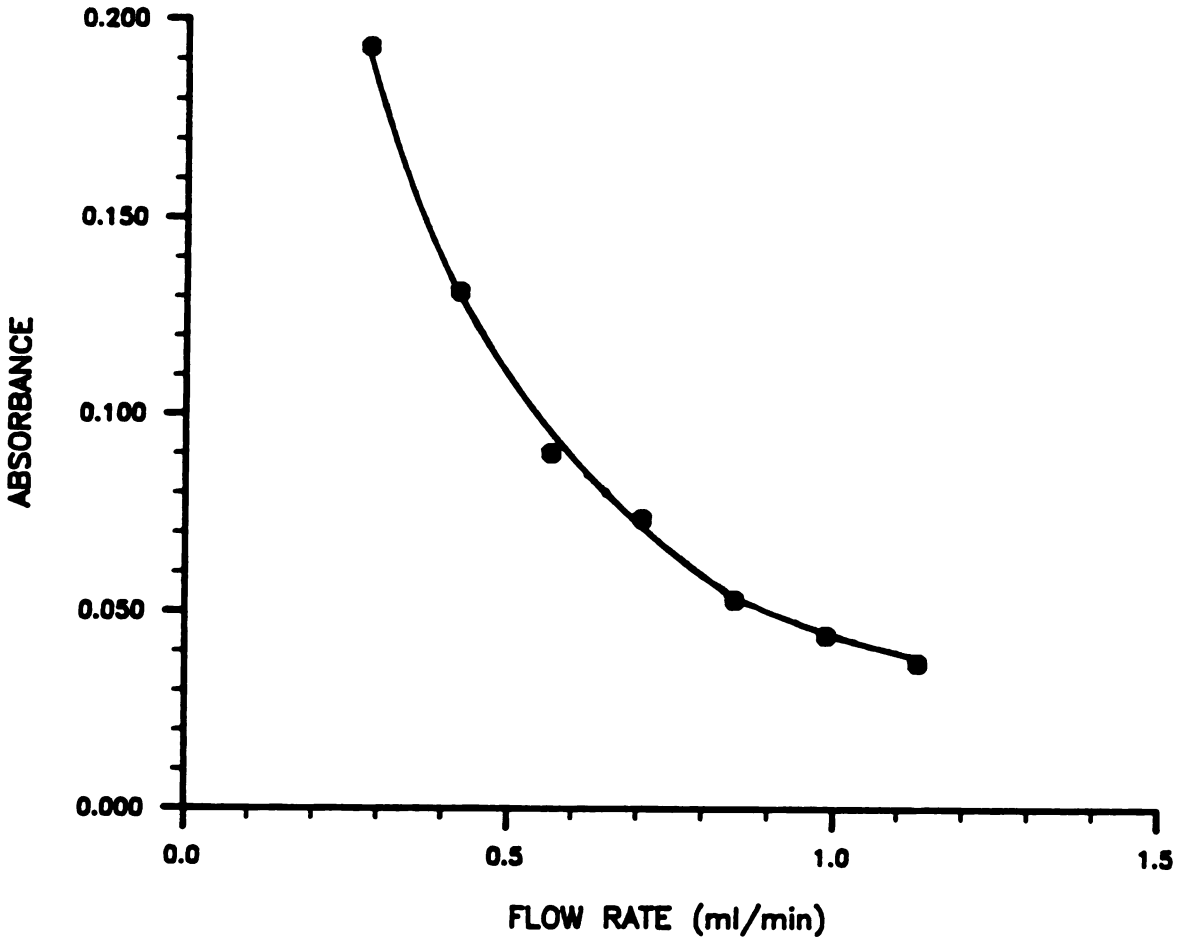

FIGURE 12 Effect of varied flow rate.

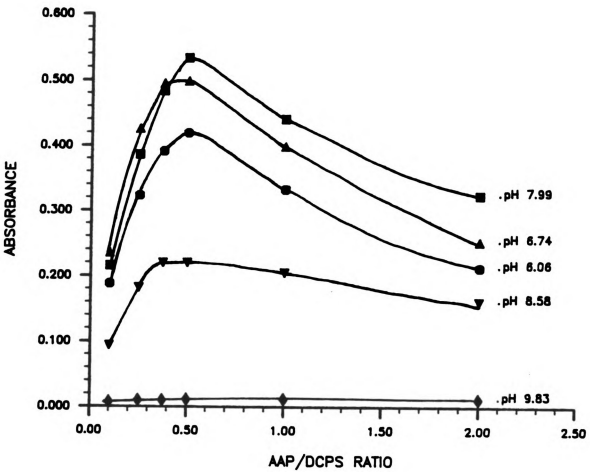

FIGURE 13 Effect of AAP/DCPS ratio.

dye was really formed by the binding of one AAP molecule to one DCPS molecule.

The possibility was entertained that the initial compound formed might be 1:1 with later addition of another DCPS. Inspection of the proposed dye compound structure would suggest that this is not highly likely since the addition of another DCPS would be sterically hindered. To rule out this possibility the diode array detection system developed by Mark Victor (61) was connected in place of the colorimeter. Spectra were acquired every second as the reacted sample plug passed through the flow cell. It was assumed that a change in the structure of the complex (formation of more double bonds) would cause a shift in the absorbance maximum. The ends of the plug, where the greatest amount of reaction occurs, seemed the most likely place for this effect to present itself. However, as shown in Figure 14, there was no detectable shift in the absorbance maximum over the entire plug.

Next, a continuous variations experiment seemed in order. The combined concentration of the two reagents was kept at 2.0 mM. Ratios of 2:1 through 1:6 (AAP:DCPS) were investigated. The highest absorbance was obtained for the 1:4 ratio. This ratio is very different from the one obtained earlier, but the AAP concentration is similar (i.e., 0.4 mM compared to 0.5 mM). Since the aminoantipyrine is considered the two-electron donor for the peroxidase (62), its concentration should be the critical factor. This is corroborated in these studies. The results also imply that for a reagent solution 0.4 mM in AAP the DCPS concentration must be at least 1.0 mM. From these experiments it is

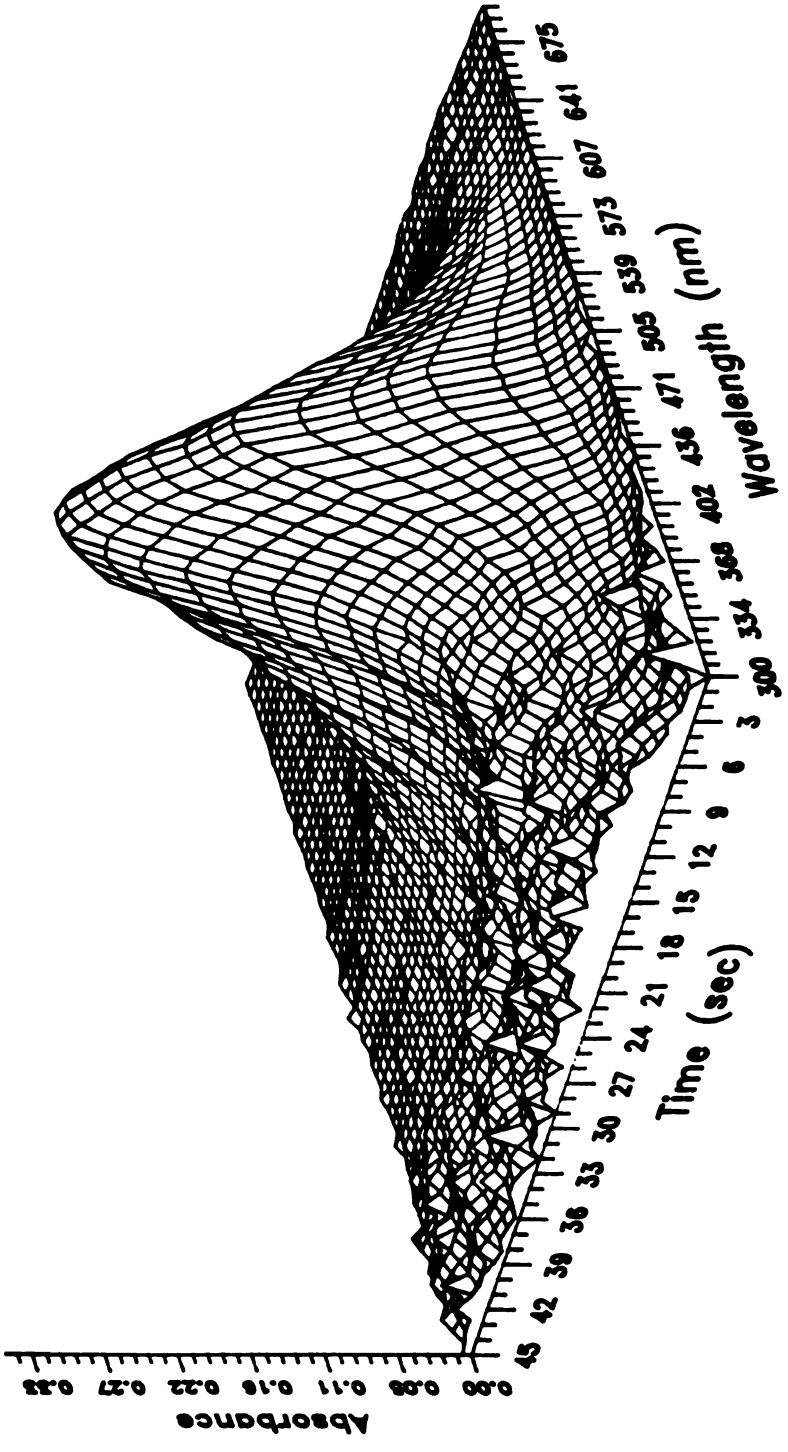

FIGURE 14 Three dimensional surface of the FIA peak for the Trinder reaction.

also apparent that there would be no great advantage in increasing the total concentration of the reagents.

The peroxidase concentration was varied from 0.05 mg ml^{-1} to 1.0 mg ml^{-1}. An 800 ppm standard was used so that the results would reflect the maximum amount of PO necessary for the range of standards normally used for calibration. A plateau region emerged as the concentration approached 0.8 mg ml^{-1} (see Figure 15). At this point a small variation in the PO concentration would not drastically affect the absorbance obtained. Since such small amounts of peroxidase are used on a daily basis it is desirable to operate in that region.

The investigation of the effect of pH was twofold. First, the type of buffer had to be determined. The four types of buffer listed above were each made to be pH 8.00, since that is in the working range of each. The experiment was conducted in the usual fashion. The phosphate and Universal buffers gave equal absorbance values while the Tris and Borax buffers proved to be less than 1. Because the Universal buffer has such a wide working range (pH 5.00-10.00) it was used for the second part of the study. The pH was varied from 5.00 to 10.00 in 0.50 increments. The results shown in Figure 16 indicate a pH optimum at 7.50. For the purpose of comparing this optimum to that obtained with other buffers, another set of experiments was carried out in which phosphate and Borax buffers were used to cover the range of pH 6 to pH 10. The maximum response was obtained at pH 7 (see Figure 17). It can be concluded from this study that the glucose oxidase/Trinder reaction is quite sensitive not only to the pH of the buffer but to the type of buffer used as well. The optimum values

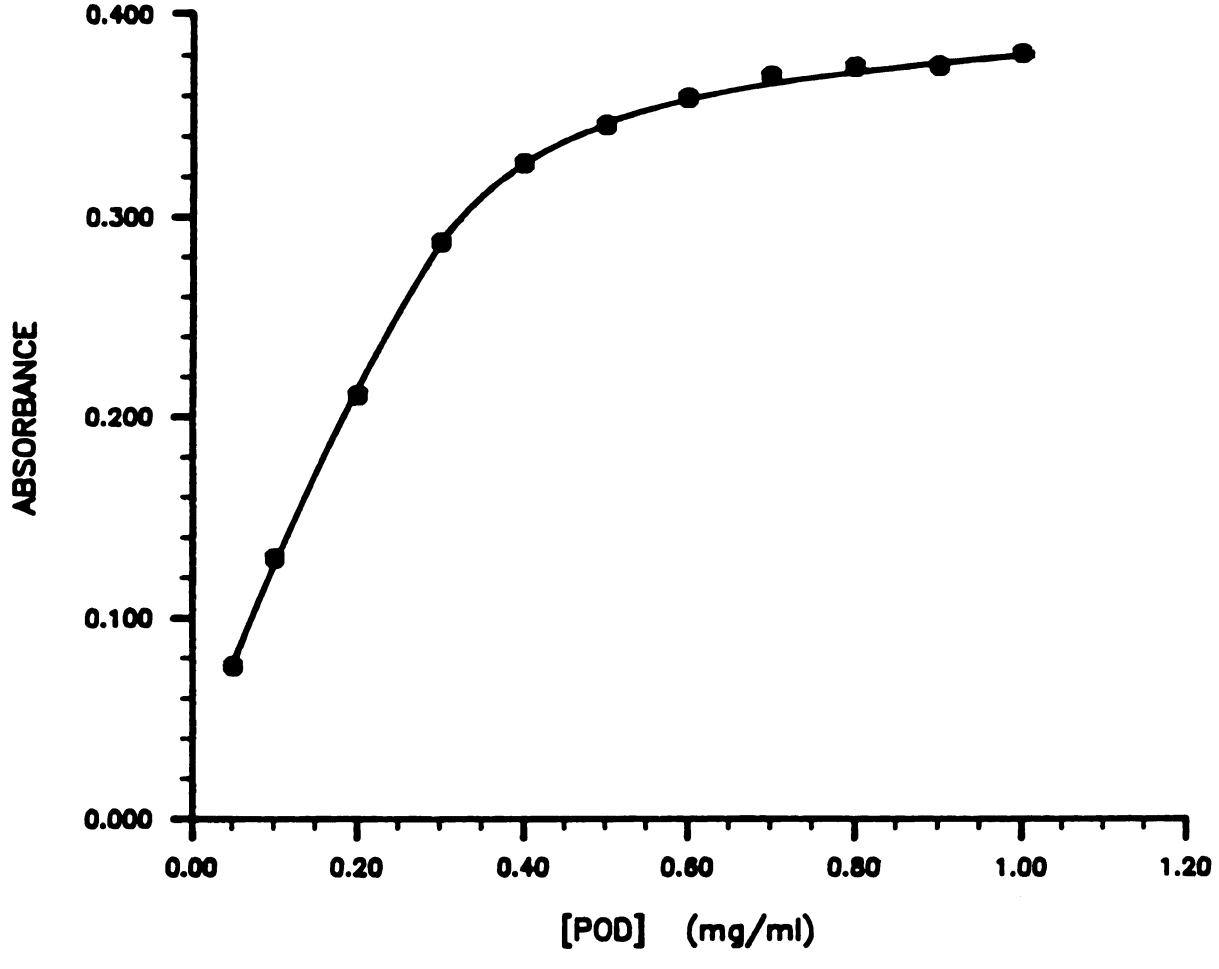

FIGURE 15 Effect of peroxidase concentration.

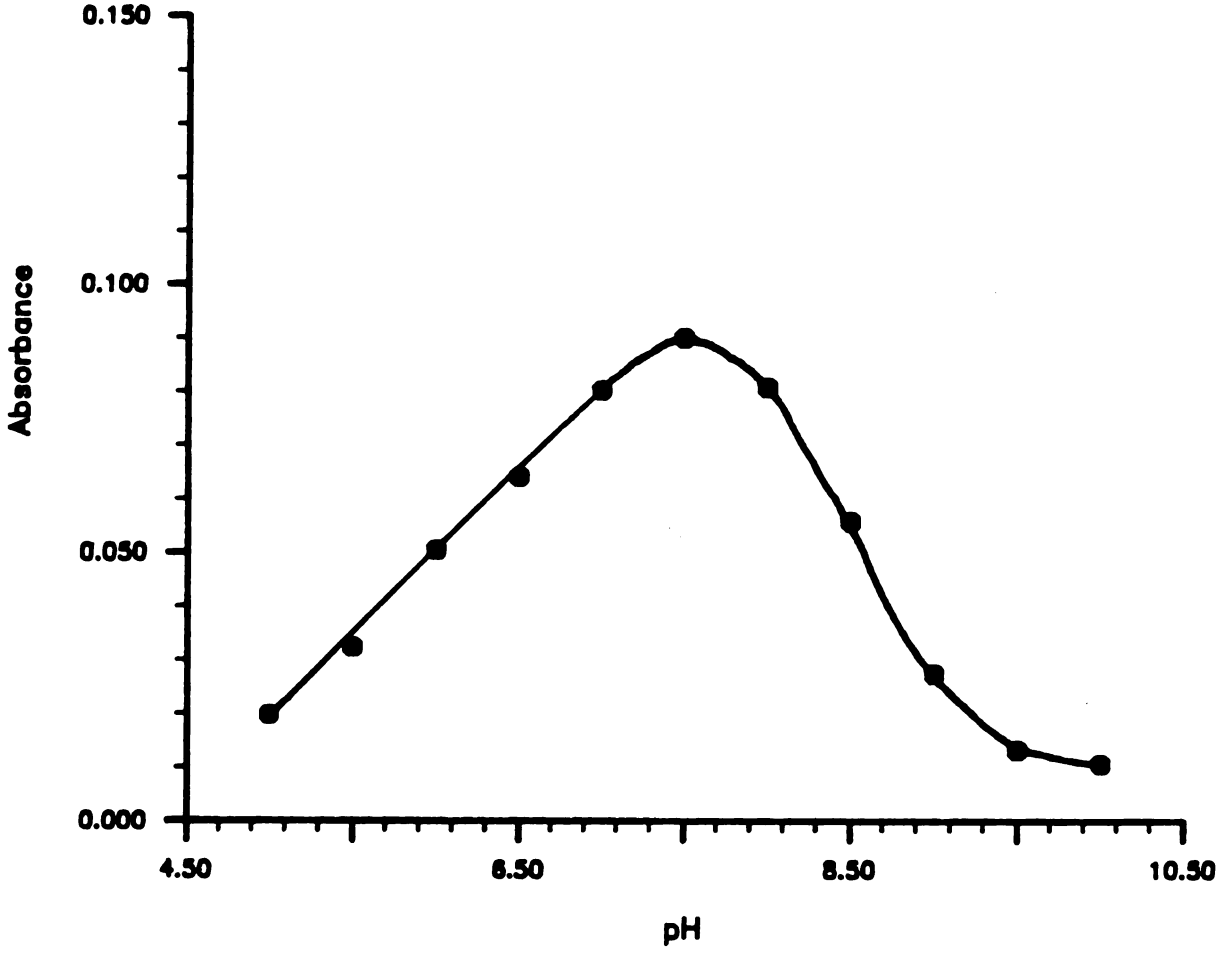

FIGURE 16 pH dependence of GO/Trinder reaction with Universal buffer.

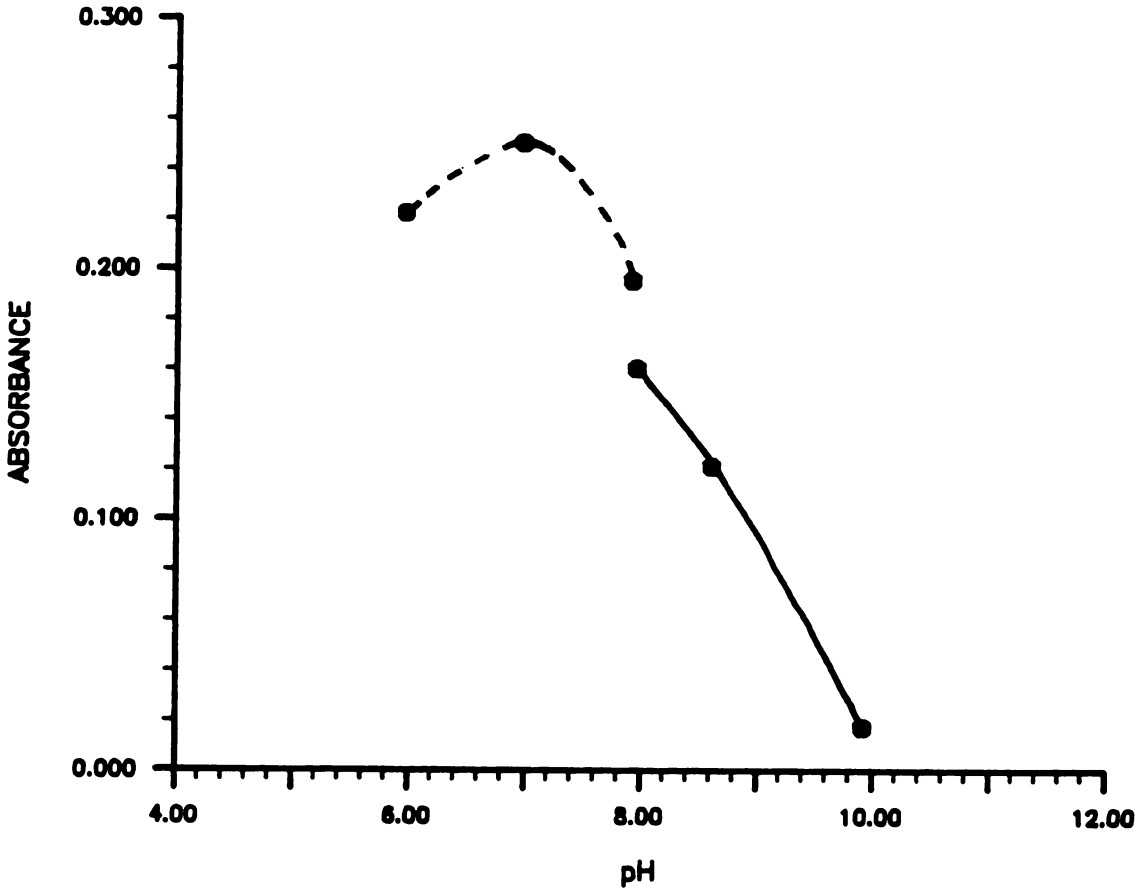

FIGURE 17 pH dependence of GO/Trinder reaction with phosphate (- -) and borax (—) buffers.

obtained here are slightly higher than the pH optimum for glucose oxidase in solution (63). This will be discussed below.

The final variable examined was the temperature of the GO SBSR. It should be noted here that the temperature of the color-forming reaction was varied over the same range as that used for the glucose oxidase reaction and no significant improvement was attained. This demonstrates that the reaction is fast compared to the time required for the reacted sample to traverse the manifold. Since it is well known that enzymes are prone to denaturation above 37°C the operational temperature range was from room temperature (21°-22°C) to a few degrees beyond this upper limit. The bath temperature was adjusted and the components were allowed to come to thermal equilibrium before the sample was injected. The response obtained increased with temperature as illustrated by the plot in Figure 18. Between 31°C and 38°C a plateau region exists, where the response is at its maximum value. Beyond 38°C the response decreases rather rapidly because of enzyme denaturation.

A complete set of univariate experiments would have involved going back to each variable systematically in order to determine a true set of optimum conditions. If such an approach were used to evaluate the optimum to within 20% in each of seven dimensions (an additional variable is created when the pH of the carrier stream is separated from that of the reagent stream), for this FIA system a total of 175 experiments would have been required. Since a great amount of time was expended in this small set of experiments, an alternative to this method was sought.

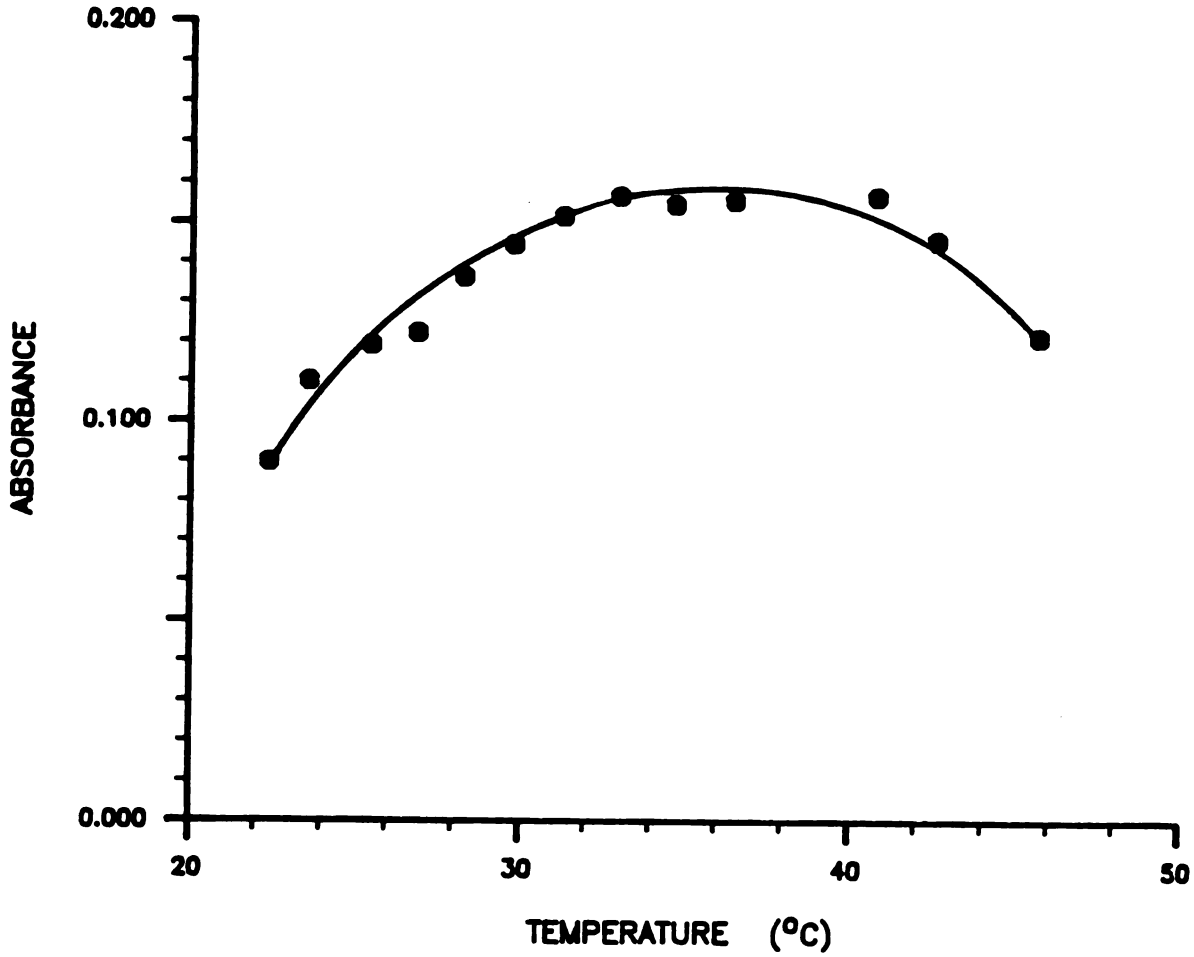

FIGURE 18 Temperature response of a 10 — cm GO SBSR.

Delay Flow Experiments

This second approach focused solely on increasing the absorbance obtained with a 400 ppm standard. Based on the results of the univariate experiments a standard set of conditions was defined: 0.5 ml min^{-1}, 22°C, pH 6.85, 1 mM AAP, 1 mM DCPS, and 0.8 mg ml^{-1} PO. By integrating the FIA peak it was found that the total absorbance obtained corresponded to conversion of 7.3% of the total amount of glucose in the sample. It was therefore suspected that significant increases could be attained by stopping the flow after the entire sample plug occupied the GO SBSR. It was thought that a delay time would allow as much reaction to occur as possible before the flow was resumed.

A preliminary study was used to determine the time at which the pump was to be stopped. The sample was injected and the pump was stopped at various times, while the delay time was kept constant at 10 s. Then the pump was restarted. The greatest response was obtained when the pump was stopped after 10 s.

The stop time was then set at 10 s and the delay time varied. Data acquisition times were adjusted to ensure complete recording of the signal. Figure 19 shows that the maximum response can be obtained when the flow is delayed for 10 s. The decrease in absorbance for longer delay times is probably due to the destruction of hydrogen peroxide; as the sample is in the reactor for a longer period of time there is a greater probability that the peroxide will come into contact with catalase and, thus, be reduced. This method only served to increase the sensitivity of the system and actually decreased the possibility of

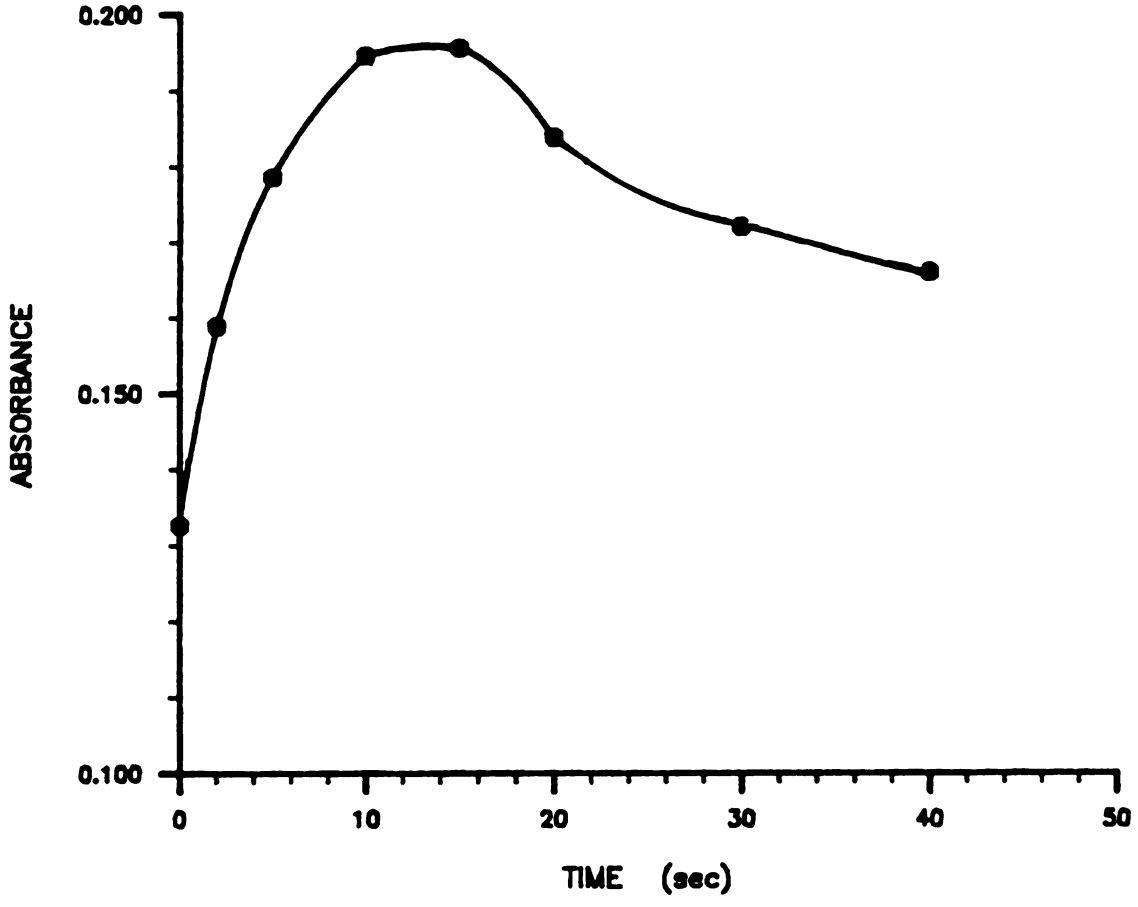

FIGURE 19 Results from delay flow experiment.

greater sample throughput. Therefore, an alternate method of optimization was sought.

Simplex Optimization

The underlying assumption in a set of univariate experiments is that there is no interaction between variables. If there is indeed some interaction a false set of optimum conditions may be found. Alternatively, a pattern search could have been used to determine the response surface for the seven variables investigated here. Under these conditions 78,125 experiments would have been required. A better alternative than these methods has been shown to be a simplex optimization (64), which allows simultaneous variation of all parameters.

The simplex method is widely applied and accepted in analytical chemistry (65). A simple two dimensional surface, as pictured in Figure 20, can be used to illustrate the principles employed. The x and y axes represent the two parameters to be varied and each concentric circle represents combinations of those two which give the same response. This surface can be thought of as a topographical map; as the circles get smaller the response increases in magnitude. The simplex is generated initially by choosing a set of experimental conditions which are known to be suboptimal. After the response from that experiment is obtained another set of conditions is specified. This process is repeated until the geometric shape made of n+1 vertices is obtained, where n is the number of parameters. In the two-parameter case, three experiments are required and the simplex takes the shape of a triangle.

The response at each vertex is ranked based on its magnitude—the largest is taken as best, the next largest as next best, etc. In the triangular case, the point that gives the worst response (point 1 in the figure) is reflected an equal distance through the line between the other two points (points 2 & 3). A new set of conditions is specified, the response obtained, and the responses are again ranked. In this example, the response surface is shown so that the movement of the simplex can be understood. Normally, the response surface is unknown and becomes defined by the movement of the simplex. As the optimum set of conditions is reached the simplex may begin to oscillate. Such behavior can be thwarted by reflecting the next best point rather than the worst.

The history of the simplex methodology (adapted from Reference 66) is summarized in Figure 21. Since the pioneering work of Morgan and Deming (67), many modifications have been suggested which attempt to improve upon the speed and reliability of the method. These have been reviewed elsewhere (68). For this work, the method chosen was the Composite Modified Simplex (69). This method has additional features such as expansion when the optimum is far away and smaller movements when the optimum is near. The composite modified simplex program (OPTIMA--written in BASICA) was provided by Betteridge and Wade (70). Simplex optimization was previously attempted on the original Trinder reaction in a static system (71), however, no optimum was found.

It has been shown that a judicious choice of a response function can expedite the optimization process (72). Such a response function allows a number of FIA parameters to be optimized simultaneously, and

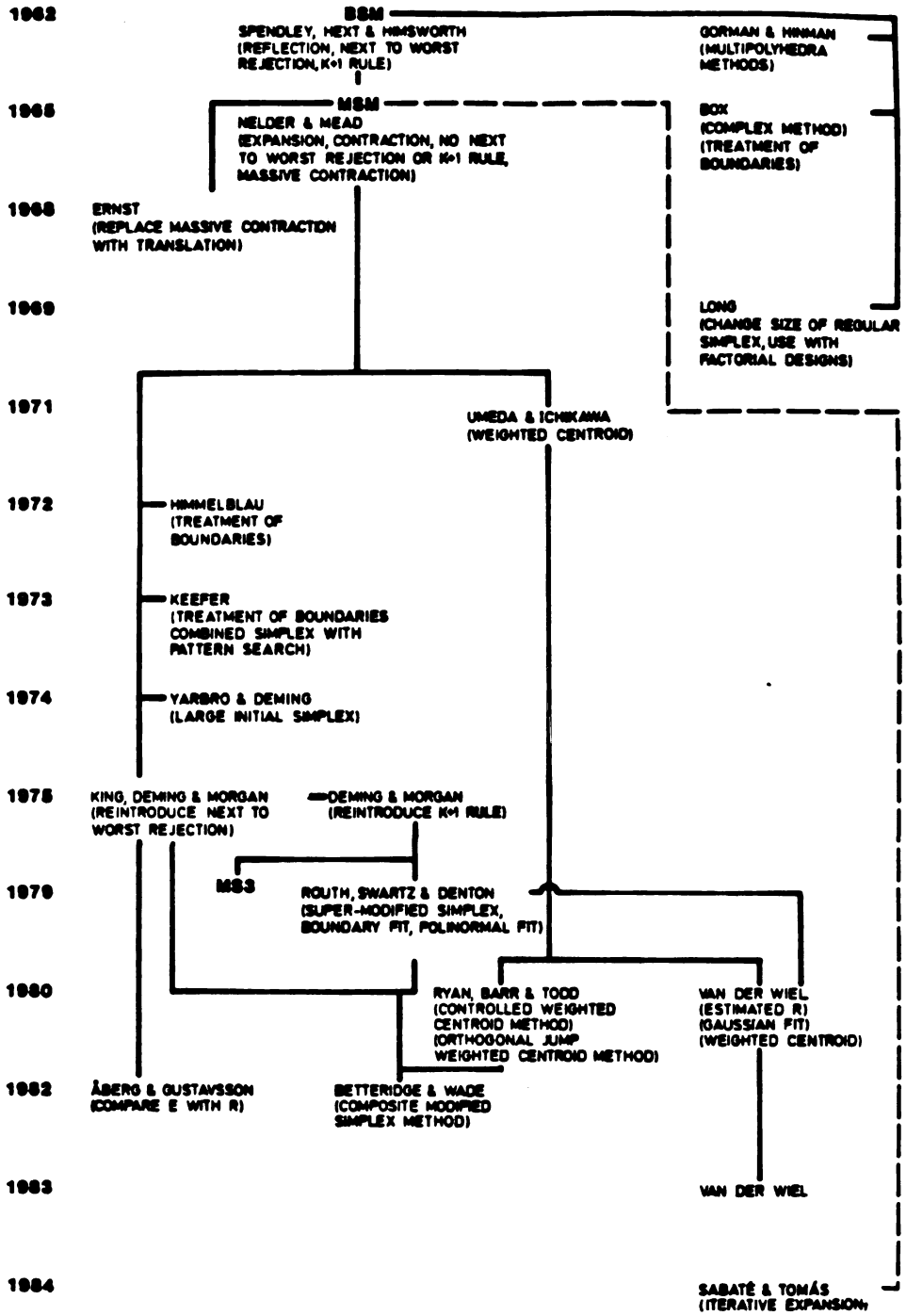

FIGURE 21 History of simplex optimization.

takes the form of a mathematical equation that combines two or more system parameters (peak height, cost, throughput, etc.) in an appropriately weighted fashion.

The response function chosen was based on three considerations. First, the activity of the enzymes involved changes over long periods of time; second, the achievement of a sampling rate of at least 60 hr^{-1} was desired; finally, the sampling rate factor should contribute no more than 30% to the overall response. The function chosen was:

$$\text{Time Corrected Absorbance Ratio} = \frac{80\ s}{60\ s + t_p} \times \frac{A_{exp}}{A_{base}}$$

where A_{exp} = Absorbance at peak maximum for a set of experimental conditions, A_{base} = Absorbance at peak maximum for the baseline set of conditions, and t_p = time (sec) after injection at which the peak maximum occured.

The initial simplex was obtained by entering the information listed in Table 5 into the composite modified simplex program. The simplex program was run on an IBM PC compatible microcomputer (PC Designs) while data were acquired with the Bruce Bus microcomputer. From the univariate experiments that were done prior to this optimization, acceptable ranges for each of the parameters were identified. The settings listed under "Reverse" are those which gave low absorbance values and those under "Forward" gave high absorbance values.

Some other considerations played a role in this decision making process as well. The minimum pump setting (flow rate) indicates that a minimum sampling rate of 24 per hour was required. The bath temperature

TABLE 5 Range and precision of variables for simplex optimization.

Experimental Variable	Foward Boundary	Reverse Boundary	Precision
Pump Setting	99	20	1
Bath Temperature (°C)	21.0	51.4	0.2
[POD] (mg ml^{-1})	0.05	1.0	0.02
[AAP] (mM)	0.1	2.5	0.01
[DCPS] (mM)	0.1	2.5	0.01
pH Carrier, Sample	10.00	5.00	0.02
pH Reagent	10.00	5.00	0.02

was bounded at the low end by room temperature and at the high end by 37°C--the maximum temperature shown to be advisable for use with this enzyme. The high end of the PO concentration was set at 0.8 mg ml^{-1} since it was desirable to limit the cost of the experiments and this concentration was in the plateau region described previously. The upper limit for the AAP and DCPS concentrations was such that if both were used in their highest concentrations the reagent solution composition would be no more than 25% (v/v) in each. The pH of the carrier and sample was made independent of that of the reagent since it was unknown whether the two reactions would have different optimal pH values. The range for each was selected on the basis that the working range of the Universal buffer is between pH 5.00 and pH 10.00.

The initial (baseline) conditions listed in Table 6 were known to be suboptimal, but exhibited acceptable reproducibility (1% RSD). It was found that a 400 ppm glucose standard, when used with a new GO SBSR, gave a maximum absorbance value that was in the middle of the detectable range and was, therefore, suitable for use in the optimization.

Since there were seven variables, eight experiments were needed to form the initial simplex. These were performed and the results entered. The first point of the simplex was the response obtained from the baseline experiment with the initial conditions. Thereafter, each time the simplex program specified a set of experimental conditions, this experiment was performed and the time-corrected absorbance ratio was calculated and entered. In reality two experiments were done in order to obtain the response for one set of conditions: one at the specified conditions and the other at the baseline conditions.

TABLE 6 Initial and optimal experimental conditions for the FIA determination of glucose.

	Exp. No.	Flow Rate ml min^{-1}	Temp. (°C)	[POD] mg ml^{-1}	[AAP] (mM)	[DCPS] (mM)	pH Carrier	pH Reagent	Time Corr. Abs. Ratio
Start	1	1.13	22.2	0.20	0.50	0.50	9.00	9.00	1.11
Top 6	59	0.52	32.8	0.94	0.27	1.34	7.18	8.10	25.0
	63	0.57	31.8	0.78	0.51	1.14	6.78	8.42	19.7
	65	0.64	28.5	0.60	0.58	1.20	7.24	8.52	19.1
	66	0.52	35.6	0.88	0.27	1.48	7.49	8.36	23.2
	68	0.54	29.5	0.74	0.49	1.22	6.62	8.32	19.9
	70	0.57	31.7	0.80	0.34	1.26	6.46	9.02	20.1
Average Optimum for top 6		0.57	31.6	0.79	0.41	1.27	6.96	8.46	21.2
Std. Dev. for top 6		0.05	2.5	0.12	0.13	0.12	0.40	0.31	2.4

The simplex rapidly improved the response at first. This was followed by a more gradual increase and then a plateau region as diplayed in Figure 22. This same pattern has been observed and explained elsewhere (73). After twenty-seven experiments, the data suggested that a "false maximum" had been found in experiment nine. To check this, that particular experiment was repeated and was found to be in error. The simplex was restarted with the original values for the first eight experiments and the new value for the ninth. After the thirtieth experiment with the new simplex it was intuitively felt that the rate of improvement might be enhanced by use of a simplex that was larger in the dimensions of temperature and PO concentration. Further optimization was carried out using the current simplex points, but replacing two of those experiments with two experiments at higher temperatures and/or POD concentrations.

The optimization process was terminated when an optimum set of conditions was deemed to have been reached. Since the composite modified simplex method is a search procedure in which contraction around a maximum will take place, it is likely that there will exist several sets of conditions in the final data set that are near a true surface maximum. By taking the average of the values for each of the parameters for the experimental conditions that gave the six largest time corrected absorbance ratios (i.e., those yielding a response that was 75% or more of the largest value found), a rough measure of the width of the optimum in each dimension was possible. These results are given in Table 6.

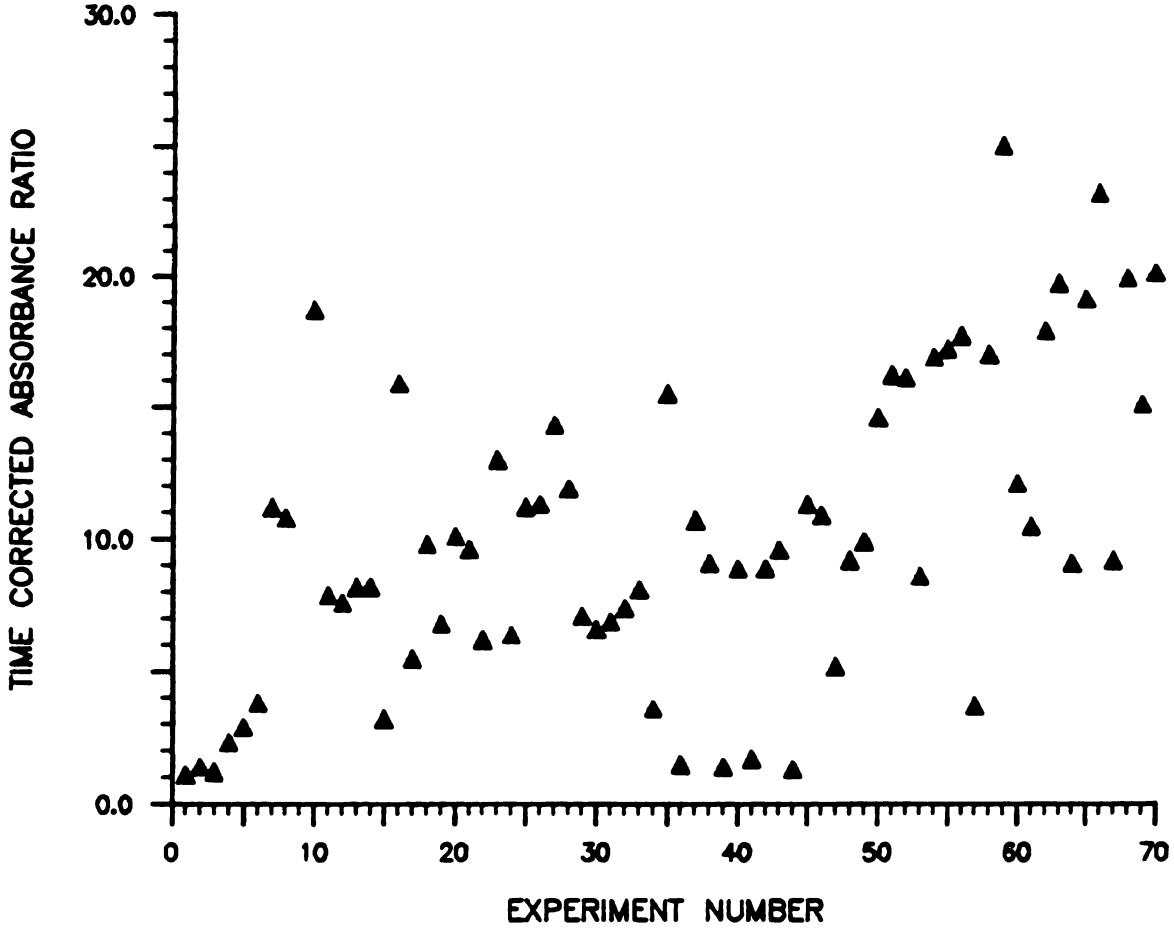

FIGURE 22 Progress of the simplex.

The values for the response function obtained for each of the seventy experiments are plotted against each of the seven variables individually. The diagrams in Figure 23 show the results. These diagrams should not be viewed as univariate experiments, because they represent experiments in which all variables are changed. For this reason, they are often called "scatter diagrams". From the conditions giving best responses and the trends in the scatter diagrams several observations can be made.

The pH of the carrier and sample showed a maximum around pH 7 (Figure 23a). This result agreed quite well with previous univariate experiments. The discrepancy between the optimum for the immobilized species and that for the soluble species may have been due to the difference between the pH of the bulk solution and that seen by the enzyme. Since the flow ratio of the carrier to the reagent stream was 10:1, it is suspected that the carrier pH would predominate and could therefore be reasonably compared to the one pH used in the univariate experiments. The optimum reagent solution pH (Figure 23b) was also found to be higher than that considered optimum for PO in solution (74), however, it is known that that the optimum is dependent upon the particular substrate and type of buffer used (75). The dilution factor may also have played a role in this. Some of the mystery concerning the real value of the pH in the manifold could be cleared in the future by inserting a micro-electrode at various points in the stream.

By inspection of the plot for the variation of flow rate (Figure 23c), a maximum response is obtained at 0.56 ml min^{-1}. This trend is not like the steadily decreasing response found in the

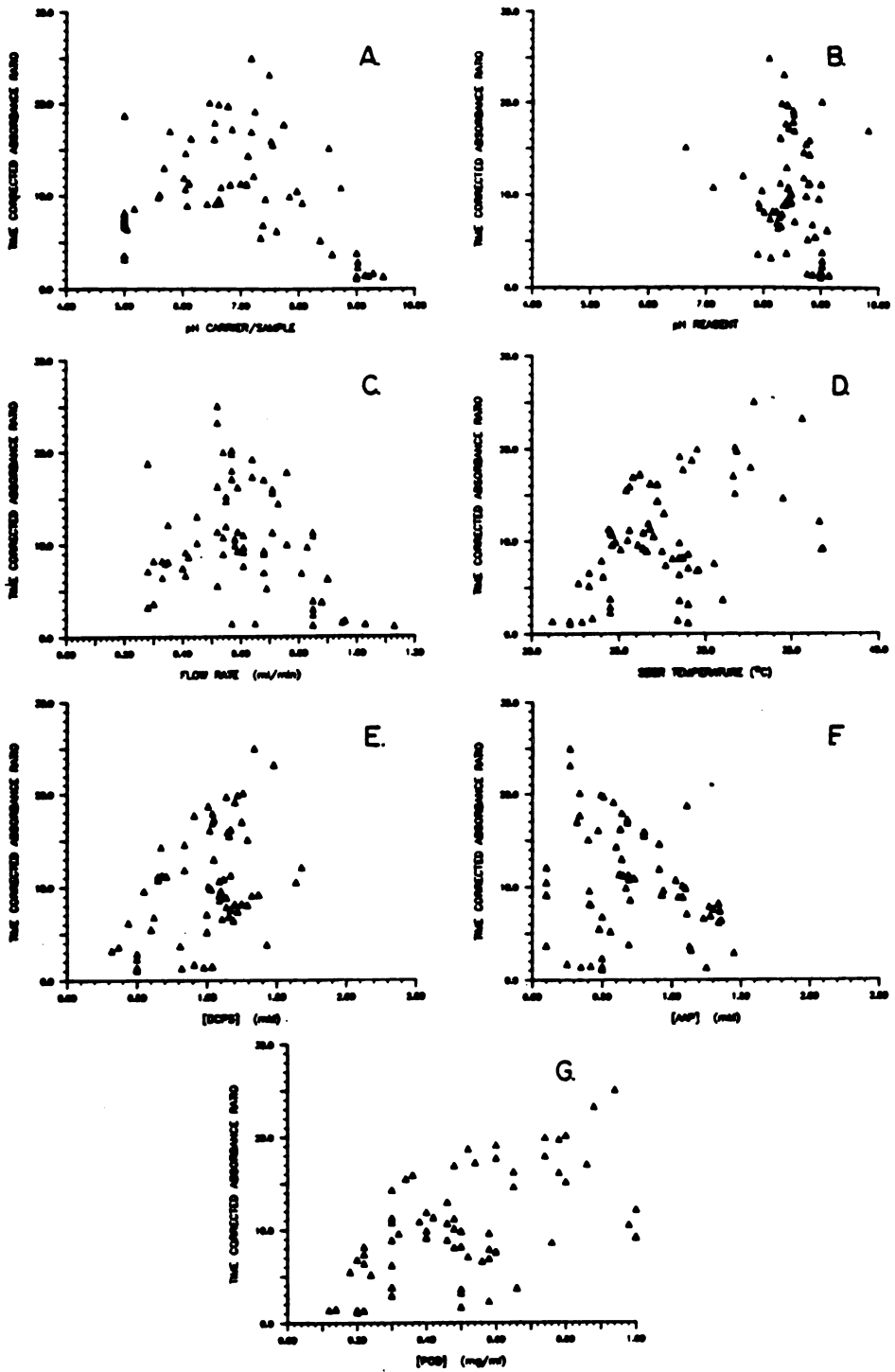

FIGURE 23 Effect of experimental variables on response function: (a) carrier pH; (b) reagent pH; (c) flow rate, ml min^{-1}; (d) SBSR temperature, °C; (e) DCPS concentration, mM; (f) AAP concentration, mM; (g) PO concentration, mg ml^{-1}.

univariate experiments. The nature of the response function accounts for this since a time factor was included.

The behavior of the response as a function of temperature (Figure 23d) did not differ markedly from what was expected and was very similar to the univariate results; there was a steady rise followed by a plateau region. A rise in temperature would be expected to increase the rate of the reaction. Modelling studies have suggested that it may also decrease the dispersion (73) thus giving higher peak heights (this issue is addressed in Chapter 6). There was no evidence of major interaction between temperature and other variables in the system.

In this case also the effect of changing the concentrations of the DCPS (Figure 23e) and AAP (Figure 23f) was significant. The results showed that the optimum ratio of the two was approximately 3:1. Once again the optimum AAP concentration was found to be between 0.4 mM and 0.5 mM and the DCPS concentration was slightly greater than 1.0 mM. The PO concentration was also found to enhance the response (Figure 23g) in a manner similar to that found in the univariate case, and exhibited a typical Michaelis-Menten shaped curve.

The performance of the system (as measured by the magnitude of the response function) was improved by a factor of 22.5 (over the initial conditions). A calibration curve obtained at the optimum conditions was linear from 0.1 to 3.3 mM glucose and usable from 0.1 to 5.5 mM glucose with the reagent concentrations specified. A comparison of the calibration curve obtained with the simplex optimum conditions is compared to that obtained with the univariate optimum conditions in Figure 24. The slope for the simplex case is higher, but the linear

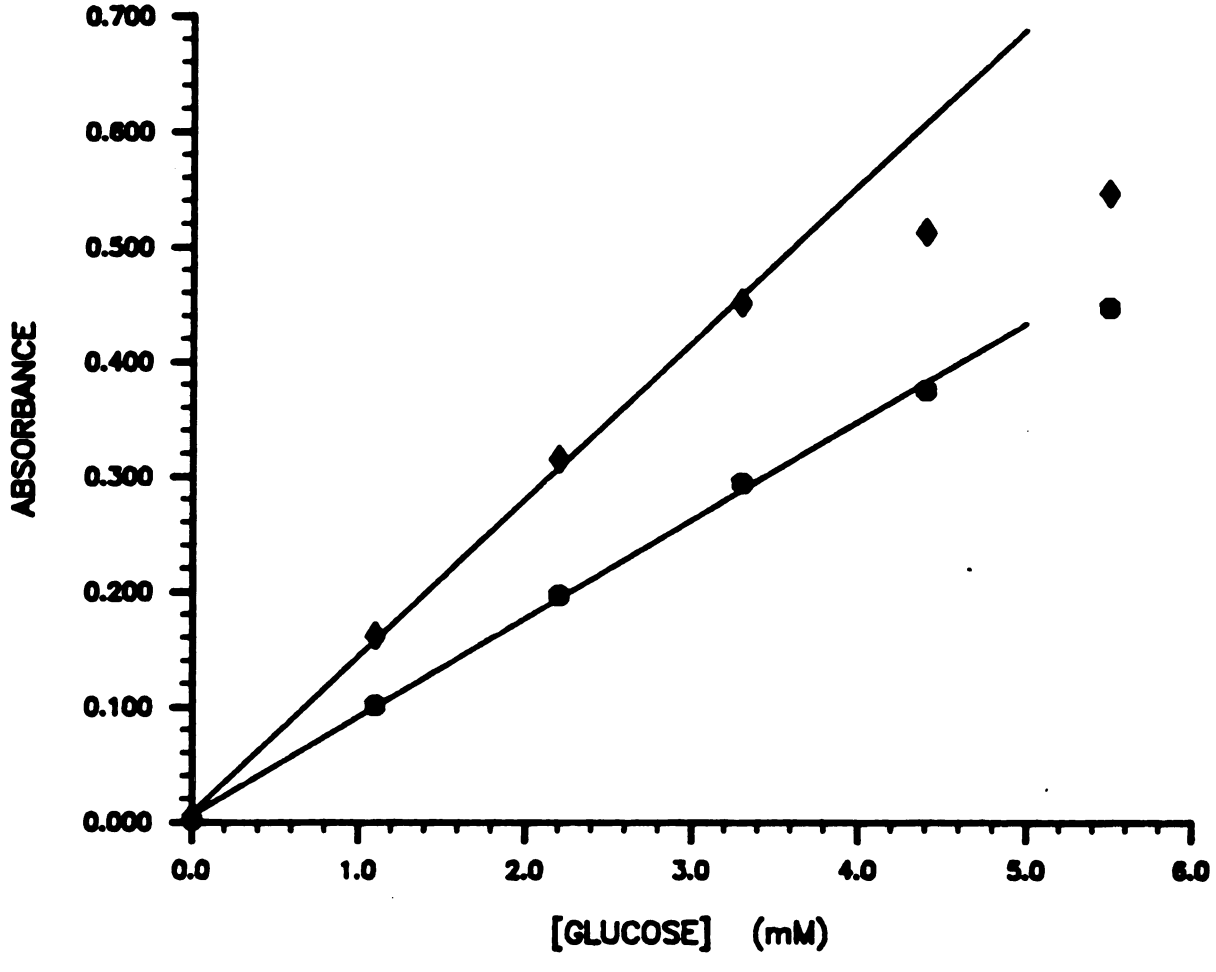

FIGURE 24 Calibration curves for optimum operating conditions arrived at by simplex optimization (♦) and by univariate experiments (●).

range for the univariate case is larger. It becomes a trade-off between the capacity to determine the concentration with high precision and the alternative capacity to analyze samples that have a wide range of concentrations. For the analysis of food samples the latter choice is appropriate. The former choice would be appropriate for clinical determinations where a narrow range of glucose concentrations is found.

CHAPTER 5

EXTENSIONS OF THE GLUCOSE OXIDASE FIA SYSTEM

After having gained a considerable amount of knowledge concerning the optimum conditions under which immobilized glucose oxidase could be used most efficiently, several possibilities for the extension of that knowledge were explored. Originally, it was hoped that the system could be miniaturized to allow greater versatility in field applications. In an effort toward that end, a microconduit was designed and tested. A second area of interest was the interference of ascorbic acid in the glucose oxidase/Trinder reaction. The problem was found to be nontrivial. Finally, the feasibility of using the glucose oxidase reactor for the analysis of samples containing sugar mixtures was investigated. An interesting offshoot of that venture resulted in the use of the reactor for monitoring the mutarotation of D-glucose in phosphate solutions. A return to the main event resulted in the assembly of a parallel system for the simultaneous determination of glucose and galactose. Each of these extensions is discussed in detail in the paragraphs that follow.

Design and Testing of the Microconduit Glucose Oxidase SBSR

In 1984, when this work was begun, the premier article on the construction and use of microconduits in flow injection analysis had just been published (29). Since determinations with enzymes are used routinely in various fields, it was felt that such a miniature system would be of great utility. A microconduit was created in the original

work by engraving a "snake like" channel onto a small block of PVC (70 x 45 x 10 mm) which was then covered with a transparent plate and sealed in place with a pressure sensitive polymeric glue. In the work by Ruzicka and Hansen the microchannel was a semicircular cross-section with a typical area of 0.8 mm^2. Flow cells were constructed within the block so as to make a self-contained unit that only had to be attached to the detector via a fiber optic at one end and to the pump at the other. More recently, there was a report of the construction of a versatile injection valve within the block (76).

A sketch of the microconduit designed for this work is shown in Figure 25. The shape of the channel was designed such that two identical plates could be used. The cross-section of the channel on each PVC plate was semicircular. By inverting and rotating one plate on top of the other a circular cross-section (with an area of 0.8 mm^2) was obtained. Thus the channel created was similar to that found in a 1-mm i.d. tube. The creation of a channel with such a small radius (0.5 mm) is not easily accomplished with ordinary tools. In this case a very smooth, uniform channel was obtained by use of a Computer Numeric Controlled milling machine (manufactured by Charnoa). The machine was programmed and operated by the workers at Mattson Tool & Die, Inc. (Belmont, MI). The length of the channel is approximately 10 cm.

Two stainless steel plates were also machined and used to sandwich the two PVC plates together. By tightening the screws at each corner enough pressure could be applied to effectively seal the reactor; this eliminated the need for any type of glue. Each metal plate had the center cut out to facilitate connection of the ends of the channel to

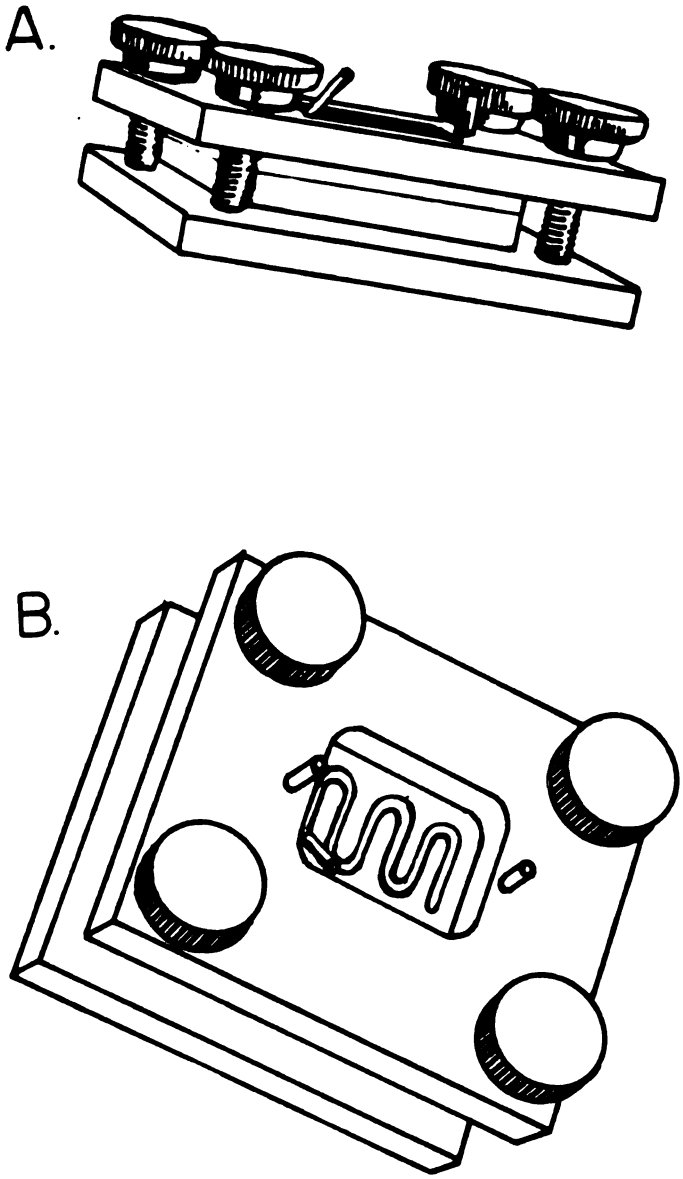

FIGURE 25 Side (a) and top (b) views of a microconduit SBSR.

external tubing. Holes were drilled perpendicular to the channel at each of its ends to accomodate short lengths of Teflon tubing which were used for the connection. Provided that the external surfaces are also very smooth and flat another set of plates could be stacked atop the first set without the need for any connecting tubing between the two sets. By increasing the length of the screws used to connect the two outer metal plates numerous reactors could be stacked together.

The microchannel reactor was packed with nonporous glass beads containing immobilized glucose oxidase. This novel single bead string reactor was used in place of the usual 10-cm GO SBSR and a calibration curve obtained. The operating conditions were the standard set adopted earlier (Chapter 4). The curve was linear to 800 ppm glucose and had a slope similar to that found for a 10-cm SBSR made from the same beads. These results make the future very bright for immobilized enzyme microconduits.

Although the size of the channel employed here is not really considered to be at the "micro" level by this author, it is identical to channel sizes in other microconduits (29). The use of a 0.5 mm i.d. cross section would fit the description more appropriately. Such miniaturization has not yet come to fruition.

Ascorbic Acid Interference Study

Ascorbic acid is known to interfere with the peroxidase catalyzed reaction. The nature of the interference is that the ascorbate acts as an alternate oxygen acceptor for the peroxide attached to the enzyme (77). In the case of the Trinder reaction, the sulfonate group

normally performs this function as it is eliminated from the DCPS. The premature abstraction of oxygen from the hydrogen peroxide may force the 3,5-dichloro-2-hydroxyphenyl sulfonic acid to obtain oxygen by another pathway or not at all. A recent report by Thompson (78) provides evidence that the former is the case. Other workers have also reported negative errors in the Trinder reaction due to ascorbate (71). It was therefore assumed that an investigation of the effect of ascorbate would be routine. That proved not to be the case.

In studies of the effect of ascorbate, the same PO reagent concentrations were used as in the delay flow experiments. A stock solution of ascorbic acid (Sigma) was prepared fresh daily by transferring 176.1 mg to a 1 liter volumetric flask and diluting to the mark with distilled water. Ascorbate standards were prepared by appropriate dilution of the stock solution. When not in use this stock solution was stored in the dark since it is light sensitive. Glucose standards were made from the stock solution described previously (Chapter 4). Six glucose standards in the range of 0 mM to 5.5 mM were used. A complete set of experiments was carried out using five sets of standards which were spiked with 0, 20, 40, 60, and 80 μM ascorbic acid, respectively. All standards were prepared with 0.05 M phosphate buffer.

In the first round of experiments an increase in peak height was concurrent with an increase in ascorbate concentration. The slope of the calibration curve decreased slightly while the intercept increased. The second round of experiments gave decreasing peak heights with increasing ascorbate concentration and the calibration curves became nonlinear. The only difference between the two rounds was that Brij-35

(a wetting agent) was added to the buffer that was used in the second round. A third round of experiments was carried out with buffer that did not contain Brij-35. Once again the intercept of the calibration curve increased in direct proportion to the concentration of ascorbate present. The slopes, intercepts, and correlation coefficients for the first and third experiments are given in Table 7 . These data suggest that the addition of the wetting agent has an adverse affect on the Trinder reaction. Brij-35 is a 30% aqueous solution of polyoxyethylene(23)lauryl sulfate. It appears that this inert surfactant has some effect on the reaction.

In order to investigate the effect of the further, a standard containing 2.2 mM glucose and 50 μM ascorbate was prepared. Injections from the solution were made at five minute intervals. The initial absorbance was lower than that obtained with a non-spiked glucose standard. However, the absorbance of the spiked standard gradually increased in each subsequent injection. Since the standard was shaken vigorously in order to obtain complete mixing the ascorbic acid may have depleted some of the oxygen in the solution, and limited the amount available for the glucose oxidase reaction. Since the container was left open to the air, some of the oxygen in the solution may have been gradually replenished.

The increase in the y-intercept merits some discussion. This trend suggests that a chromophore of some type is formed when only ascorbic acid is present. It may be that the ascorbate binds directly to the peroxidase, thus creating a complex that absorbs at 510 nm. The other possibility is that the ascorbate in some way facilitates the

TABLE 7 Effect of ascorbic acid in experiments without Brij-35.

Expt. No.	[Ascorbate] (μM)x10^4	slope x10^3	intercept	corr. coef.
1	0	4.31	0.78	0.99997
	20	4.26	6.1	0.99999
	40	4.25	13.0	0.99999
	60	4.08	27.8	0.9998
3	0	6.11	-5.7	0.9991
	20	6.08	8.4	0.998
	40	6.19	23.1	0.9996
	60	6.24	40.2	0.9996
	80	6.15	57.2	0.9995

coupling of the AAP to DCPS. By using the diode array detection system one could look at the spectrum of the flowing stream just prior to and while the sample plug containing ascorbic acid passes through the flow cell. A decrease at any of the wavelengths associated with PO absorbance combined with an increase at 510 nm in the absence of peroxide would confirm the formation of an ascorbate-PO complex. A second set of spectra could be taken with a reagent stream consisting of only AAP and DCPS to ascertain whether or not there is any direct interaction between the ascorbate and the two color-forming reagents.

The effect of ascorbic acid on the Trinder reaction has proved to be a nontrivial matter. Since this FIA system could be used ultimately to determine the sugar content in food this interference is important. Further investigation should yield concrete solutions to the problems identified in this work. Because this was a substantial deviation from the main goals of this project it was decided to leave this investigation for the future.

Kinetic Study of D-Glucose Mutarotation

The major use of immobilized enzyme systems has been for the determination of specific substrates in various types of samples (11). Chibata (7) gives an excellent review of other ways in which immobilized enzymes can be used (e.g. structural analysis of biopolymers and the elucidation of enzyme mechanisms). A novel way of implementing the immobilized enzyme reactor is by using it to follow the kinetics of a batch reaction which produces a substrate for which the enzyme is specific.

Previously described kinetic studies by FIA are predominantly those of reactions that occur in the manifold. In one method the flow is stopped and the absorbance of a species monitored as it reacts within the flow cell (19). In another, the sample plug circulates continuously in a loop that contains the detector (79). Painton and Mottola recently showed that the rate constant for a reaction in a single sample plug can be determined by comparison of the signal profile with those from numerical simulations (80). FIA has only recently been used to study the kinetics of relatively slow batch reactions (81-83). This is accomplished by injecting a sample from the solution in the batch reactor onto the FIA manifold at prescribed time intervals. The previously discussed FIA system containing a GO SBSR was employed to study the mutarotation of D-glucose.

This reaction is well-characterized (84, 85) and therefore can be easily used as a model since the kinetic parameters are well known. The reaction (see Figure 26) proceeds by a first order reversible process until equilibrium is reached. The integrated form of the rate equation for this process is:

$$-\ln \frac{(\beta - \beta_{eq})}{(\beta_0 - \beta_{eq})} = (k_1 + k_2)t$$

where β_0, β_t, and β_{eq} are the concentrations of the β anomer initially, at time t, and at equilibrium, respectively. The term, $k_1 + k_2$, is known as the mutarotation coefficient. It is more common to use the optical rotation of the solution in place of the concentration of the β anomer (86). However, since glucose oxidase is specific for the β

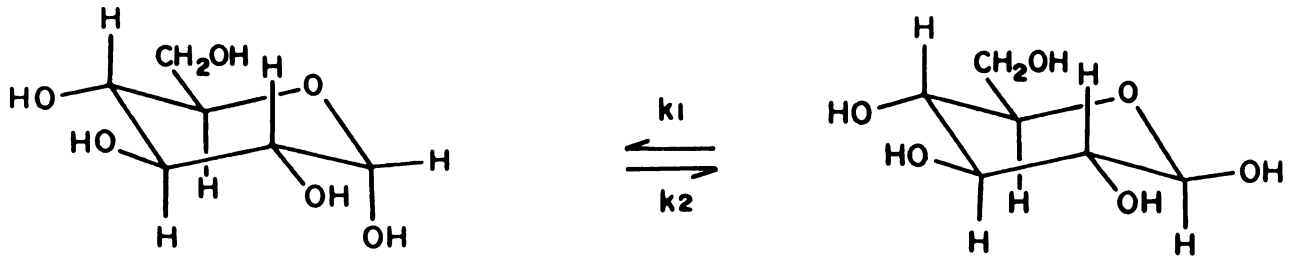

α-D-glucose

β-D-glucose

FIGURE 26 Mutarotation process for D-glucose.

anomer of D-glucose the absorbance from the product of the Trinder reaction can be used.

A set of experiments was designed in which the apparatus (described in Chapter 4) was used to follow the mutarotation kinetics of D-glucose in the presence of various concentrations of phosphate. The mutarotation process was also followed for D-glucose in the presence of D-galactose. Since D-galactose also mutarotates, the conventional method for this type of study (polarimetry) would be more complex than the method described here.

A 0.2 M phosphate buffer stock solution was prepared by adding 13.609 g of KH_2PO_4 (Mallinckrodt) and 14.196 g of Na_2HPO_4 (Fisher Scientific Co.) to a 1 liter flask and diluting to the mark with DW. Additional buffer solutions were made by dilution of the stock solution. In each case the pH was adjusted to 6.84 by addition of 0.2 M NaOH (made with pellets from E.M. Science).

The reagent solution for the Trinder reaction was prepared in a volumetric flask immediately before use. It was composed of 0.8 mg ml^{-1} PO, 1 mM AAP and 1 mM DCPS, diluted to the mark with 0.05 M phosphate buffer.

Glucose solutions were prepared at the time of use by measuring 15.0 mg of the appropriate anomer into a 25.0 ml volumetric flask and diluting to the mark with the appropriate solution. For the experiments in which galactose was also in solution, 15.0 mg of D-galactose was added to the 15.0 mg of glucose before transfer to the volumetric flask.

The overall flow rate was increased to 1 ml min^{-1}. Four different phosphate concentrations were used: 0.00, 0.05, 0.10, and 0.20 M. Only

the 0.05 M phosphate buffer was used in the case where galactose was added. The mutarotation process was followed in both the forward and reverse directions, starting with the pure α and β forms, respectively. For each anomer in each concentration of phosphate, the following experiment was repeated 2-4 times. The anomer was transferred to the volumetric flask and the clock was started. The sample was diluted as described above and allowed to dissolve completely. The tube leading to the sample injection valve was inserted into the flask and the pump started. After 90 s the solution had had sufficient time to occupy the sample loop and the first injection was made. Subsequent injections were 60 s apart. Each injection was followed by monitoring the output voltage from the detector.

Mutarotation coefficients were obtained by means of a simplex fitting routine which was based on the method of Nelder and Mead (87) and written by Pete Wentzell. It was necessary to provide the program with an equation describing the relationship of the x and y values to the constants that result from the fit. The following model was used to find the best values of the three parameters—($\beta_o-\beta_{eq}$, k_1+k_2, and β_{eq}):

$$\beta_{calc} = \beta_{eq}+(\beta_o-\beta_{eq})*EXP(-t*(k_1+k_2))$$

This is simply a different version of the previous equation in which all of the β values represent peak absorbance rather than concentration of the β anomer. The calculated β value, β_{calc}, was obtained during the fit. All points were weighted equally. Initial values of the three parameters were supplied by the user. In the case of the α anomer, β_o was assumed to be zero. For the β anomer, β_o could not be measured directly, and therefore the peak absorbance vs. time data were

extrapolated back to t = 0. Initial β_{eq} values were calculated from the average of the last two peak absorbance values, except in the case of the water solution. It is known from polarimetric measurements (86) that at room temperature 64% of the D-glucose is in the β form at equilibrium and thus β_{eq} for the water solution was estimated by appropriate multiplication of the β_0 value. Initial estimates of k_1+k_2 were obtained by calculating the initial slope of the curve for each set of data points.

The initial simplex consisted of four vertices and was calculated from initial estimates and an appropriately chosen step size for each of the three parameters. At each vertex the following procedure was performed. For each value of t in the data set a value of β_{calc} was computed. The squares of the differences between this value and the experimentally obtained value (β) were summed for all values of t using the function: $R = \Sigma (\beta-\beta_{calc})^2$. The magnitude of this sum of the squares of the residuals, R, was a measure of how closely the current estimates for the three parameters matched the experimental behavior. The simplex moved through successive iterations as it tried to minimize R (i.e., to obtain the closest match possible). Convergence was assumed when the sum of the squares of the residuals did not decrease after further iterations.

Determination of Mutarotation Coefficients

Convergence of the simplex was usually obtained in less than 100 iterations and was not more than 140 in any instance. Complete separation of β_0 and β_{eq} values in the equation used for the fitting

procedure was investigated. This did not decrease the number of iterations necessary nor did it improve the final R value obtained. The experimental points (shown in Figure 27) are connected by the corresponding fitted curves. The fitted curves show good agreement with the experimental data. The standard error of the estimate was less than 10% and the between run deviation was at most 5%. The mutarotation coefficients obtained with α and β anomers in various phosphate concentrations are listed in Table 8.

The generally accepted value for the mutarotation coefficient of D-glucose in water at 20°C is 0.015 min^{-1} (50, 88). The value of 0.018 min^{-1} at 21°C obtained here is in good agreement with the literature value. The small deviation can be accounted for by the slight temperature difference and the standard error of the measurement.

Effect of Phosphate Concentration

It is well known that phosphate ion catalyzes the mutarotation of D-glucose (84). Preliminary experiments indicated that the phosphate concentration had no affect on the GO/Trinder reaction for an equilibrium mixture of α- and β-D-glucose. Therefore, the increase in exponential character of the curves (Figure 27) is attributed to the catalytic effect of the phosphate ion on the batch reaction alone. The results, shown in Table 8, indicate the mutarotation coefficient to be linear with phosphate concentration. This same trend was observed in the polarimetric studies of Murschhauser (89). The slopes, intercepts, and correlation coefficients are given in Table 8. The mutarotation coefficient obtained when the D-glucose is initially in the α

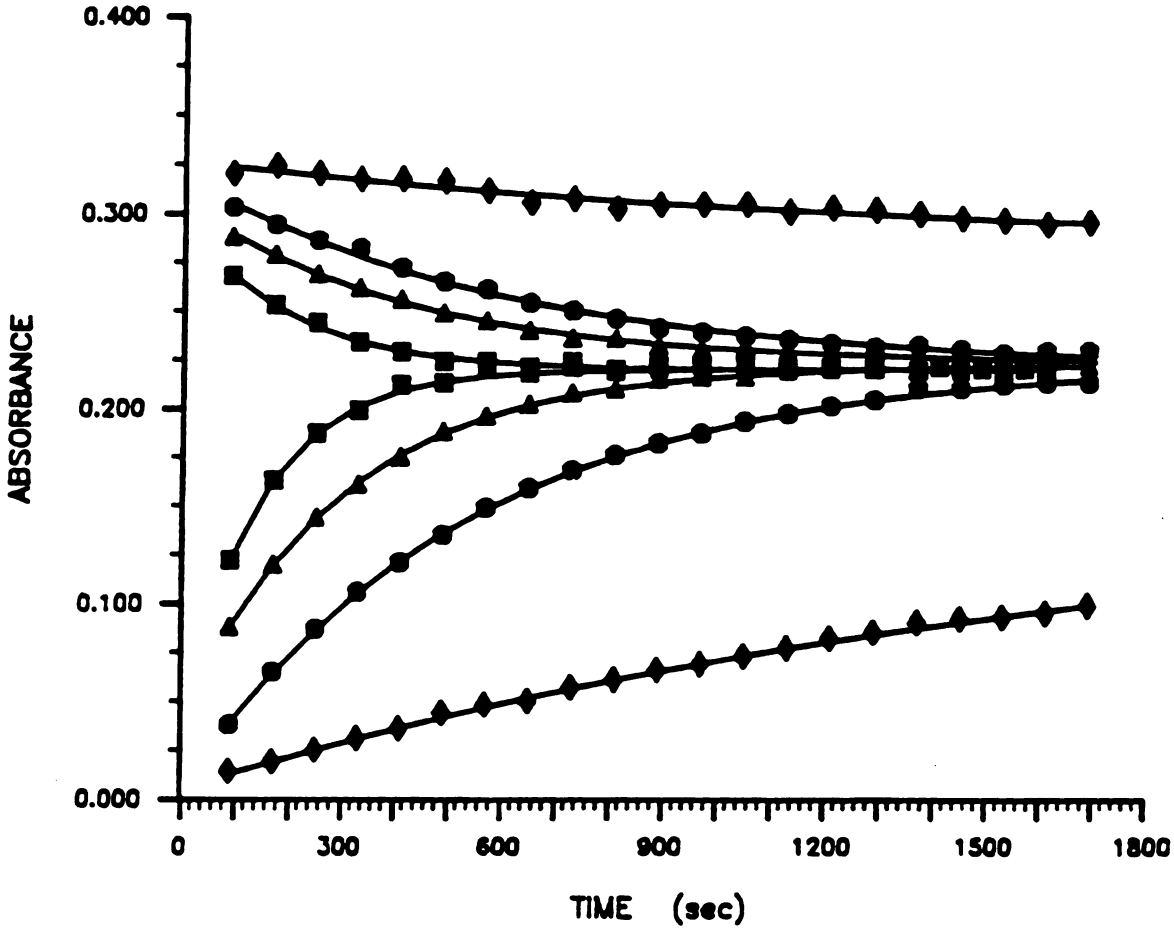

FIGURE 27 Effect of phosphate concentration on rate of D-glucose mutarotation. Lines represent curves of best fit. Upper curves were obtained with only β-D-glucose initially present. Lower curves were obtained with only α-D-glucose initially present. Phosphate buffer concentrations were: (◆) 0.00 M, (●) 0.05 M, (▲) 0.10 M, (■) 0.20 M.

TABLE 8 Mutarotation coefficients for D-glucose at 21°C.

Phosphate Buffer Concentration (M)	Coefficient x 10^3 (s^{-1}) only α initially	only β initially
0.00	0.3	0.3
0.05	1.9	1.5
0.10	3.3	2.6
0.20	6.9	5.0
slope ($M^{-1}s^{-1}$)	0.033	0.024
intercept (s^{-1})	0.00016	0.00027
correlation coeff.	0.998	0.999

conformation is larger than that for the β conformation by approximately 30%. The values for the y-intercepts in the equations relating phosphate concentration to the mutarotation coefficient indicate that the coefficient in water ought to be 0.009-0.018 min^{-1}, which compares favorably with literature values.

Effect of Galactose

Since the apparatus employed here could be used to investigate the mutarotation of D-glucose in the presence of other sugars and mutarotase, it was desirable to demonstrate the selectivity of the GO reactor. The main interference envisioned was that of galactose since its mutarotation is catalyzed at a rate similar to that for glucose. The mutarotation coefficients for D-glucose in the presence of an equal amount of galactose were found to be 1.9×10^{-3} s^{-1} and 1.7×10^{-3} s^{-1} for the α and β forms, respectively. These values agree with those obtained for the solutions containing glucose alone, and thus demonstrate the selectivity of the glucose oxidase reactor. This further substantiates the claims of specificity made in Chapter 3.

Since the enzyme is specific for a single sugar, this method facilitates the study of the mutarotation process for that sugar in a matrix of other optically active species (e.g., a mixture of sugars several of which mutarotate). The mutarotation of some sugars is complex since, when in solution, furanose as well as pyranose structures are present (84). It may be possible to investigate separately the slow reactions of the pyranose form of other sugars with an apparatus similar to that described here.

Parallel Determination of Sugars

Galactose oxidase was chosen as a complementary enzyme to glucose oxidase. The interest in the determination of galactose arises from both the nutritional aspect as well as the clinical standpoint. It is considered one of the six nutritionally-significant sugars (90). The reaction of galactose with galactose oxidase also produces hydrogen peroxide. From the clinical standpoint the condition of galactosemia sometimes found in infants causes elevated levels of galactose in the urine. The conventional method of diagnosis is based on a negative glucose test and a positive test for reducing substances, followed by identification of the reducing substances (91). This procedure could be greatly simplified by determining the galactose level directly. Since galactose oxidase is more expensive than glucose oxidase, immobilization of the enzyme was thought to be cost effective.

The Galactose Oxidase SBSR

The procedure used to immobilize glucose oxidase was also used for galactose oxidase. The critical parameters of pH and enzyme concentration were pondered. Assay procedures employing galactose oxidase specify a pH between 6 and 7 (92, 93). This would suggest that the enzyme is most active in that pH range. Therefore, since it is desirable to immobilize the enzyme in its most active state the same phosphate buffer was used. The concentration of the enzyme solution was determined by calculating the amount of enzyme necessary to give an equivalent number of Units of activity as that obtained for glucose oxidase. The appropriate portion of galactose oxidase (E.C.1.1.3.9,

Sigma Type V from Dactylium dendroides, specific activity approximately 70 U mg^{-1} at 25°C) was diluted with 5 ml of phosphate buffer. This solution was used in the place of the glucose oxidase solution in the immobilization procedure. Other workers have immobilized galactose oxidase on porous glass (94, 95), but this is the first time nonporous glass beads have been used.

The nonporous glass beads containing the enzyme were put into a 50-cm piece of Teflon tubing since it was suspected that the activity would be less than that available from the GO SBSR. A galactose stock solution was prepared by transferring 200 mg to a 100 ml volumetric flask and dilutin to the mark with DW. Galactose standards were prepared from the stock by appropriate dilution with phosphate buffer. Although the actual absorbance values obtained were much less than those for GO, the calibration curve was linear from 0.13 to 3.3 mM galactose.

Immobilized Galactose Oxidase Specificity

The galactose (GA) SBSR was tested for specificity against the other five nutritionally-important sugars: maltose, lactose, glucose, sucrose, and fructose. Standard solutions (3.3 mM) of each sugar were prepared by transferring the appropriate amount of powder to a volumetric flask and diluting to the mark with phosphate buffer. The results are given in Table 9 as a percentage of the response obtained with galactose. An interesting phenomenon occured with the sucrose and maltose samples: negative peaks were produced. This was probably not a result of a reaction, but rather a change in refractive index which caused an apparent decrease in absorbance. Significant absorbances were

TABLE 9 Galactose oxidase activity toward other sugars.

Sugar	Ratio
galactose	1.00
glucose	0.12
fructose	-
sucrose	-
lactose	0.28
maltose	-

"-" indicates no detectable response

obtained with glucose and lactose. This may be the result of a slight glucose oxidase impurity in the enzyme preparation. The relatively high response to lactose was expected. Other workers have used GA reactors for the determination of lactose in the absence of galactose in substances such as milk (94, 95). Lundback (95) devised a procedure by which the enzyme is further purified prior to the immobilization procedure. This could be implemented in the future to obtain greater activity per gram of beads.

Galactose oxidase requires more care than glucose oxidase. It is recommended that the immobilized version be stored in a copper sulfate/EDTA/Tris buffer solution in order to maintain the activity of the enzyme (95). The copper(III) in the enzyme changes to copper(I) as it catalyzes the reaction. Via a side reaction it sometimes reaches an inactive state (copper(II)) which can be restored by use of hexacyanoferrate. For future experiments these procedures should become routine. Consideration must also be given to inactivation of the enzyme by high galactose concentrations.

Design of the Parallel FIA System

The FIA system was modified to accomodate the two immobilized enzyme SBSRs. The sample size was increased to approximately 70 µl and a tee placed immediately after the injection valve. The GO SBSR was connected to one arm of the tee and the GA SBSR to the other. In order to accomplish even splitting of the stream, a 40-cm plain SBSR was added between the tee and the GO SBSR. This compensated for the pressure drop associated with the 50-cm GA SBSR. Pump tubing and speed were adjusted

so that the overall flow rate was maintained at 0.5 ml min^{-1} and a flow ratio of 10:1 preserved. The manifolds were identical following each immobilized enzyme reactor--the same as that used for one reactor. The parallel system is shown in Figure 28.

Alizarin red (0.00025 M) was injected into a stream of 0.05 M phosphate buffer to determine the actual percentage of sample going to each side. Plain SBSRs of the same dimensions replaced the respective enzyme SBSRs. Each peak obtained was integrated and the area taken as representative of the total amount of sample reaching that reactor. The GA SBSR was recipient of 50.6% of the injected sample.

Analysis of Real Samples

Two sets of calibration standards were prepared from stock solutions of glucose and galactose. One set contained glucose and the other set contained galactose. The range of standards was 0.0 to 5.5 mM. The calibration curve for glucose was linear from 0.1 mM to 5.5 mM. The linear range for galactose was from 0.1 mM to 3.3 mM. The glucose oxidase did exhibit a small, but perceptible response to the galactose standards. As mentioned earlier, there was also a small response to glucose by the galactose oxidase. As a preliminary check on the system's ability to perform accurate determinations of glucose and galactose simultaneously, a mixture containing known amounts of the two sugars was prepared. The amounts determined were found to be within 10% of known values.

A few real samples were analyzed with this system. The peaks obtained are shown in Figure 29. Pepsi was found to have 4.92% glucose

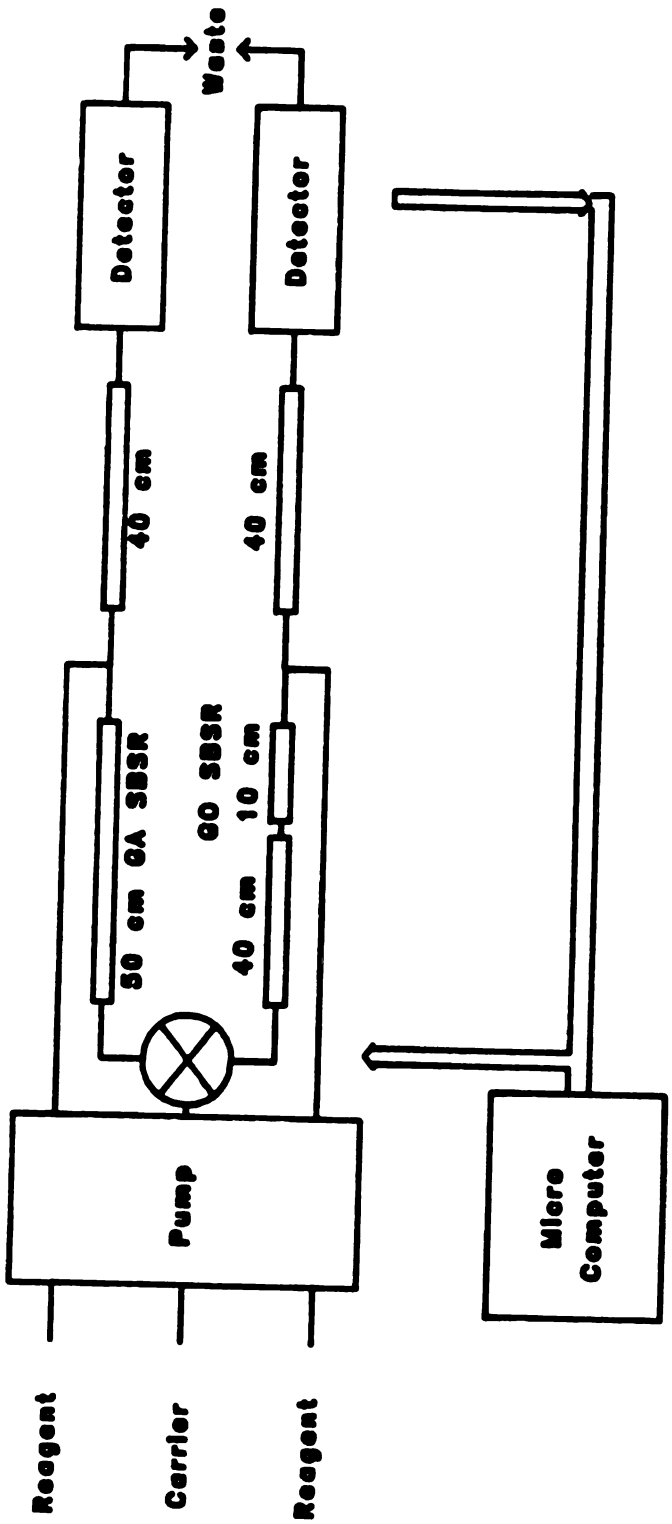

FIGURE 28 FIA system for parallel determination of glucose and galactose.

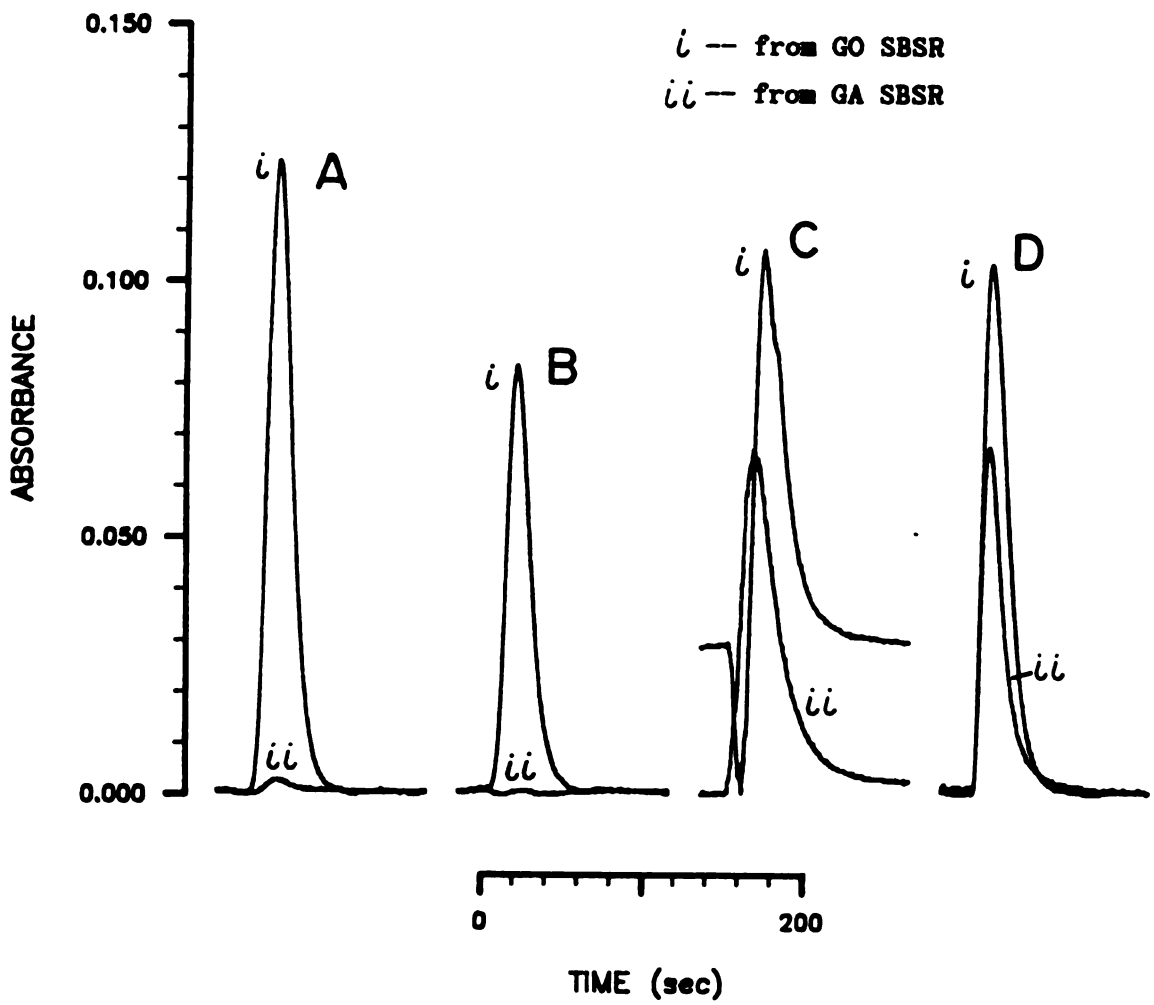

FIGURE 29 FIA profiles for : (a) Pepsi, (b) Sunglo fruit punch, (c) diluted serum, (d) deproteinized serum.

and no galactose. This result agrees well with the value (4.95%) determined by a different method (42) and the nominal value reported in that same work (4.3%). Sunglo fruit punch was found to contain 3.48% glucose and no galactose. Reconstituted serum samples (SeraChem by Fisher) were also tested. The first peak was obtained from a 1:5 dilution of the serum with DW. The glucose concentration was found to be 77 mg dl^{-1}, compared to 78 ± 10 mg dl^{-1} given in the manufacturer's data sheet. The initial negative peak obtained from the glucose oxidase reactor was probably due the difference in viscosity between the carrier and the sample. This effect has been observed by other workers (96).

To correct for the baseline interference in the GO reactor the serum sample was deproteinized. To 1.0 ml of serum in a centrifuge tube was added consecutively 1.5 ml $Ba(OH)_2$ solution (20 g l^{-1}) and 1.4 ml $ZnSO_4$ solution (20 g l^{-1}). After the solution was thoroughly mixed, it was centrifuged for three minutes. The supernatant was used directly for the determination and found to contain 74 mg dl^{-1} glucose. In addition to the good agreement with the published value, the FIA profile was much improved. The presence of protein did not affect the determination (i.e., the two values were equivalent within the experimental precision of this system--an RSD of 5% for three replicate determinations); this substantiates an earlier report (71). The activities of the reactors were not adversely affected by reaction with a sample containing protein--the slopes of the calibration curves remained constant.

The large response of the galactose oxidase reactor to the serum sample was beyond the range of the calibration curve. The data sheet

did not list any substances which might have caused such a high response. Each successive injection yielded an increased response. This indicates that some type of activation was taking place and provides solid evidence that further precautions need to be taken when working with this enzyme.

From these results it can be concluded that parallel determination of sugars is quite feasible. A major improvement in the system performance could be attained with a sample selector. This would allow the individual optimization of each channel.

CHAPTER 6

THE EFFECT OF TEMPERATURE ON DISPERSION

Considerable attention has been given to the study of dispersion in flow injection analysis (19, 73, 97-101). Flow injection brought to analytical chemistry a concept that was entirely new, that of "manipulated dispersion" (102). Prior to this, complete mixing of sample and reagent solutions was considered a prerequisite for performing a chemical analysis. In most cases it is desirable to control dispersion rather than minimize it, since some amount of dispersion is usually required to facilitate a chemical reaction, dilute the sample, or produce a gradient. Sample throughput may be dispersion-limited for systems that merely transport a sample, and in these minimum dispersion is advantageous.

In an attempt to quantify dispersion a numerical technique was used to solve the diffusion-convection equation (97). Elsewhere, Reijn et al indicated the additive dispersive effects of the processes of injection, transport, and detection (98). Other workers have studied the various aspects of system design and experimental parameters which affect these. Ruzicka and Hansen recognized the importance of dispersion when they included sample volume, tube length, flow rate, and the presence of a mixing chamber into seven rules for developing FIA systems (19). Vanderslice et al (99) indicated that the diffusion coefficient and tube radius play a role in dispersion. A further dispersive effect during the transport process has been attributed to chemical reaction (19, 31, 73, 103). Painton and Mottola (104) also

point out that the usefulness of the "practical dispersion number" can be invalidated or obscured when chemical reactions take place. The nature of the reaction manifold used (straight tubes, coiled tubes, single bead string reactors, etc.) has been shown to be a key factor (105). Dispersion introduced during detection was recently partially attributed to the flow cell configuration (106). A recent article by Stone and Tyson (107) provides a model for the dispersion process that takes into account the flow rate, tube length, tube inner diameter, and method of injection. The complex interactions of all these factors in the ever widening range of flow injection analyses are still not well characterized. It is obvious that deeper theoretical and practical studies of the processes that cause a sample plug to become dispersed as it travels through a flow injection analyzer are necessary (102).

In all of the discussion concerning various sources of dispersion there has been little mention of the effect of temperature. A hypothesis can be made regarding the relation ship of dispersion and temperature from the equation derived by Ruzicka and Hansen that describes the relationship of dispersion, D, to various experimental parameters. It is as follows:

$$D = \frac{V_r}{S_v} \left(\frac{L\ Q}{12\ D_m} \right)^{1/2} \pi\ r^2$$

where V_r is reactor volume, S_v is sample volume, L is tube length, Q is flow rate, and r is tube radius. The molecular diffusion coefficient, D_m, is proportional to temperature. This implies that dispersion is inversely proportional to temperature.

No experimental studies have been published until now (108) that substantiate this hypothesis, although the case for such is strong in light of the circumstantial evidence available. For example, (i) in FIA viscometric studies temperature control was necessary to obtain the required reproducibility of peak height measurements (103); (ii) simulation studies indicated that an increase in temperature (and the resultant decrease in viscosity) would promote radial mixing, decrease longitudinal dispersion and increase peak height (73, 106); (iii) peak shapes changed as the temperature of one flow injection system was increased (109). The reaction kinetics which take place in flow injection analyzers are often favored by higher temperatures. For slow reactions this can be used to achieve greater sensitivity or decreased time per analysis, since the "optimum" experimental conditions will change.

An investigation was launched in an effort to validate the aforementioned hypothesis. Four types of reactions were studied in order to ascertain the effect of temperature on the on the FIA peak profile. The first type involved the injection of a dye into a non-reactive carrier stream. The results from this are compared to those obtained for a fast reaction, that of p-nitrophenol with sodium hydroxide. The complexation reaction of nickel and PAR (4-(2-pyridylazo)resorcinol) was used for the investigation of a moderate speed reaction. The same apparatus configuration was used for all three reactions and is therefore described first. And last, but certainly not least, the effect of temperature on the glucose oxidase/Trinder reaction was used as a model of a slow reaction.

The Apparatus for Cases 1 through 3

The FIA system for this set of experiments was assembled from the basic components described earlier (Chapter 4) and is shown in Figure 30. The manifold in this case was very simple. The sample was injected into a carrier stream which flowed through 1 m of coiled 0.8 mm i.d. microline tubing (2.0 cm coil diameter) to the detector.

The sample container, reagent container, and manifold coil were immersed in a water bath. This consisted of a large pyrex recrystallization dish filled with water and placed on a hotplate which had an adjustable heating control. A thermometer was immersed in the water at the level of the coil and containers.

Accurate compensation for the slight heat loss that occurred as the solutions travelled from the thermostatted vessels to the detector flow cell was attained by measuring the temperature of the stream as it entered the flow cell. The precision 30-kΩ thermistor was used as described earlier (Chapter 4) to obtain temperature calibration curves at various flow rates. Distilled water was pumped through the system for this process. Table 10 shows the slope, intercept and correlation coefficient for the linear relationships between bath temperature (T_b) and manifold temperature (T_m) at each flow rate.

Data acquisition was accomplished with the Bruce Bus microcomputer. A data set was obtained from five replicate injections for each 5° increment of temperature. The files for each of the replicates were then transferred to the DEC LSI 11/23 minicomputer where the counts were converted to absorbance units and plots of each peak were obtained with the aid of a two pen plotter. A baseline correction

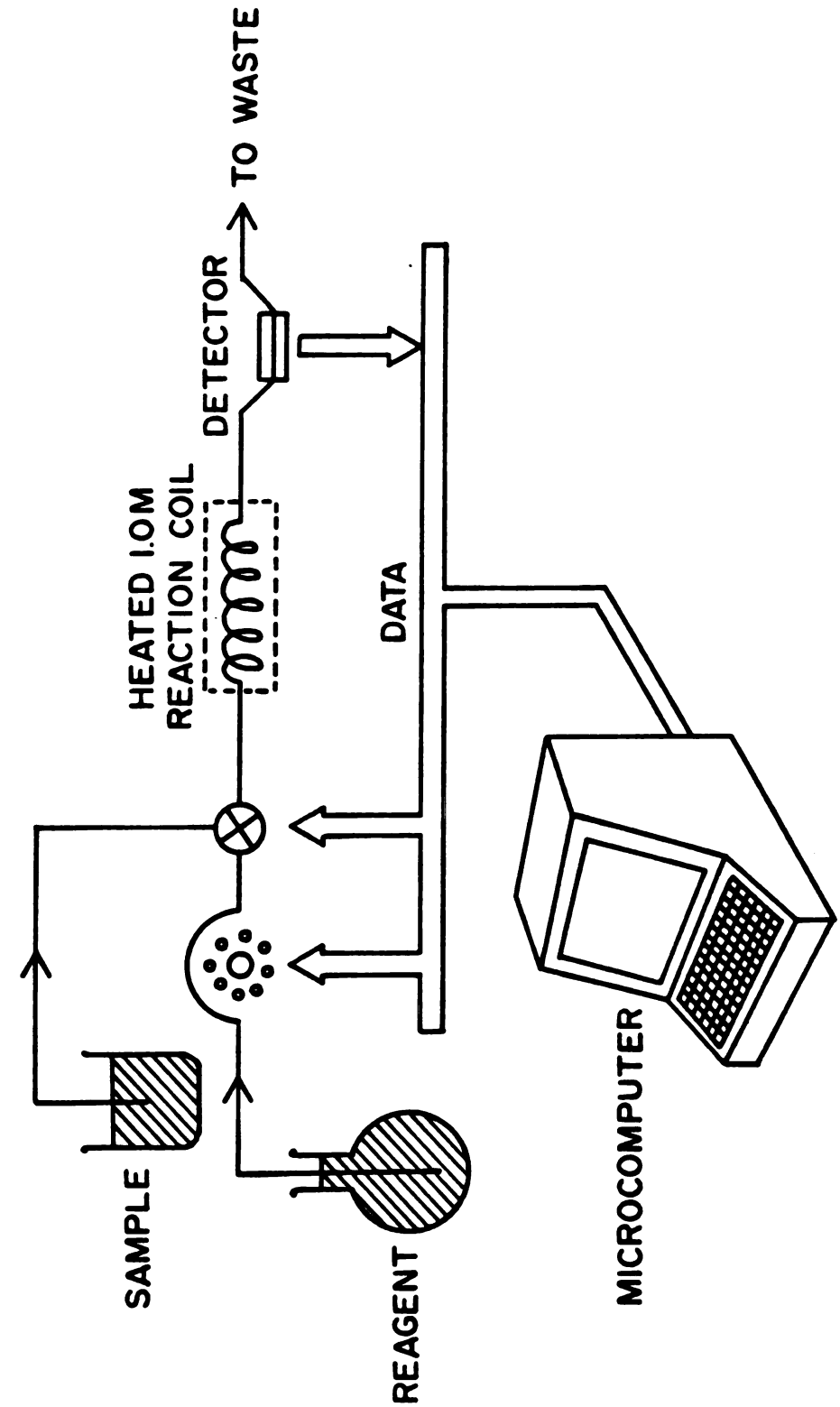

FIGURE 30 FIA system for temperature studies.

TABLE 10 Temperature correction equations for various flow rates.

Equation: $T_M = a*T_B + b$

Flow Rate (ml min^{-1})	a	b	Correlation Coefficient
0.56	0.947	1.17	0.9999
1.20	0.952	1.02	0.9999
1.88	0.860	3.25	0.9997
1.00	0.650	7.46	0.9999

for each plot was obtained by measuring the height of each peak by hand. For convenience, the FWHM (full width at half the maximum height) was also measured by hand. A program written in FORTRAN was used to obtain the area of each peak by integration with Simpson's rule. In each case the average of the five replicates was taken as the "true" value.

Case 1: No Reaction

A solution of alizarin red (0.00048 M) was prepared on the day of use by adding 33.1 mg of the powder to a 200 ml volumetric flask and diluting to the mark with 0.05 M phosphate buffer. The solution was stirred until dissolution was complete.

The dispersion characteristics of the single line manifold were investigated for a temperature range of 20-70°C at flow rates of 0.56, 1.20, and 1.88 ml min^{-1}. Before injection, the sample solution, carrier solution, and reaction manifold were allowed to come to temperature equilibrium with the water bath. A 30-µl sample of alizarin red solution (0.00048 M) was injected into a stream of phosphate buffer (0.05 M) which flowed through the coiled manifold. The absorbance of the stream was monitored at 510 nm.

In an additional set of experiments, the peak height for the undiluted dye, H_{max}, was measured. The same procedure was used as above, except that the sample 'injection' was a continuous stream of the dye, rather than a finite plug.

The effect of temperature on dispersion for the system without reaction is shown in Figure 31. The dispersion values were calculated by dividing H_{max} by H. For each of the flow rates studied, the same

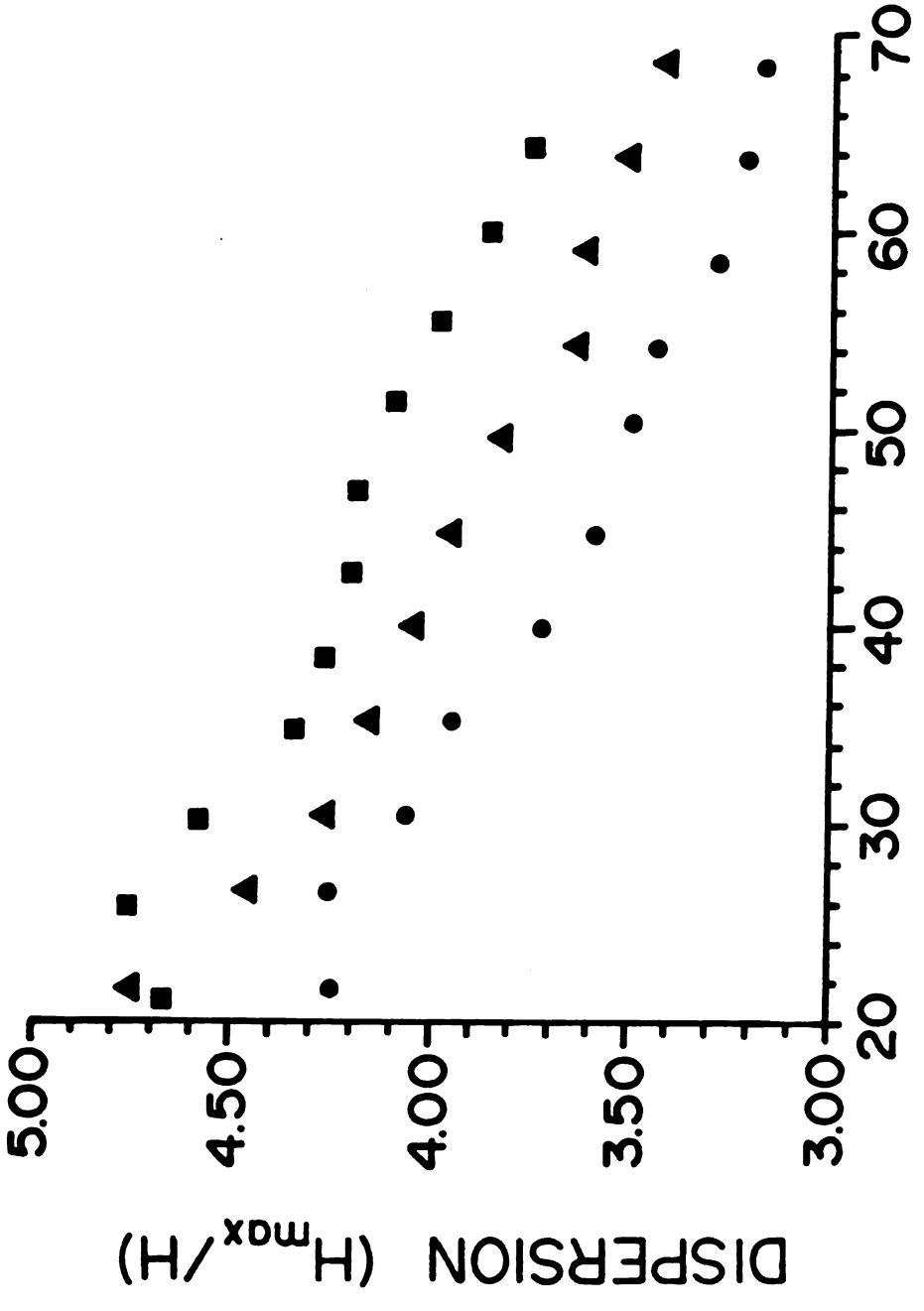

FIGURE 31 Effect of temperature on dispersion without reaction. Flow rates were: (●) 0.56 ml min^{-1}, (▲) 1.20 ml min^{-1}, and (■) 1.88 ml min^{-1}.

trend was seen; increased temperature resulted in decreased dispersion. Since no change in the total amount of dye present was expected, it was initially concluded that the change in dispersion was due to temperature. Over the temperature range of 26°C to 70°C, for the flow rates of 0.56, 1.2 and 1.88 ml min^{-1}, the dispersion, D, decreased by 24.5, 21.1 and 21.1% respectively.

To ensure that no change in total absorbance occurred as the dye travelled through the manifold, the effect of temperature on peak area was investigated. The horizontal lines obtained (Figure 32a) indicated that, indeed, the peak areas did not change with temperature. The "areas" shown for the three different flow rates indicate that the integration of peak height was originally carried out over time, not volume. When these areas were multiplied by the appropriate flow rates they became equal within the limits of experimental error.

Figure 32c shows that the peak height increased with increased temperature and decreased flow rates. The experimental flow rate dependence has been reported elsewhere (109) and is in accordance with trends predicted by theory (19, 73, 106).

Figure 32e shows that the peaks became narrower as the temperature increased. Also, the steepness of the initial slope decreased as the flow rate increased. This was thought to be due to action of the flow rate and temperature upon the dispersion process. Theoretical predictions and interpretations given elsewhere (73, 106) indicate that decreased longitudinal dispersion may be directly attributed to an increase in radial mixing.

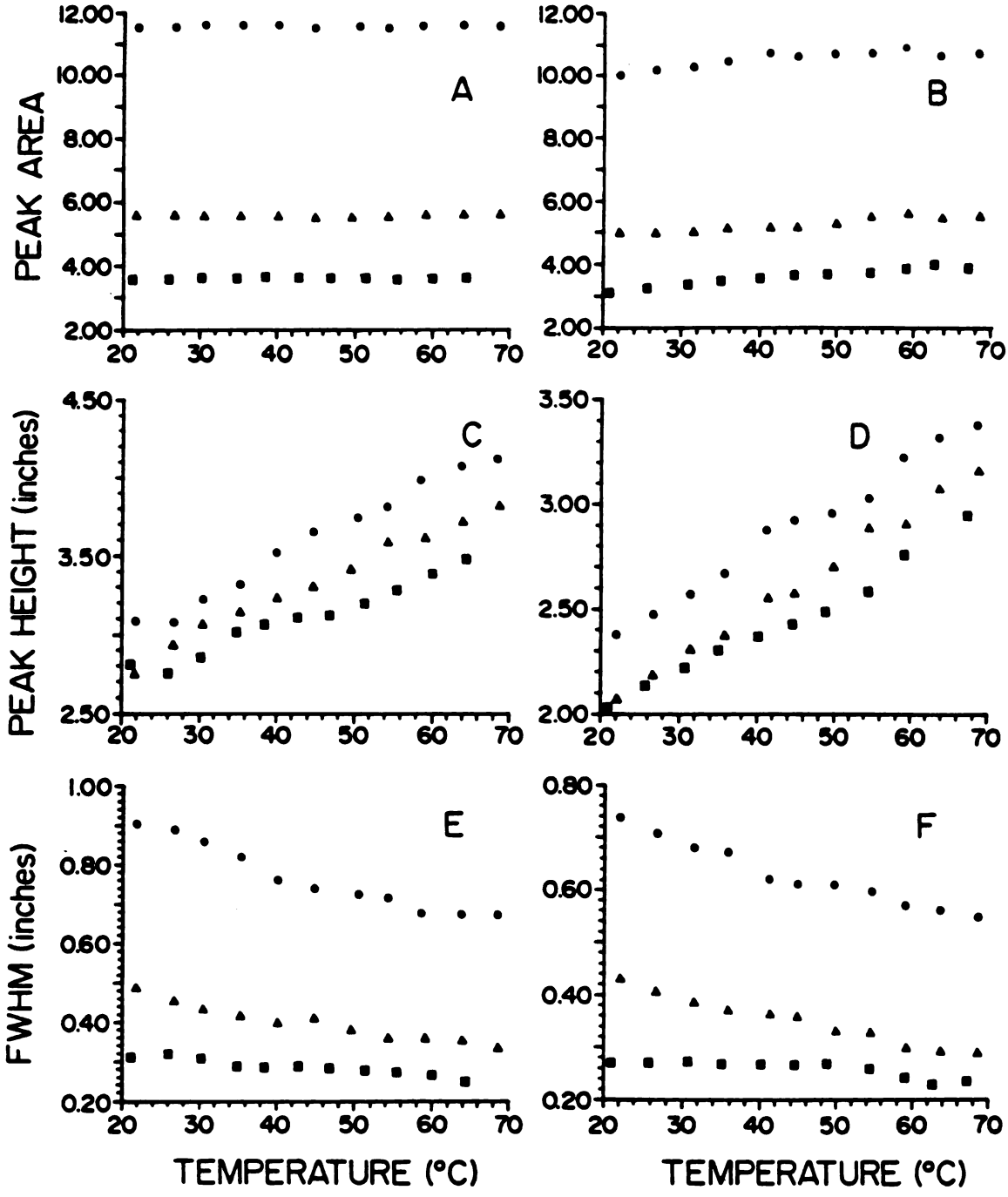

FIGURE 32 Effect of temperature on peak area without reaction (a), peak area with fast reaction (b), peak height without reaction (c), peak height with fast reaction (d), FWHM without reaction (e), and FWHM with fast reaction (f). Flow rates were: (●) 0.56 ml min^{-1}, (▲) 1.20 ml min^{-1}, and (■) 1.88 ml min^{-1}.

Case 2: Fast Reaction

A p-nitrophenol stock solution (0.01 M) was prepared by adding 0.6958 g p-nitrophenol to a 500 ml volumetric flask and diluting to the mark with DW. The solution was stirred until dissolution was complete and then transferred to an amber bottle and stored at 4°C. On the day of use a 0.0002M solution of p-nitrophenol was made by appropriate dilution of stock solution with DW. A sodium hydroxide stock solution (0.2 M) was prepared by diluting 12 ml of 50 % (w/v) aqueous sodium hydroxide to 1 liter with DW. The other desired sodium hydroxide solutions were made by subsequent dilutions of the stock solution with DW. The sodium hydroxide solutions were then standardized by titration against anhydrous potassium hydrogen phthalate with phenolphthalein as the indicator (110).

Since the interaction of p-nitrophenol with NaOH is a simple acid-base reaction, it was assumed to be fast. Prior to the FIA experiments a stopped-flow experiment was carried out to confirm this. A p-nitrophenol solution (0.0008 M) was instantaeously mixed with NaOH solution (0.01 M). The data acquisition rate was set at 1 ms^{-1} (the fastest available on the custom built apparatus (111, 112)). A nonzero absorbance in the range expected for the completed reaction was observed immediately--no change was observed for a period of 100 ms. This showed that the reaction rate is very rapid compared to the time that would be required for the sample to travel through the FIA manifold.

The experimental parameters employed in this set of experiments were the same as those for Case 1. A 30-µl sample of p-nitrophenol solution (0.0002 M) was injected into a stream of sodium hydroxide

(0.01 M) which flowed through the coiled manifold. The absorbance of the stream was monitored at 420 nm.

The slight positive slope below 50°C for the areas of the p-nitrophenol curves (Figure 32b) indicated that the peak areas (and hence, total absorbance of product) were increased by temperature. It was thought that this effect might be due to a shift in the chemical equilibrium, rather than a reaction rate or mixing phenomenon. Therefore, static experiments were carried out to see if product absorbance increased with temperature, irrespective of any sample dispersion effect. Since the sample would see a range of hydroxide concentrations in the flow injection system, a range of hydroxide concentrations was used in these confirmatory experiments. Three premixed solutions containing 0.0002 M p-nitrophenol and, respectively, 0.005 M, 0.01 M, and 0.05 M sodium hydroxide were used. These solutions were passed sequentially through the FIA apparatus without injection. The absorbance was monitored at 420 nm relative to DW over the same temperature range as above, except that 15°C temperature increments were used. No change in absorbance with temperature was observed. Thus, the change in peak area observed could not have been due to a shift in equilibrium and another avenue of investigation was pursued.

The reaction of p-nitrophenol with sodium hydroxide is very fast compared to the time the sample takes to traverse the manifold (milliseconds compared to seconds). Thus, the most likely cause of the observed effect was one of temperature on the sample dispersion, i.e., in this flow injection system, at temperatures below 50°C, insufficient mixing occurred to facilitate complete reaction. This was corroborated

by calculation of the number of tanks, N, for this system. Here N was approximately 5 for all three flow rates. This low value indicated incomplete mixing. An additional set of experiments was carried out with a 3.0 m coil in place of the 1.0 m coil. It was found that under these conditions the peak area did not increase with temperature. Thus, incomplete mixing was confirmed as the cause of the artifact in the original data set.

The effect of temperature on peak height for the reaction (Figure 32d) was similar to that observed in the system without reaction. An exception was noted for the 1.20 ml min^{-1} flow rate; the peak height was lower than expected for temperatures below 40°C. This deviation could not be attributed to experimental error, and does not lend itself to an easy explanation. The trends for the values of the FWHM (Figure 32f) were the same as those in Case 1.

A typical set of peaks obtained at different temperatures for this fast reaction is displayed in Figure 33. It is of interest to note that there is an increasing amount of noise in the baseline as the temperature increases. This could have a significant effect on the limit of detection at high temperatures. The nature of this artifact would make an interesting topic for future investigation.

Case 3: Moderate Reaction

A nickel(II) stock solution (10^{-2} M) was prepared by measuring 0.2908 g $Ni(NO_3)_2$ $6H_2O$ into a 100 ml volumetric flask and diluting to the mark with DW. A stock solution of PAR was prepared by transferring 25.5 mg to a 100 ml volumetric flask followed by dilution to the mark

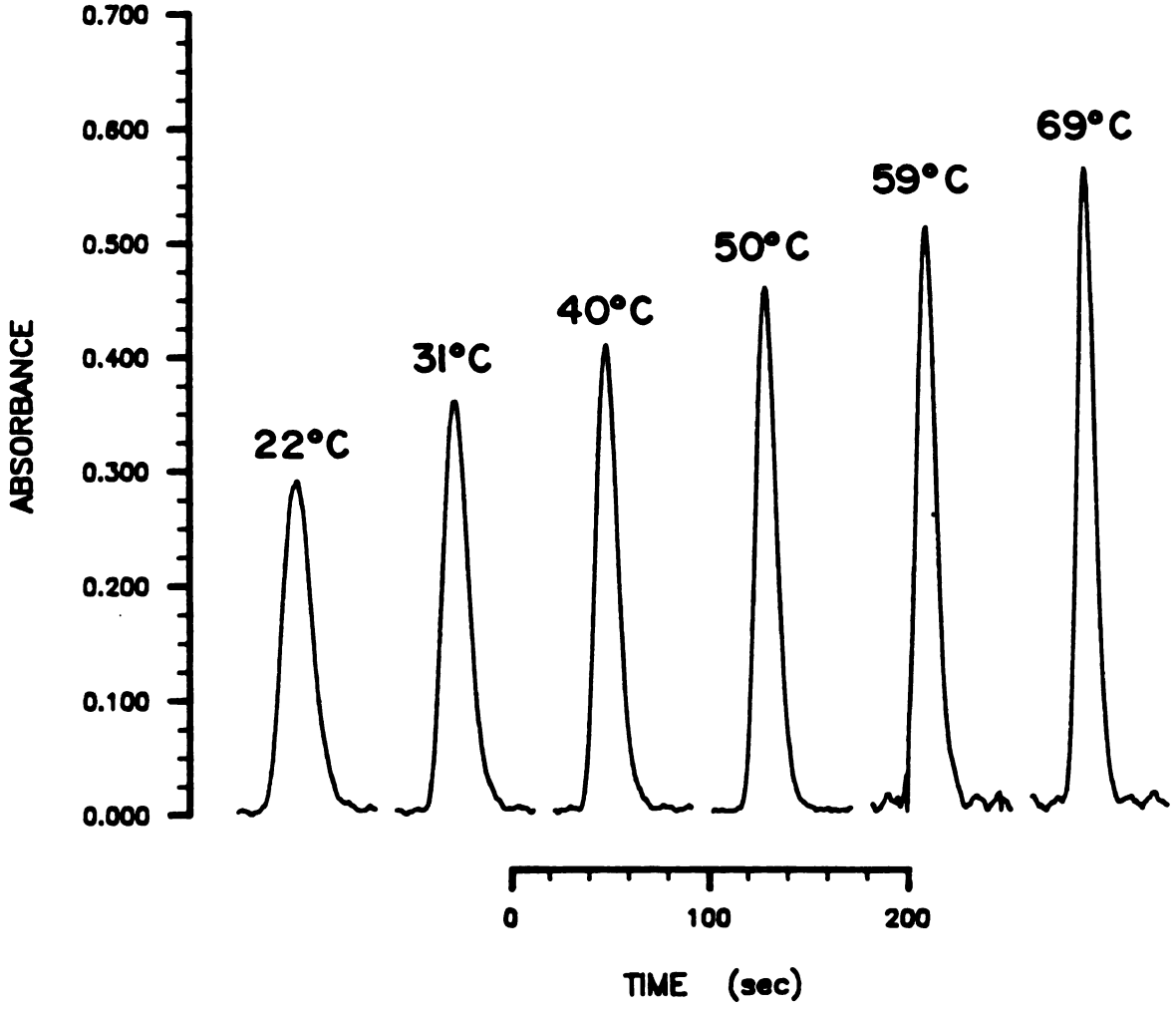

FIGURE 33 FIA profiles obtained for the experiment with p-nitrophenol under the following conditions: flow rate 1.20 ml min^{-1}; coil length 3.0 m; and temperature range 20-70 °C.

with DW. The nickel and PAR reagent solutions were made on the day of use and were 2 x 10^{-5} M and 10^{-4} M, respectively. Since the complex is 1:2 a 1 to 5 reagent concentration ratio was deemed sufficient. Since the complexation reaction is pH-sensitive, a 0.05 M phosphate buffer was used to make the solutions used for the experiment. The pH of this buffer (6.85) is well within the pH range over which complexation takes place, and chosen to be less than pH 8 so that no precipitation would occur.

As in the case for the fast reaction, a stopped-flow experiment was carried out to determine the length of time required for the reaction to reach completion. The reagent solutions were prepared as indicated above. A data acquisition rate of one point per 800 ms was used to obtain the reaction curve shown in Figure 34. The nonzero absorbance present at the initiation of the run was due to the background absorbance of PAR at 510 nm. The progress of the reaction approaches a plateau region after 80 s. This information was utilized in the choice of coil length used in the study.

The apparatus as described earlier was modified slightly for the nickel/PAR experiments. The jacketed reagent vessels connected to the thermostatted water bath (previously used in the enzyme studies) replaced the make-shift water bath on the hotplate. The reaction coil was immersed in a 250-ml jacketed flask (also connected to the water bath) filled with water. As before, compensation was made for the loss in heat by calibration with the precision thermistor. The flow rate of the carrier stream (PAR reagent solution) was 1 ml min^{-1}. Nickel reagent solution (30 µl) was injected into the carrier stream, passed

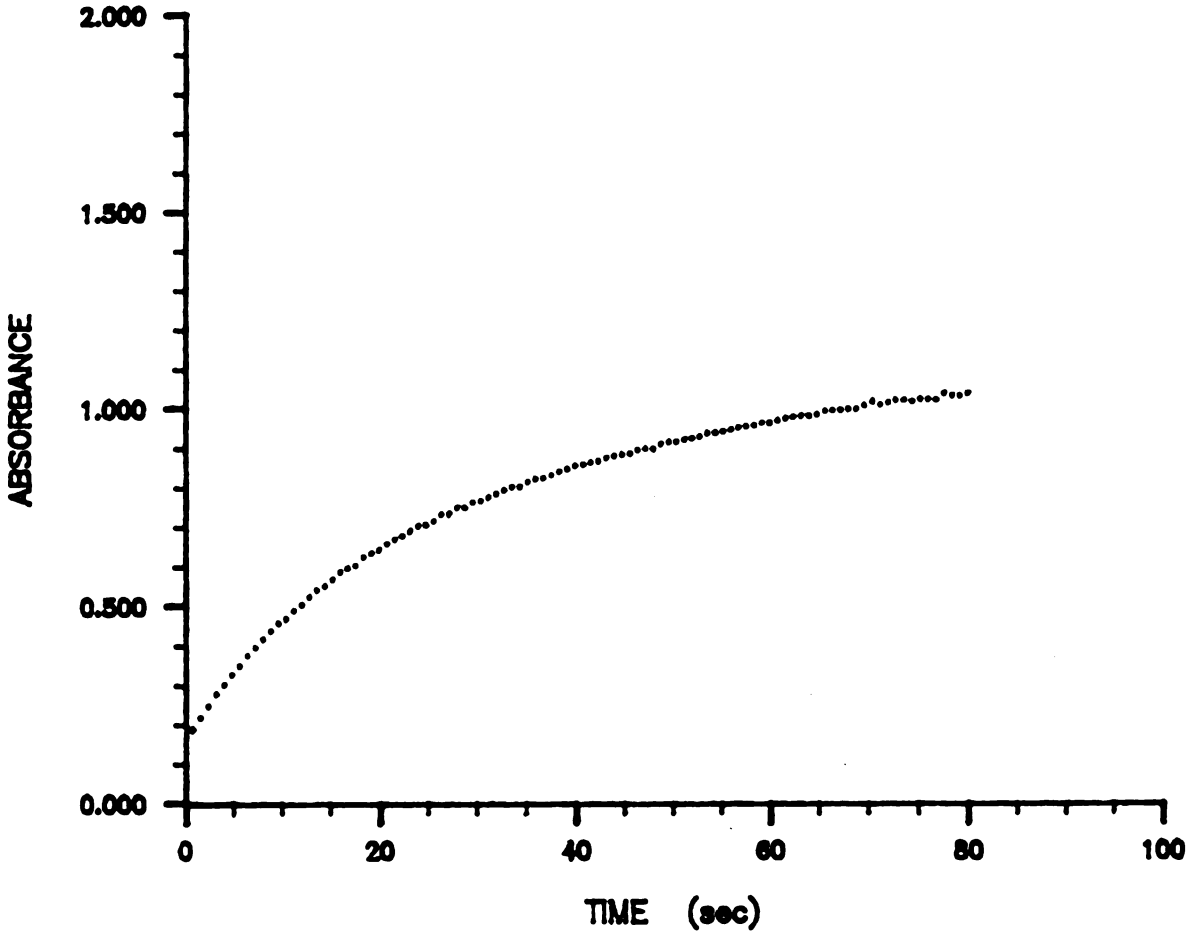

FIGURE 34 Reaction progress curve for nickel ($2x10^{-5}$ M) with PAR (10^{-4} M) at pH 6.85.

through the reaction coil to the detector where the absorbance was monitored at 510 nm. Two different lengths of reaction coils were used. A 1.0-m coil was selected based on the fact that it would provide a reaction time (30 s) which was much less than that required for the reaction to reach completion. A 3.0-m coil was chosen to provide a reaction time (90 s) longer than that required for the complete reaction.

The effect of temperature on the peak area for the two different coil lengths is depicted in Figure 35a. The trend for the shorter coil is as expected; as the temperature is increased there is a rapid increase in total absorbance created by an increased amount of reaction. The data points obtained with the longer coil do not exhibit the ideal straight-line behavior seen in the previous case studies, but the trend is similar. The scatter of the points was probably a result of integrating a noisier than normal signal.

Inspection of the effect of temperature on peak height (Figure 35b) reveals an increase for both reaction times. The increase with temperature is much more marked for the shorter reaction time. This is reasonable since the dispersion of the sample plug undergoing a shorter reaction time is affected both physically and chemically. In the longer coil the effect of chemical reaction on plug dispersion becomes a constant and the physical process predominates.

The random walk theory for FIA shows that an increase in temperature increases the physical process of radial diffusion and therefore enhances mixing. On a short time scale more complete reaction is predicted (73, 106). The nickel/PAR experiments lend credence to

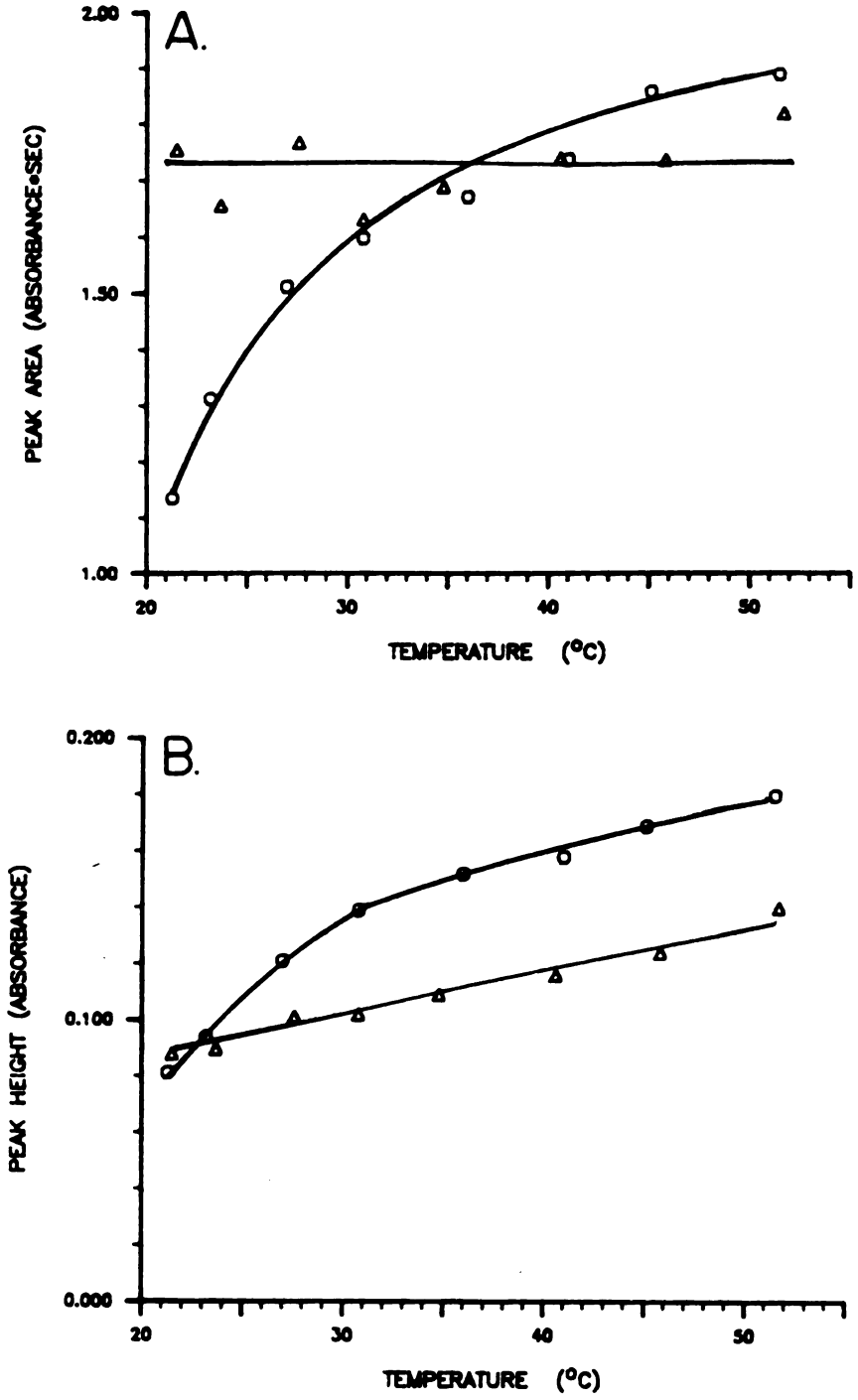

FIGURE 35 Effect of temperature on peak area (a) and peak height (b) for medium reaction with 1-m (O) and 3-m (Δ) coils.

these predictions. The chemical enhancement observed here may be due to better mixing or an actual increase in the reaction rate, or to a combination of these effects.

The theory also predicts that a temperature-induced reaction rate enhancement will affect slower reactions more noticeably. The last case presented was undertaken in an effort to substantiate this. An enzyme system provides a classic example for temperature-induced rate effects since a very small change in temperature can bring about a large change in reaction rate. The rapid increase in product absorbance with increased temperature noted earlier (Chapter 4) illustrates this effect.

Case 4: Slow Reaction

The FIA system for the glucose oxidase/Trinder reaction was used as described earlier (Chapter 4). The operating conditions were the standard set specified by the univariate experiments. Peroxide standards were prepared by appropriate dilution of 30% hydrogen peroxide. The stock solution was titrated with standardized thiosulfate on the day of use (110). Two calibration curves—one for peroxide, the other for glucose—were prepared in order to determine the peroxide concentration that would give an absorbance equivalent to that obtain with a 300 ppm glucose standard.

Data were taken at four different temperatures between 20°C and 40°C. Two glucose standards and their equivalent peroxide standards were used. The peak heights obtained at each temperature are plotted versus temperature in Figure 36b. The values obtained for the peroxide standards at room temperature are a bit higher than those for the

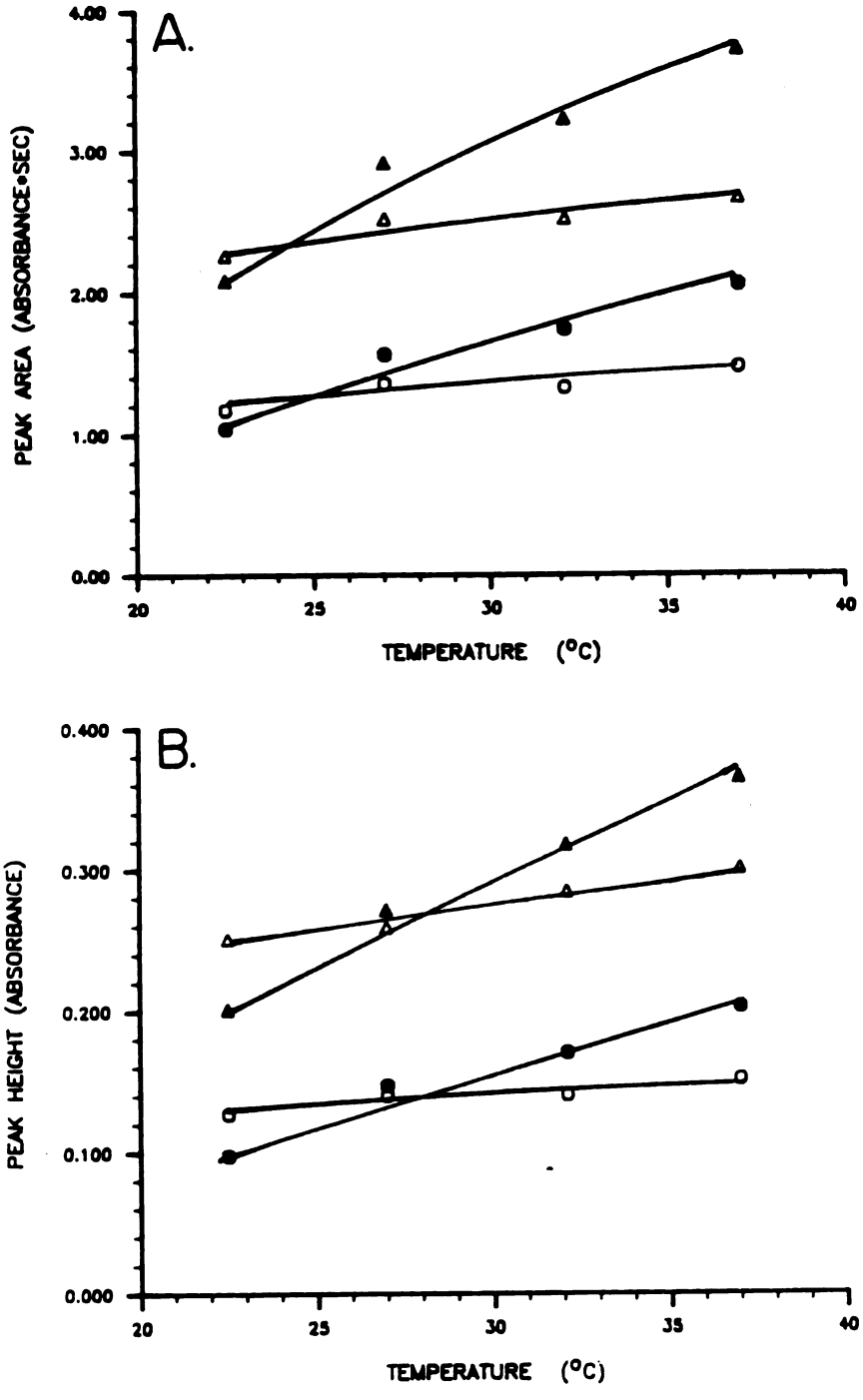

FIGURE 36 Effect of temperature on peak area(a) and peak height (b) for slow reaction. Concentrations of standards were: (●) 1.65 mM and (▲) 3.3 mM glucose; (○) 0.14 mM and (△) 0.28 mM H_2O_2.

glucose standards due to a slight mismatch of concentrations. This results in a crossover at the second temperature. A relatively small increase in absorbance takes place when peroxide is used compared to the large increase for the glucose standards. The effect of temperature on the peroxide part of the reaction is due to the physical factor and possibly the reaction as well. By integration of the peaks, the cause of the increase in peak height can be ascertained.

If it is the case that only the physical factor predominates, then one would expect to see a horizontal line as in Cases 2 and 3. If the chemical reaction is also responsible, an increase in peak area would be expected. The plot of peak area versus temperature (Figure 36a) suggests that the latter is the case, but only to a very small extent. This was expected since earlier results indicated that the peroxidase reaction is not drastically affected by changes in temperature. The temperature effect on the peak area for the glucose standards is much more severe. This is corroborated by the knowledge that the glucose oxidase reaction is slower than the peroxidase reaction.

The percent increase in response for each glucose standard over that obtained for the respective peroxide standard was calculated. The values can be found in Table 11. The percentage increase is linearly related to the temperature. This relationship could be used to "correct" for temperature the response obtained from the enzyme FIA system. In a "field" situation this would be a very useful technique since the temperature may vary by a few degrees over a short period of time. As illustrated here, that small temperature variation could result in a rather large measurement error.

TABLE 11 Temperature effect on glucose oxidase/ Trinder reaction.

Glucose Standard	Temperature	% incr. in peak area due to Reaction
1.65 mM	27.0°C	35
	32.1	54
	37.0	72
3.3 mM	27.0	28
	32.1	43
	37.0	6I

In summary, this experimental study shows that sample dispersion in flow injection analyzers decreases with increasing temperature and substantiates the theoretical predictions of Betteridge *et al* (73, 106). This effect is especially important when high precision results are required as, for example, in viscometry. Since the magnitude of the effect can readily be quantified, the experimentalist is in a better position to decide whether rigorous temperature control is necessary for a particular flow injection analysis application.

For well-characterized reactions it may be possible to "correct" a system for temperature changes as demonstrated in Case 4. Improved repeatability without temperature control could be obtained. Temperature sensitive devices could be incorporated into FIA manifolds routinely. Results which are independent of temperature could then be obtained by applying an appropriate multiplier to the peak height obtained, or by carrying out some transform on the peak shape. Such an approach could be of considerable utility for process control since a wider range of temperature conditions is more prevalent there than in the laboratory. One specific case in which this might be a useful technique is in food process control where an automated immobilized enzyme FIA system is used on-line.

CHAPTER 7

DEVELOPMENT OF A FLOW REVERSALS/MERGING ZONES FIA SYSTEM

It has been shown by Wade *et al* (113) that the effective length of the FIA manifold can be extended by reversing the flow direction of the stream after its first pass through the detector. Several reversals allow multidetection to be accomplished by this technique with only one detector. The FIA profile is different after each reversal. The peak shape becomes more Gaussian and the width at the base increases as the sample plug is allowed more time to disperse. In the case where a reaction occurs between the injected sample and the carrier stream, an increased amount of product (for moderate or slow reactions) would be detected after each reversal. The situation would become more complicated if the product were degraded in a period of time that corresponded to the timescale of the reversals. This is a rather simple example in which a single concentration gradient is present.

In order to exploit the use of flow reversals fully, a more complex case was considered. A complexation reaction which is sensitive to pH was selected. By overlapping a concentration gradient with a pH gradient, and then allowing the extent of overlap to increase with time, a two dimensional chemical surface is generated. It was thought that with a flow reversal experiment this surface could be mapped using the information obtained from a single injection. Computer simulation studies (114) indicated that this is a real possibility.

The FIA Flow Reversals System

The goal of this project was to assemble a semi-automated flow injection analysis system which could be used to obtain this two dimensional information for the complexation of metals with PAR. This task was performed under the supervision of Adrian Wade, a postdoctoral research associate in the Chemistry department. The FIA apparatus was put together as shown in Figure 37. The same pump, light source, and detector were used as in the studies presented in the previous chapters. The two sample injection valves, V1 and V2, were manually operated six-port sample injection valves with 70-µl sample loops (Rheodyne). The computer-controlled pneumatic actuator was attached to a third six-port valve, V3. The connections on this were rearranged so that the flow could be reversed by changing the position of the valve from "fill" to "inject" and vice versa. The sample passed through a detector into a 5-m holding coil. A slider valve (Alltech), V4, was used during the reversal to bring a second 5-m holding coil into line. The coils were 0.8 mm i.d. Microline tubing. Most of the connections were made with HPLC type threaded fittings joined with 0.8 mm i.d. Teflon tubing.

To ensure precise simultaneous injection of the two sample plugs, S1 and S2, the pump was stopped, the valves switched to the "inject" position, and the pump restarted. The two plugs were then merged at a tee to create the overlap. This technique is commonly known as "merging zones" (19). Asymmetric overlap was obtained by insertion of a short piece of tubing, C1, into one arm of the tee as shown in the figure. The two merged gradients were then joined with the reagent stream, R, at another tee. The flow of the stream was reversed by changing the

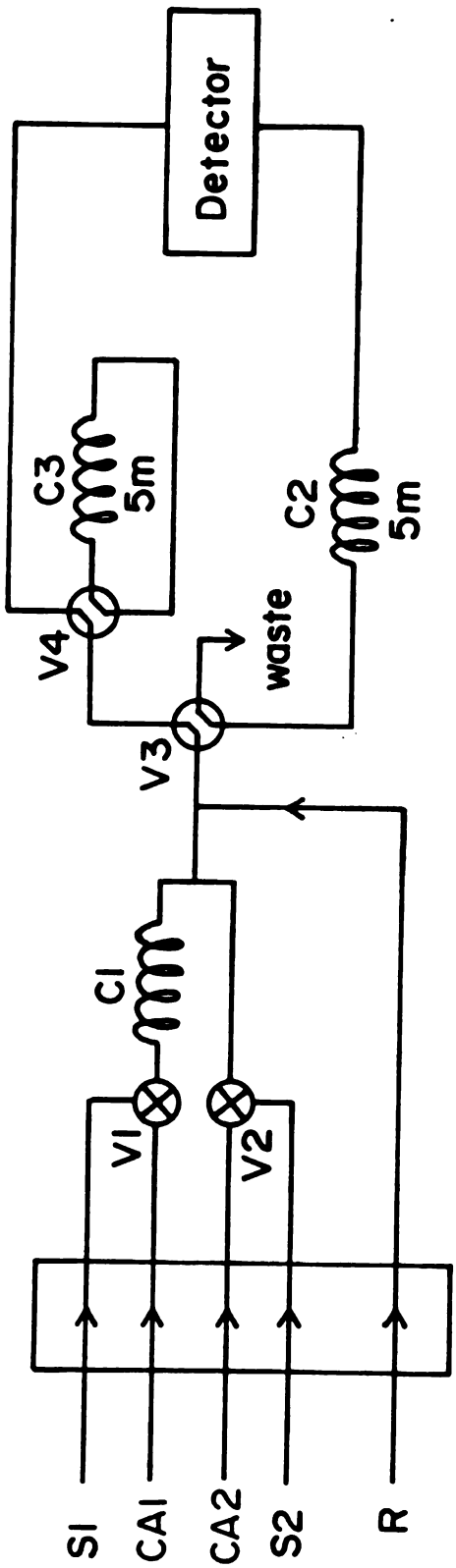

FIGURE 37 FIA system for flow reversal/ merging zones experiments.

position of V3. The holding coil was simultaneously brought into line by manually switching the position of V4; this prevented loss of the sample plug to waste upon the first reversal.

Computer control of the flow reversal was of paramount importance. The time at which each reversal takes place must be known and totally reproducible. This is because dye samples are used to determine the shape of the sample plug each time it passes through the detector. For a select chemical system it was presumed that there would be only specific regions within the plug where product would be detected. The absorbance would result from the convoluted effect of the concentration and pH gradients. To ensure that the same plug shape was produced for each set of reversals on each injection, computer control was necessary. This facilitated accurate mapping of the surface.

The 8088-based microcomputer (Bentley-Model T) was programmed as mentioned previously (Chapter 4). The BASIC program, FIADATA, was supplemented with a few extra lines of code in order to perform the reversals. The reversal times were included in a DATA statement. On each occasion that a set of A/D conversions was averaged, the current time was calculated. This time was compared with the reversal time; if it was equal to or greater than the reversal time, V3 was switched. Data acquisition was the same as described earlier. A sampling rate of 2 Hz was used.

Calibration with Dye

A solution of Alizarin Red (0.00048 M or 0.00025 M) in 0.05 M phosphate buffer was prepared. Three experiments were performed. In

all cases the reagent stream, R, and the two carrier streams, CA1 and CA2, were 0.05 M phosphate buffer, and the overall flow rate was 1.0 ml min^{-1}. The dye was first injected as S1 into CA1, then as S2 into CA2, and then simultaneously into both carrier streams (i.e., S1 and S2 were merged). In each case the absorbance of the stream flowing through the detector was monitored continuously. This set of experiments was done for both configurations of the system, i.e., both with and without the delay coil in place. This technique was adopted because it was previously shown that this type of characterization can be used to predict the shape of a pH gradient in an FIA system (115). The flow was reversed every 80 s in these experiments.

To investigate the location of experimental points on the two dimensional surface referred to earlier, S2 absorbance is plotted against S1 absorbance. The curves shown in Figure 38 were obtained for the system without the delay coil. The peak maximum for S2 (Figure 38b) occurs slightly later than that for S1 (Figure 38a). This indicated that the overlap was not complete (i.e., there was some asymmetry present). Figure 38c illustrates the small amount of peak broadening that occurs as a result of the asymmetry when the two samples are injected simultaneously. If the overlap of the two plugs is complete and the plugs are identical, a straight line of 45° slope is expected when S2 absorbance is plotted versus S1 absorbance. However, due to slight differences in sample volume and dispersion characteristics of the plugs (a result of inhomogeneity in the apparatus) the straight line becomes an ellipse as shown in Figure 39. This is because the absorbance of S1 initially rises faster than that of S2, then the S2

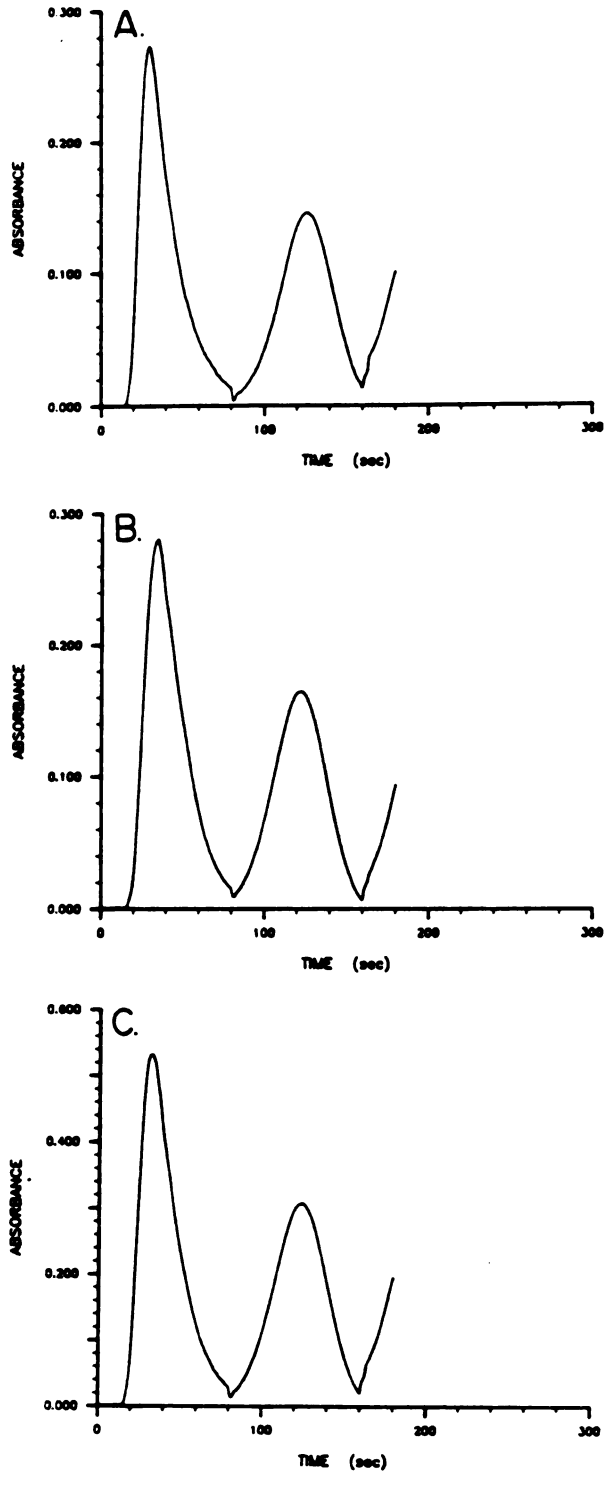

FIGURE 38 FIA profiles for two reversals and one detector. The three injections were: (a) S1 only; (b) S2 only; and (c) S1 plus S2.

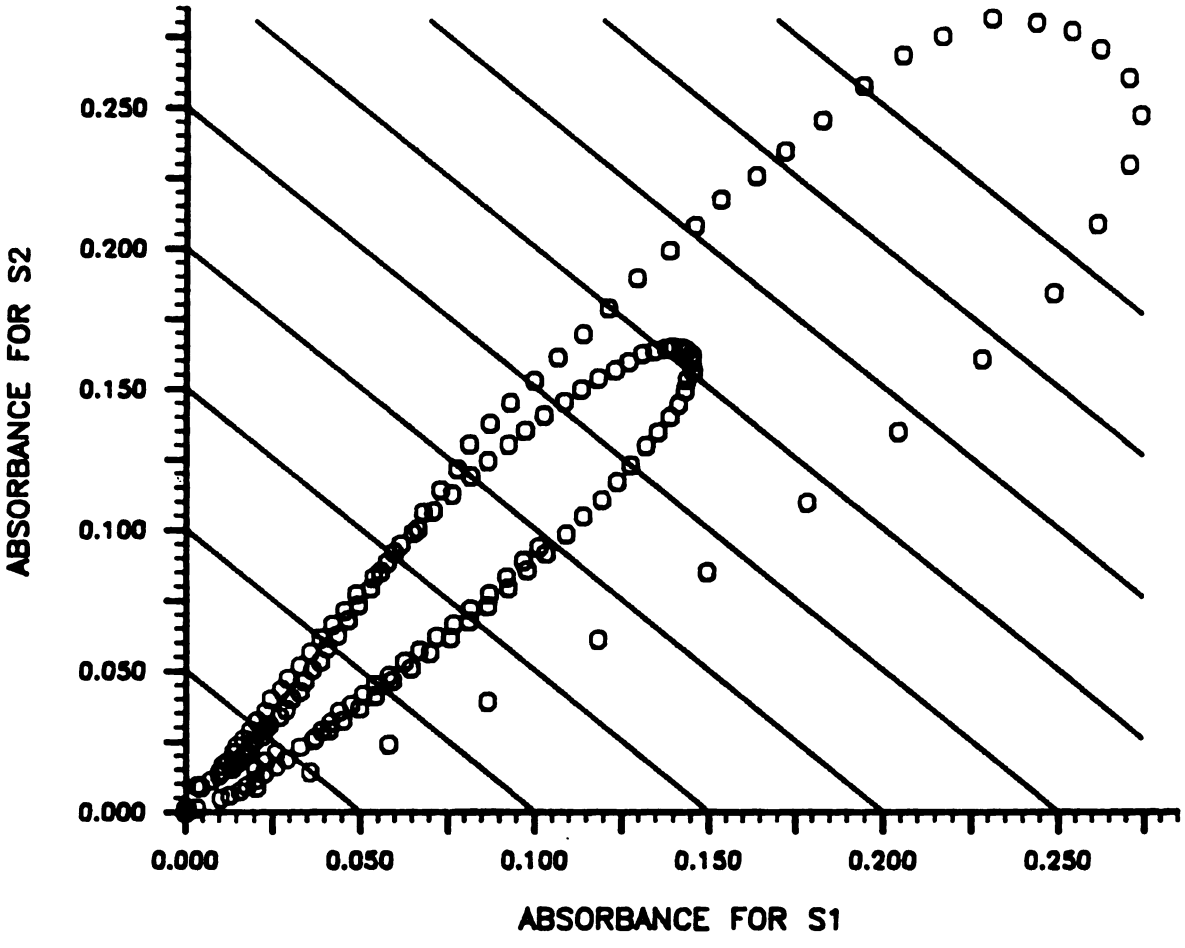

FIGURE 39 Contour plot for two reversals and one detector.

absorbance decreases slower than that of S1. If the sample volumes were different, but the dispersion characteristics identical, a single curved line would be expected.

By comparison of the FIA profiles shown in Figure 40 the effect of the delay coil can be seen. The sample plug, S2, arrives at the detector noticeably later than S1. This design allows S1 to experience the chemical environment of CA1 completely before a gradient is imposed by merging with S2 in CA2. For this set of experiments two detectors were used in series; the first detector was separated from the second by 50 cm of Microline tubing. By the time the two plugs reach the second detector it is evident that more dispersion has taken place.

A number of interesting observations can be made about the S2 versus S1 plot in Figure 41. The asymmetric nature of the outermost ellipse is due to the asymmetric nature of the peaks. The distribution of the sample becomes more Gaussian after each reversal. This is illustrated by the increased symmetry of the ellipse. With each reversal the ellipse contracts since the sample undergoes more longitudinal dispersion and is better mixed with the carrier, which makes the gradient less steep. As can be seen from the diagram, as this lobe contracts a greater density of points defines the lobe. By changing the data acquisition frequency, one could adjust the number of points so that enough are taken to define the shape and yet not so many that the information becomes redundant. Otherwise, a surface fitting routine with continuously adjustable weighting factors may be required in order to generate a good fit over the entire surface.

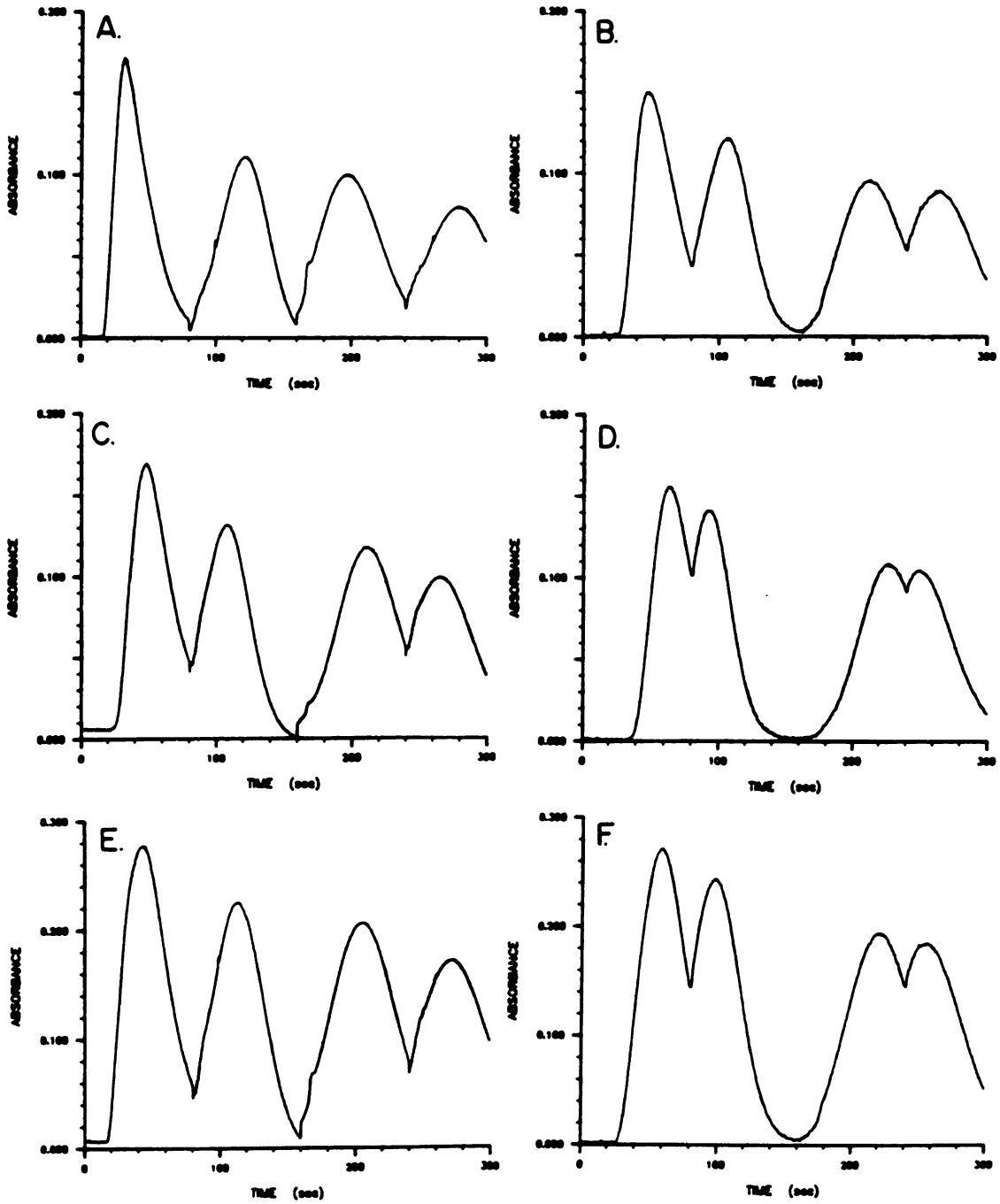

FIGURE 40 FIA profiles for three reversals and two detectors. The three injections were: (a) S1 only through the first detector; (b) S1 only through the second detector; (c) S2 only through the first detector; (d) S2 only through the second detector; (e) S1 plus S2 through the first detector; (f) S1 plus S2 through the second detector.

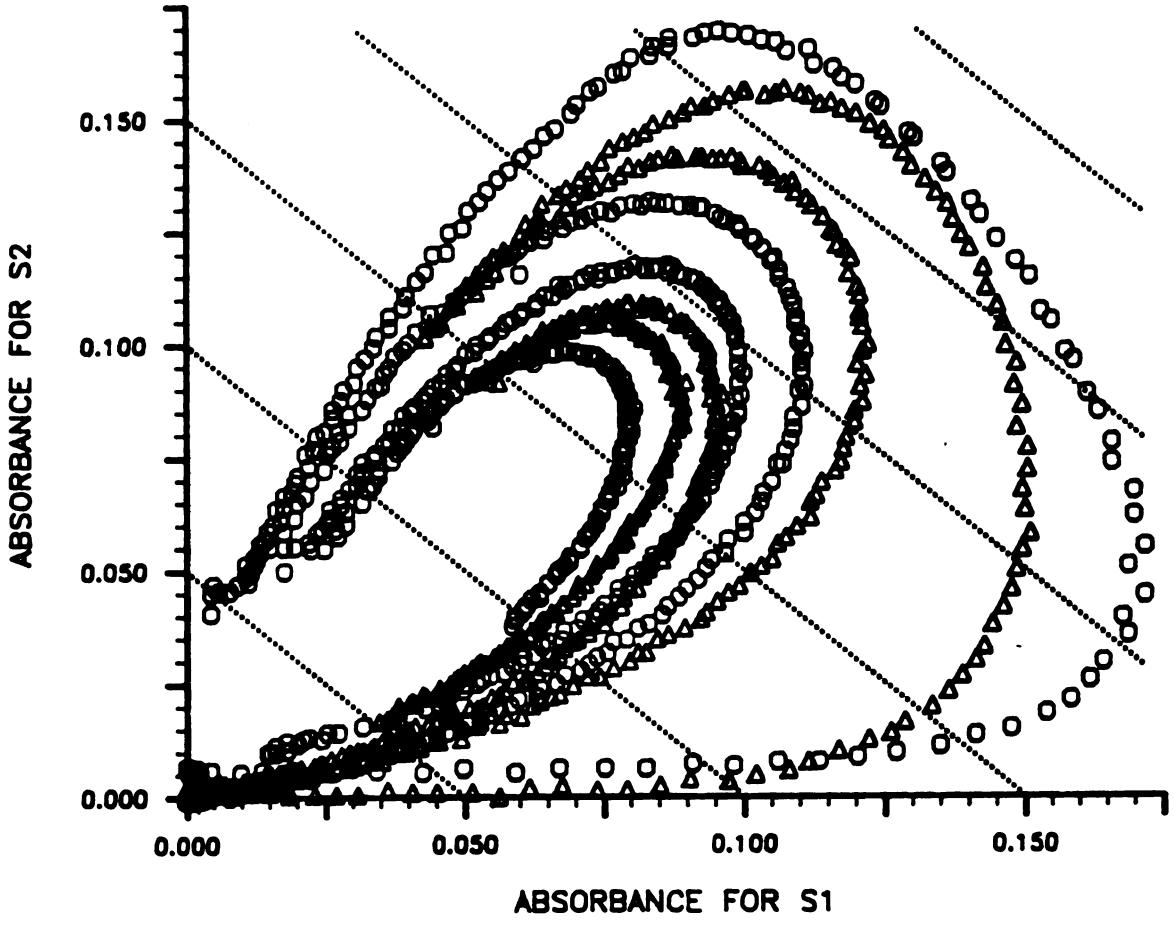

FIGURE 41 Contour plot for three reversals through the first detector (o) and the second detector (Δ).

It is also apparent that without the second detector there would be a large gap in information between that obtained in the initial pass through the detector and that after the first reversal. This illustrates how the use of a second detector can greatly contribute to the characterization of the dispersion behavior as the samples pass through longer lengths of tubing. The simulation showed that by use of as many as eight detectors, excellent surface coverage would be expected (114).

In Figures 39 and 41 the diagonal lines represent the contours of the surface. These were generated for the two sets of data with a fitting routine (based on the Kalman Filter) which was written by Pete Wentzell (116). The results from the injection of S1 and S2 individually were used as the base response. The results from the injection of S1 and S2 simultaneously were matched to this model. Since dye was used it would be expected that the match would be exact and thus generate diagonal straight lines. The diagonal nearest the origin represents the lowest iso-response area. The subsequent diagonals represent areas of increasing response which reflect increasing total dye concentration. By matching the results obtained from a chemical reaction within the two plugs to the non-reactive model of the two dye plugs, one would expect to obtain curved contours which would describe the two dimensional chemical surface.

Extension to a Chemical System

The complexation of various metals with PAR was chosen as the reaction to be implemented in this apparatus. The extent of

complexation for each metal is governed by pH. Metals such as copper and/or vanadium would be interesting examples. Copper forms two complexes with PAR, one begins to form at pH 2 while the other is formed above pH 9. Vanadium forms a complex between pH 6 and pH 8 but not above pH 9. Injection of metal, S1, into a stream of citric acid (low pH) and PAR followed by merging with S2, a plug of hydroxide (high pH), should provide the ideal environment to map the reaction surface for the two complexes.

Another consideration for the experiment with reaction is that PAR also absorbs at the same wavelength (480 nm) as either of the two complexes. Therefore it will be necessary to use the proper dilution of the reagent stream in the reference channel of the colorimeter. When PAR is mixed with hydroxide its absorbance increases. Therefore, a baseline experiment will be necessary. The baseline experiment with hydroxide must be subtracted from the other results. A number of static experiments should also be done in order to correlate complex absorbance and pH.

The apparatus constructed here is rather makeshift but has shown in the dye experiments that it should be possible to obtain meaningful results for the chemical system of interest. The technique of flow reversals, in general, could be very useful in other areas as well. It is a unique alternative to closed loop recycling (117) or multiple detectors (118, 119). For the immobilized enzyme work presented in the bulk of this work this methodology could be used to optimize reactor lengths in an automated system and may also be useful in determination of kinetic parameters.

CHAPTER 8

WHERE DO WE GO FROM HERE?

There are number of unfinished projects which have surfaced as a result of this research. The development of an on-line correction method for ascorbic acid interference with the Trinder reaction would be useful. Such a method could be implemented with other types of reactors. This would be especially useful in clinical applications since ascorbic acid is the only remaining interferent in serum after deproteinization.

Increased interest in the past few years concerning miniaturization of FIA systems indicates that there is a future for the extension of immobilized enzymes to microconduits. Studies with smaller tubing would provide the necessary information concerning lengths and inner diameters of channels that could be used with the pumps currently available. Immobilization of the enzyme on smaller particles should not be a problem since many workers have used controlled pore glass for many years.

A longer term project involves the construction of a parallel sugars analyzer. Glucose is one of six nutritionally-important sugars (aldohexoses) (90). There are enzyme reactions for each of the sugars which generate hydrogen peroxide and could therefore be coupled to the Trinder reaction. Enzyme reactors to determine glucose, galactose, maltose, sucrose, fructose, and lactose could each be incorporated into one channel of a six channel system. A possible configuration for this system is shown in Figure 42. The sample would be injected into one of

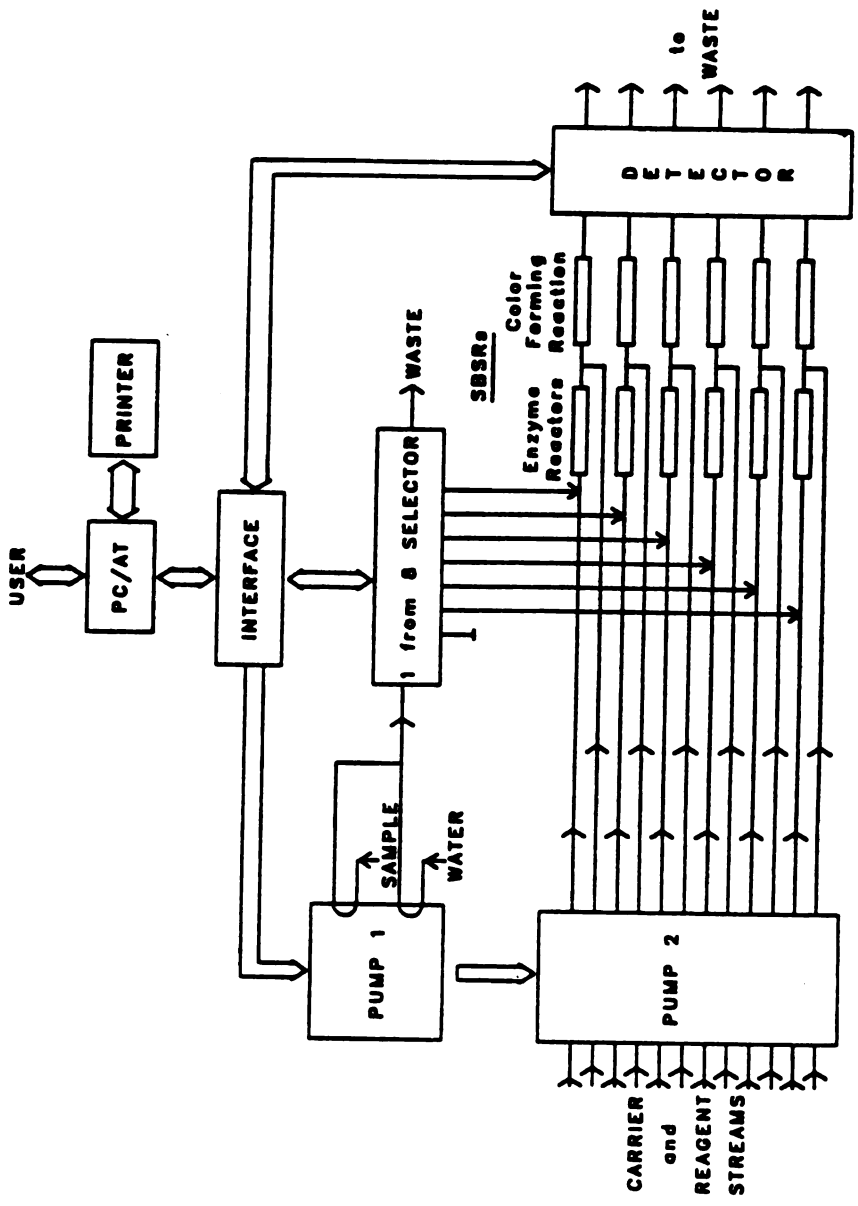

FIGURE 42 Six channel parallel FIA system for simultaneous determination of glucose, galactose, maltose, lactose, sucrose, and fructose.

the six channels by a selector. A simpler detection system could be used for each channel. The circuit designed by Betteridge *et al* (120) could be used effectively. This system could be miniaturized by constructing individual microconduits. A further enhancement would be provided by the use of an optrode that is sensitive to hydrogen peroxide. This could incorporate immobilized peroxidase. The results obtained with glucose and galactose indicate that development of a parallel analyzer employing SBSRs is feasible.

There a few more general FIA studies that could result from the insights gained here. As was noticed in the temperature study, the noise in the baseline increases with temperature. This merits further investigation since it could affect the reproducibility of results obtained by FIA. The source of this "ripple" needs to be identified.

The flow reversals work is far from complete. The data obtained from experiments with dye on any merging zones system could be used to determine the nature of the overlap. The S2 versus S1 plots are much more revealing than a simple look at the FIA profile. The speciation of metals using the apparatus discussed in Chapter 7 needs to be undertaken as well.

This research has opened new avenues for exploration. It is hoped that the practical issues addressed in this work will aid others in the pursuit of greater achievements in the use of immobilized enzymes and flow injection analysis.

LIST OF REFERENCES

LIST OF REFERENCES

1. O. Zaborsky, *Immobilized Enzymes*, CRC Press: Cleveland, 1973.

2. M. Salmona, C. Saronio, S Garattini, *Insolubilized Enzymes*, Raven Press: New York, 1975

3. R.A. Messing, Ed., *Immobilized Enzymes for Industrial Reactors*, Academic Press: New York, 1975.

4. H.H. Weetall, Ed., *Immobilized Enzymes, Antigens, Antibodies, and Peptides*, Marcel Dekker: New York, 1975.

5. L.B. Wingard, E. Katchalski-Katzir, and L. Goldstein, Eds., *Applied Biochemistry and Bioengineering, Vol. 1*, Academic Press: New York, 1976.

6. T.M.S. Chang, *Immobilized Enzymes and Proteins, Vols. 1 and 2*, Plenum Press: New York, 1977.

7. I. Chibata, Ed., *Immobilized Enzymes: Research and Development*, John Wiley & Sons: New York, 1978.

8. R. Mosbach in *Immobilized Enzymes* (S.P. Kolowick and N.O. Kaplan, Eds.) *Methods in Enzymology, Vol. 44*, Academic Press: New York, 1978.

9. M.D. Trevin, *Immobilized Enzymes*, John Wiley & Sons: New York, 1980.

10. P.W. Carr and L.D. Bowers, *Immobilized Enzymes in Analytical and Clinical Chemistry*, John Wiley & Sons: New York, 1980.

11. G.G. Guilbault, *Analytical Uses of Immobilized Enzymes*, Marcel Dekker: New York, 1984.

12. L.D. Bowers and P.W. Carr, *Anal. Chem.* 1976, *48*, 544A.

13. D.N. Gray, M.H. Keyes, and B. Watson, *Anal. Chem.* 1977, *49*, 1067A.

14. M.M. Fishman, *Anal. Chem.* 1978, *50*, 261R.

15. L.D. Bowers, P.W. Carr, *Adv. Biochem. Eng.* 1980, *15*, 89.

16. M.M. Fishman, *Anal. Chem.* 1980, *52*, 185R.

17. L.D. Bowers, *Trends Anal. Chem.* 1982, *1*, 191.

18. L.D. Bowers, *Anal. Chem.* 1986, *58*, 513A.

19. J. Ruzicka and E.H. Hansen, *Flow Injection Analysis*, John Wiley & Sons: New York, 1981.

20. M. Valcarcel and M.D. Luque de Castro, *Flow Injection Analysis: Principles and Applications*, John Wiley & Sons: New York, 1987.

21. J. Ruzicka and E.H. Hansen, *Anal. Chim. Acta* 1986, *179*, 1.

22. *Flow Injection Analysis Bibliography*, Tecator AB: Hoganas, Sweden, 1985.

23. J.M. Nelson and E.G. Griffin, *J. Am. Chem. Soc.* 1916, *38*, 1109.

24. F.I. Onuska, M.E. Comba, T. Bistricki, and R.J. Wilkinson, *J. Chrom.* 1977, *142*, 117.

25. M.C. Gosnell, R.E. Snelling, and H.A. Mottola, *Anal. Chem.* 1986, *58*, 1585.

26. L. Skeggs, *Am. J. Clin. Pathol.* 1957, *13*, 451.

27. K.K. Stewart, G.R. Beecher, P.E. Hare, *Fed. Proc.* 1974, *33*, 1439.

28. J. Ruzicka and E.H. Hansen, *Anal. Chim. Acta* 1975, *78*, 145.

29. J. Ruzicka and E.H. Hansen, *Anal. Chim. Acta* 1984, *161*, 1.

30. J.M. Reign, W.E. van der Linden, and H. Poppe, *Anal. Chim. Acta* 1981, *123*, 229.

31. C.C. Painton and H.A. Mottola, *Anal. Chim. Acta* 1984, *158*, 67.

32. G.P. Hicks and S.J. Updike, *Anal. Chem.* 1966, *38*, 726.

33. S.J. Updike and G.P. Hicks, *Nature (London)* 1967, *214*, 986.

34. S.J. Updike and G.P. Hicks, *Science* 1967, *158*, 270.

35. P. Cremonisi and R. Bovara, *Biotech. Bioeng.* 1976, *18*, 1487.

36. G.J. Moody, G.S. Sanghera, and J.D.R. Thomas, *Analyst* 1987, *112*, 65.

37. T. Yao, M. Sato, Y. Kobayashi and T. Wasa, *Anal. Chim. Acta* 1984, *165*, 291.

38. B. Watson, D.N. Stifel, and F.E. Semersky, *Anal. Chim. Acta* 1979, *106*, 233.

39. M. Masoom and A. Townshend, *Anal. Chim. Acta* 1985, *171*, 185.

40. R. Appelqvist, G. Marko-Varga, L. Gorton, A. Torstensson, and G. Johansson, *Anal. Chim. Acta* 1985, *169*, 237.

41. B. Olsson, B. Stalbom, and G. Johansson, *Anal. Chim. Acta* 1986, *179*, 203.

42. C.A. Koerner and T.A. Nieman, *Anal. Chem.* 1986, *58*, 116.

43. R.Q. Thompson, Ph.D. Dissertation, Michigan State University, East Lansing, MI, 1982.

44. J.N. Miller, B.F. Rocks, and D.T. Burns, *Anal. Chim. Acta* 1977, *93*, 353.

45. H.A. Mottola, *Anal. Chim. Acta* 1983, *145*, 27.

46. G. Johansson, L. Ogren, and B. Olsson, *Anal. Chim. Acta* 1983, *145*, 71.

47. M.H. Ho and M.U. Asouzu, *Use of Immobilized Enzymes in Flow Injection Analysis*, *Ann. N.Y. Acad. Sci.* 1984, *434*, 526.

48. L. Holland, *The Properties of Glass Surfaces*, John Wiley & Sons: New York, 1964.

49. M. C. Gosnell and H.A. Mottola, *Anal. Chem.* 1986, *58*, 631.

50. D. Keilin and E.F. Hartree, *Biochem. J.* 1952, *50*, 331.

51. P. Trinder, *Ann. Clin. Biochem.* 1969, *6*, 24.

52. D. Barham, and P. Trinder, *Analyst* 1972, *97*, 142.

53. P.J. Worsfold, *Anal. Chim. Acta* 1983, *145*, 117.

54. L. Gorton and L. Ogren, *Anal. Chim. Acta* 1981, *130*, 45.

55. C.L.M. Stults, A.P. Wade, and S.R. Crouch, *Anal. Chim. Acta* 1987, *192*, 155.

56. C.J. Patton and S.R. Crouch, *Anal. Chim. Acta* 1986, *179*, 189.

57. *YSI Precision Thermistors*, Yellow Springs Instruments, Yellow Springs, Ohio, 1977.

58. B.H. Newcome and C.G. Enke, *Rev. Sci. Instrum.* 1984, *55*, 2017.

59. P.R. Kraus, Ph.D. in progress, Michigan State University.

60. H.T.S. Britton and R.A. Robinson, *J. Chem. Soc.* 1931, 1456.

61. M. Victor, Ph.D. in progress, Michigan State University.

62. B.W. Griffin and P.L. Ting, *Biochemistry* 1978, *17*, 2206.

63. D. Keilin and E.F. Hartree, *Biochem. J.* 1948, *42*, 221.

64. D. Betteridge, T.J. Sly, A.P. Wade, and J.E.W. Tillman, *Anal. Chem.* 1983, *55*, 1292.

65. S.N. Deming and S.L. Morgan, *Anal. Chim. Acta* 1983, *150*, 183.

66. A.P. Wade, Ph.D. Dissertation, University of Wales, 1985.

67. S.N. Deming and S.L. Morgan, *Anal. Chem.* 1974, *46*, 1170.

68. D. Betteridge, A.P. Wade, and A.G. Howard, *Talanta* 1985, *32*, 723.

69. D. Betteridge, A.P. Wade, and A.G. Howard, *Talanta* 1985, *32*, 709.

70. D. Betteridge and A.P. Wade, British Petroleum Research Centre, Sunbury- on-Thames, UK, Personal communication, February 1986.

71. J.A. Lott and K. Turner, *Clin. Chem.* 1975, *21*, 1754.

72. D. Betteridge, A.F. Taylor, and A.P. Wade, *Anal. Proc.* 1984, *21*, 373.

73. D. Betteridge, C.Z. Marczewski, and A.P. Wade, *Anal. Chim. Acta* 1984, *165*, 227.

74. H.U. Bergmeyer, Ed., *Methods of Enzymatic Analysis*; Verlag Chemie: Weinheim, 1965; p. 990.

75. K. Zeile in *Die Methoden der Fermentforschung* (E. Bamann and K. Myrback, Eds.); reproduced by Academic Press: New York, 1941; p. 2601.

76. B.C. Erickson, B.R. Kowalski, and J. Ruzicka, *Anal. Chem.* 1987, *59*, 1246.

77. B. Chance, *J. Biol. Chem.* 1943, *151*, 553.

78. R.Q. Thompson, *Anal. Chem.* 1987, *59*, 1119.

79. A. Rios, M.D. Luque de Castro, and M. Valcarcel, *Anal. Chim. Acta* 1986, *179*, 463.

80. C.C. Painton and H.A. Mottola, *Anal. Chim. Acta* 1984, *158*, 67.

81. M.A. Koupparis, *2nd Int'l Symp. on Kinetics in Analytical Chemistry*, Preveza, Greece, September, 1986.

82. H. Hirano, Y. Baba, N. Yoza, and S. Ohashi, *Anal. Chim. Acta* 1986, *179*, 209.

83. C.L.M. Stults, A.P. Wade, and S.R. Crouch, *Anal. Chem*, accepted for publication.

84. W. Pigman and H.S. Isbell, *Advan. Carbohyd. Chem.* 1968, *23*, 11.

85. H.S. Isbell and W. Pigman, *Advan. Carbohyd. Chem. Biochem.* 1969, *24*, 14.

86. C.S. Hudson and J.K. Dale, *J. Am. Chem. Soc.* 1917, *39*, 320.

87. J.A. Nelder and R. Mead, *Comput. J.* 1965, *7*, 308.

88. G. Livingston, F. Franks, and L.J. Aspinall, *J. Solution Chem.* 1977, *6*, 203.

89. H. Murschhauser, *Biochem. Z.* 1920, *110*, 181.

90. G.F. Stewart and M.A. Amerine, Eds., *Introduction to Food Science and Technology, 2nd Ed.*; Academic Press, NY, 1982, p. 137.

91. Faulkner, W.R., Ed. in Chief *Selected Methods in Clinical Chemistry*, 1982, *9*, 379.

92. *Galactose Oxidase Product information Sheet:* Sigma Chemical Co., St. Louis, MO, 1987.

93. H.U. Bergmeyer, *Methods of Enzymatic Analysis, Volume 2,* Verlag Chemie: Weinheim, 1983.

94. S.K. Dahodwala, M.K. Weibel, and A.E. Humphrey, *Biotech. Bioeng.* 1976, *18*, 1679.

95. B. Olsson, H. Lundback, and G. Johansson, *Anal. Chim. Acta* 1985, *167*, 123.

96. D. Betteridge, *Talanta* 1976, *23*, 409.

97. V. Ananthakrishnan, W.N. Gill, and A.J. Barduhn, *A. I. Ch. E. J.* 1965, *11*, 1063.

98. J.M. Reijn, W.E. van der Linden, and H. Poppe, *Anal. Chim. Acta* 1981, *126*, 1.

99. J.T. Vanderslice, K.K. Stewart, K.K., A.G. Rosenfeld, and D.J. Higgs, *Talanta* 1981, *28*, 11.

100. H. Wada, S. Hiroaka, A. Yuchi, and G. Nakagawa, *Anal. Chim. Acta* 1986, *179*, 181.

101. J.F. Tyson, *Anal. Chim. Acta* 1986, *179*, 131.

102. J. Ruzicka and E.H. Hansen, *Anal. Chim. Acta* 1980, *114*, 19.

103. D. Betteridge, W.C. Cheng, E.L. Dagless, P. David, and T.B. Goad, *Analyst* 1983, *108*, 17.

104. C.C. Painton and H.A. Mottola, *Anal. Chem.* 1981, *53*, 1713.

105. D.C. Stone and J.F. Tyson, *Anal. Proc. (London)* 1986, *23*, 23.

106. C.D. Crowe, H.W. Levin, D. Betteridge, and A.P. Wade, *Anal. Chim. Acta*, in press.

107. D.C. Stone and J.F. Tyson, *Analyst* 1987, *112*, 515.

108. C.L.M. Stults, A.P. Wade, and S.R. Crouch, *Anal. Chim. Acta* 1987, *192*, 301.

109. A.P. Wade, unpublished results, 1983.

110. I.M. Kolthoff, E.B. Sandell, E.J. Meehan, and S. Bruckenstein, *Quantitative Chemical Analysis, 4th Ed.;* Macmillan: NY, 1969.

111. P.M. Beckwith, Ph.D. Dissertation, Michigan State University, 1972.

112. R.G. Harfmann, Ph.D. in progress, Michigan State University.

113. D. Betteridge, P.B. Oates, and A.P. Wade, *Anal. Chem.* 1987, *59*, 1236.

114. A.P. Wade, C.L.M. Stults, S.R. Crouch, and D. Betteridge, *13th Annual FACSS Meeting*, St. Louis, MO, October 2, 1986.

115. D. Betteridge and B. Fields, *Anal. Chim. Acta* 1981, *132*, 139.

116. P.D. Wentzell, Ph.D. in progress, Michigan State University.

117. J. Ruz, A. Rois, M.D. Luque de Castro, and M. Valcarcel, *Talanta* 1986, *33*, 199.

118. D. Betteridge, W.C. Cheng, E.L. Dagless, P. David, and T.B. Goad, *Analyst* 1983, *108*, 1.

119. D.J. Hooley and R.E. Dessy, *Anal. Chem.* 1983, *55*, 313.

120. T.J. Sly, D. Betteridge, D. Webberley, and D.G. Porter, *J. Automated Chem.* 1982, *4*, 186.